GEAR TOOTH OPTIMIZATION FOR NONSTANDARD CYLINDIRICAL INTERNAL AND EXTERNAL AEROSPACE GEAR PAIRS

A THESIS SUBMITTED TO
THE GRADUATE SCHOOL OF NATURAL AND APPLIED SCIENCES
OF
MIDDLE EAST TECHNICAL UNIVERSITY

BY

ORHAN NURI KARACA

IN PARTIAL FULFILLMENT OF THE REQUIREMENTS
FOR
THE DEGREE OF MASTER OF SCIENCE
IN
MECHANICAL ENGINEERING

SEPTEMBER 2019

Approval of the thesis:

GEAR TOOTH OPTIMIZATION FOR NONSTANDARD CYLINDIRICAL INTERNAL AND EXTERNAL AEROSPACE GEAR PAIRS

submitted by **ORHAN NURI KARACA** in partial fulfillment of the requirements for the degree of **Master of Science in Mechanical Engineering Department, Middle East Technical University** by,

Prof. Dr. Halil Kalıpçılar
Dean, Graduate School of **Natural and Applied Sciences** _____

Prof. Dr. M. A. Sahir Arıkan
Head of Department, **Mechanical Engineering** _____

Prof. Dr. Metin Akkök
Supervisor, **Mechanical Engineering, METU** _____

Examining Committee Members:

Prof. Dr. F. Suat Kadıoğlu
Mechanical Engineering, Middle East Technical University _____

Prof. Dr. Metin Akkök
Mechanical Engineering, METU _____

Prof. Dr. Orhan Yıldırım
Mechanical Engineering, Middle East Technical University _____

Prof. Dr. Ömer Anlağan
Mechanical Engineering, Bilkent University _____

Assist. Prof. Dr. Orkun Özşahin
Mechanical Engineering, Middle East Technical University _____

Date: 02.09.2019

I hereby declare that all information in this document has been obtained and presented in accordance with academic rules and ethical conduct. I also declare that, as required by these rules and conduct, I have fully cited and referenced all material and results that are not original to this work.

Name, Surname: Orhan Nuri Karaca

Signature:

ABSTRACT

GEAR TOOTH OPTIMIZATION FOR NONSTANDARD CYLINDIRICAL INTERNAL AND EXTERNAL AEROSPACE GEAR PAIRS

Karaca, Orhan Nuri
Master of Science, Mechanical Engineering
Supervisor: Prof. Dr. Metin Akkök

September 2019, 162 pages

Aerospace gears are produced by grinding method and can have arbitrary addendum circle and dedendum circle radii and rounded gear root as opposite to the gears produced by traditional method such as rack and pinion generation method. The aerospace gears have also nonstandard module, pressure angle and helix angle. In this study, helical external and internal aerospace gear pairs are optimized by considering bending stress, contact stress and scuffing limitations. Pinion and gear number of teeth, normal module, helix angle, pressure angle, pinion shifting coefficient, center distance, pinion addendum radius, gear addendum radius, pinion dedendum radius and gear dedendum radius are taken into consideration as the design parameters which are to be optimized. Pinion and gear rotational speeds, input power, Young Modulus and Poisson ratios of the pinion and gear material, Contact and Bending strength of the gear material are taken as input parameters. All the possible gear pairs are considered in terms of contact stress, bending stress, scuffing temperature, tiff clearance, top land thickness, root form radius and tip clearance limitations. AGMA 908-B89 is used for evaluating the contact stress geometry factor. AGMA 2001-D04 is used for evaluating the bending and contact stress. The rounded gear root evaluation is conducted for cylindrical gear pairs. The bending stress geometry factor is implemented for gear pairs which have rounded gear root. AGMA 925 is used for evaluating the flash

temperature and scuffing evaluations. The analytical method is conducted in MATLAB. All the obtained results are compared with KISSOFT commercial tool and it is observed that KISSOFT uses only the transverse plane in the gear root evaluation and does not consider the backlash effect on the bending stress geometry factor evaluation. The minimum center distance optimization has a crucial role in aerospace applications to decrease the weight of an air vehicle. The minimum weight design solutions are obtained by using the minimum center distance optimization.

Keywords: Gear tooth profile optimization, grinding, rounded gear root, aerospace gear optimization,

ÖZ

HAVACILIKTA KULLANILAN STANDART DIŞI SİLİNDİRİK İÇ VE DIŞ DİŞLİ ÇİFTLERİNDE DİŞ OPTİMİZASYONU

Karaca, Orhan Nuri
Yüksek Lisans, Makina Mühendisliği
Tez Danışmanı: Prof. Dr. Metin Akkök

Eylül 2019, 162 sayfa

Havacılık dişlileri taşlama yöntemi ile üretilir ve dişli kol-fener dişli gibi geleneksel yöntemlerle üretilen dişlilerin aksine herhangi bir istenen diş üstü dairesi yarıçapına ve diş dibi dairesi yarıçapına sahip olabilir. Bu çalışmada havacılıkta kullanılan helisel iç ve dış dişli çiftlerinin profil optimizasyonu, eğilme gerilimi, temas gerilimi ve sürtme aşınması limitasyonları yapılmıştır. Havacılık dişlileri ayrıca standart dışı modül, basınç açısı ve helis açısına sahiplerdir. Döndüren ve döndürülen dişlilerin diş sayıları, normal modül, helis açısı, basınç açısı, pinyon profil kaydırma katsayısı, dişli merkezleri arası mesafe, döndüren dişli diş dibi dairesi yarıçapı, dönen dişli diş dibi dairesi yarıçapı, döndüren dişli diş üstü dairesi yarıçapı ve döndürülen dişlinin diş üstü dairesi yarıçapı optimize edilmesi gereken tasarım parametreleri olarak alınmıştır. İhtimal dahilindeki bütün dişli çiftleri temas gerilimi, eğilme gerilimi, sürtünme aşınması sıcaklığı, tiff aralığı, diş üstü kalınlığı, diş kökü yarıçapı ve diş üstü aralığı limitasyonları incelenmiştir. AGMA 908–B89 standardı temas gerilimi geometri faktörü hesaplamasında kullanılır. AGMA 2001-D04 standardı eğilme ve temas gerilimi hesabı için kullanılır. Yuvarlatılmış dişli kökü hesabı silindirik dişliler için yapılır. Eğilme gerilimi geometri faktörü hesabı yuvarlatılmış dişli köküne sahip silindirik dişliler için yapılır. AGMA 925 standardı sürtünme aşınması sıcaklığı hesabında kullanılır. Analitik metot MATLAB programında kodlamalar geliştirilerek

düzenlenmiştir. Bütün sonuçlar KISSOFT ticari yazılımı ile karşılaştırılmıştır ve KISSOFT programının dişli kökü hesabında enine düzlemi kullandığı ve dişli boşluğunun eğilme gerilimi geometri faktörü hesabı üzerindeki etkisini ihmal ettiği gözlemlenmiştir. Minimum dişli merkezleri arası mesafe optimizasyonu bir hava aracının ağırlığını azaltmak için önemli bir role sahiptir. Minimum ağırlık tasarım çözümleri minimum dişli merkezleri arası mesafe optimizasyonu yapılarak elde edilir.

Anahtar Kelimeler: Dişli dişi optimizasyonu, taşlama, yuvarlatılmış dişli kökü, havacılık dişli optimizasyonu

To my beautiful country…

ACKNOWLEDGEMENTS

I would like to thank my supervisor Prof. Dr. Metin Akkök for his supervision, help and guidance from the beginning to end of this dissertation.

I want to thank Mahir Gökhan Orak for his endless support and encouragement throughout this study.

I also want to special thanks to my lovely cousin Emirhan Boyraz for his endless support and encouraging me throughout my research.

I want to thank my family; Zeki Karaca, Hatice Karaca and Hanife Melike Karaca for their endless support and encouragement throughout this study.

TABLE OF CONTENTS

LIST OF TABLES

TABLES

LIST OF FIGURES

FIGURES

LIST OF ABBREVIATIONS

ABBREVIATIONS

SAP	start of active profile
$LPSTC$	lowest point of single tooth contact
$HPSTC$	highest point of single tooth contact
EAP	end of active profile
$LACR$	low axial contact ratio

LIST OF SYMBOLS

a_{ref}	reference center distance
a_w	operating center distance
A	radius of the gear root
b	vertical distance of the center of the circular root
$b_{H_{(i)}}$	semi-width of Hertzian contact band
B_M	thermal contact coefficient
c	root clearance
C_e	mesh alignment correction factor
C_f	surface condition factor
C_h	helical factor
C_H	hardness ratio factor
C_{ma}	mesh alignment factor
C_{mc}	lead correction factor
C_{mf}	face load distribution factor
C_p	elastic coefficient
C_{pf}	pinion proportion factor
$C_{R_{avg_x}}$	surface roughness constant
C_{pm}	pinion proportion modifier
$C_1, C_2, \ldots\ldots\ldots, C_6$	distances along line of action

C_ψ	helical overlap factor
d	diameter
E	modulus of elasticity
E_r	reduced modulus of elasticity
F	effective face width
$(F_t)_{nom}$	nominal tangential load
F_{wn}	normal operating load
$h_{c_{(i)}}$	central film thickness at a given point
h_f	height of Lewis parabola
$H_{c_{(i)}}$	dimensionless central film thickness
I	geometry factor for contact strength
I_c	involute clearance
j	circular backlash
k_{sump}	parameter for calculating θ_m
K	flash temperature constant
K_B	rim thickness factor
K_D	combined derating factor
K_f	stress correction factor
K_m	load distribution factor
K_o	overload factor
K_R	reliability factor

K_s	size factor
K_T	temperature factor
K_v	dynamic factor
K_ψ	helix angle factor
L_{hv}	load height
L_{min}	minimum length of contact lines
L_x	filter cutoff of wavelength x
m	module
m_F	axial contact ratio
m_G	gear ratio
m_N	load sharing ratio
m_p	transverse contact ratio
n	rotational speed
p	circular pitch
P_b	base pitch
P_d	transverse diametral pitch
P_{nd}	normal diametral pitch
P_x	axial pitch
Q	tail area of the normal probability function
r	reference radius or pitch circle radius
r_a	addendum circle radius

r_b	base circle radius
r_f	root radius or dedendum circle radius
r_{cr}	critical radius
r_{nL}	load radius
r_{tf}	tip form radius
R_c	reserve factor for contact stress
R_f	root form radius
R_m	mean radius
R_t	reserve factor for bending stress
$R_{a_{1x}}, R_{a_{2x}}$	average surface roughness (pinion, gear) at L_x
s	tooth thickness
s_c	contact stress number
s_t	bending stress number
s_b	bending stress number
S_F	tooth thickness at critical section
S_n	normal tooth thickness in reference circle
S_t	transverse tooth thickness in reference circle
s_{ac}	allowable contact stress number
s_{at}	allowable bending stress number
s_{na}	top land thickness
s_{acp}	permissible allowable contact stress number

s_{atp}	permissible allowable bending stress number
tc	tip chamfer
$Tiff$	tiff clearance
$U_{(i)}$	speed parameter
$v_{e_{(i)}}$	entraining velocity
$v_{s_{(i)}}$	sliding velocity
$v_{r_{(i)}}$	rolling (tangential) velocity
w	rotational velocity
w_n	normal unit load
$W_{(i)}$	load parameter
W_t	transmitted tangential load
x	profile shift coefficient
y	profile shift
Y	tooth form factor
Y_N	bending strength stress cycle factor
z	number of teeth
Z	active length of line of action
Z_n	contact strength stress cycle factor
α	pressure angle
α_{nL}	load angle
α_{nW}	pressure angle at load application point

β	reference helix angle
β_b	base helix angle
η_{40}	dynamic viscosity at temperature $40^{\circ}C$
η_{100}	dynamic viscosity at temperature $100^{\circ}C$
η_m	dynamic viscosity at gear tooth temperature θ_m
θ_m	tooth temperature
$\theta_{fl_{(i)}}$	flash temperature
θ_{oil}	oil inlet or sump temperature
θ_s	mean scuffing temperature
λ_m	heat conductivity
$\mu_{m_{(i)}}$	mean coefficient of friction
ν	Poisson's ratio
$\xi_{(i)}$	pinion roll angle at point i along the line of action
ρ	radius of curvature of profiles at point of contact stress calculation
ρ_m	radius of curvature of the pinion profile at mean radius
X_Γ	load sharing factor
$\pm$	upper sign for external pair lower sign for internal pair
$\mp$	upper sign for external pair lower sign for internal pair
&&	and operator in MATLAB

CHAPTER 1

INTRODUCTION AND LITERATURE SURVEY

1.1. Introduction

Gears are widely used in transmission systems to transmit power. There are numerous gear types used in industrial applications. Cylindrical gears are not only used in automotive industry, they are also used in aerospace applications especially in planetary stage and accessory gear box. They are also used as collector gear in some helicopters. Cylindrical gears used in automotive industry are usually produced by traditional techniques such as hobbing and shaping. However, aerospace cylindrical gears are mostly produced by grinding. Grinding manufacturing is also called as direct gear design in the literature. Aerospace gears can have arbitrary addendum and dedendum radii since the grinding wheel can be dressed into whatever shape is desired. Dressing the grinding wheel in desired shape also makes obtaining the rounded gear root possible. However, the addendum circle and dedendum circle radii depends on the cutter shifting in traditional manufacturing techniques and obtaining the arbitrary addendum circle and dedendum circle radii is not possible. This dependency does not allow the design nonstandard gears.

Numerous different gears can be manufactured by using direct gear design technique. Therefore, different gear pairs can be manufactured to satisfy a wide range of working conditions.

Optimization is a required process at the beginning of a design project to obtain the optimum design which satisfies the requirements and the desired stress values to maintain a robust design against the compelling operational conditions. Gear design optimization takes an important place in helicopter transmission system projects. The minimum weight consideration is one of the most important design approach in

aerospace applications. Therefore, the gear pairs which have minimum center distance are more desirable when the whole system is considered. Minimum center distance makes the casing weight minimum. Hence, the weight of the gear box is also minimized.

There are numerous optimization techniques. Traditional optimization techniques are not suitable for the complex gear optimization. Nontraditional optimization methods are commonly used in gear optimization due to this complexity. However, the gear optimization studies conducted by nontraditional optimization method do not cover so many design parameters as considered in this study. Most of the studies are suitable to use nontraditional optimization methods due to including less design parameters and constraint functions as compared to current study. The different optimization method is required for the current study due to its complexity. The fine sizing optimization methodology which is explained in a detailed way in the following sections is determined as the optimization procedure. The fine sizing optimization method is used in commercial gear design and analysis computer programs like MASTA and KISSOFT. In this method, all the possible gear pairs are constituted by giving a range for all design parameters and then by combining all of them. The related constraints are evaluated for all the possible gear pairs. Gear pairs which do not satisfy the required constraints are eliminated. The remaining gear pairs after the all constraint eliminations are completed are the gear pairs which satisfy the all the geometrical and material strength requirements. Fine sizing method vanishes the possibility of the converging a local minimum such a complex gear optimization like the current study.

Commercial gear design and analysis computer programs makes the gear optimization by considering only the gears produced by traditional manufacturing techniques. The arbitrary addendum radius, dedendum radius and the rounded gear root are not considered in these programs. Addendum and dedendum radii are dependent on the shifting coefficient and taking the arbitrary values for these radii is not allowed. MASTA and KISSOFT programs are also not capable to calculate the bending stress for the gears which have rounded root. Bending stress geometry factor is calculated as

if the gear root is produced by traditional techniques and has a trochoidal shape despite the software allows the user to implement arbitrary addendum and dedendum radii as input parameters.

In the current study, the optimum gear pair is obtained by considering the direct gear design methodology. The rounded gear root and arbitrary addendum and dedendum radii are considered. Pinion and gear number of teeth, normal module, pressure angle, helix angle, center distance, shifting coefficient, addendum and dedendum radii of the pinion and the gear are taken as the design variables. Contact stress, bending stress and scuffing limitations are considered with the geometrical constraints.

1.2. Objective of the Thesis

The main aim of the study is to obtain optimum helical external and internal gear pairs for given input and given output speeds under a specified input power. Geometrical calculations of the helical external and internal gear pairs are evaluated. Bending stress, contact stress and scuffing calculations are conducted. The optimum gear design is obtained by using fine sizing method.

1.3. Literature Survey

The conducted studies in the literature about the cylindrical gear pairs are investigated in this part of the thesis.

Mohan and Seshaiah [1] conducted an optimization study on spur gear sets by taking the center distance, weight and tooth deflections as objective functions. Module, face width and number of teeth on pinion were taken into consideration as decision variables. Since the optimum problem is multi objective function and involves constraints, it is a very challenging issue to obtain the optimum result with a traditional optimization technique. Therefore, they used a nontraditional optimization technique called as Genetic Algorithm. However, they also used the traditional optimization methods to compare the traditional and nontraditional optimization techniques. They concluded that genetic algorithm gives more accurate and more optimal results than

the traditional approach. They stated that since genetic algorithm is random search and optimization technique, the chance of getting global optimum is possible. The weak side of their study is that they used very simple formulas for contact stress and bending stress evaluations. The contact stress formula proposed by them does not cover Hertzian Contact theory. Bending stress formula proposed in their study does not cover the geometry factor evaluated in AGMA standards. Therefore, geometry of the gear root was not included in their study. Another weak side of their study is that they didn't clarify how the possibility of finding a local optimum is vanished. They also didn't evaluate the scuffing temperature. Saxena et al. [2] investigated the optimization of internal spur gear design by using genetic Algorithm. They specified the minimum center distance as the objective function. They specified some limits on the contact ratio, gear ratio and tip interference. They also proposed a requirement to eliminate the involute interference. They examined the face width as a constraint function. They determined the required face width which meets bending and contact stress requirements. The weak side of the study is that they used some charts to evaluate the face width for the bending stress and for the contact stress. However, the proposed charts do not include any information about the tooth geometry. Therefore, the proposed formulas for face width evaluation can give the same results for the gears which have different geometric shape with respect to each other. They stated that the global optimum result was found by using genetic algorithm. However, Wu [3] stated that genetic algorithm can give the local optimum. To overcome this issue, he proposed an algorithm includes an improved genetic and simulated annealing algorithm with the function of disturbance. Saxena et al. didn't propose an improved genetic algorithm and they stated that the global optimum was reached in their study. They didn't clarify how the possibility of finding a local optimum is vanished by using genetic algorithm. Revar et al. [4] investigated the optimization of helical gears. They considered the face width and helix angle as design variables. They changed the helix angle and face width by keeping the other parameters constant. They evaluated the maximum bending stress and the maximum contact stress by trial and error method. They tried to find the optimum design that gives the maximum contact stress and

bending stress in certain limits. They made finite element analysis in ANSYS. They concluded the effect of the helix angle and the face width on the contact stress and bending stress. They stated that less thickness and helix angle give better and maximum contact stress and bending stress. The weak side of the study is that they didn't use any optimization technique to obtain the optimum result. They tried to find optimum solution by trial and error method. They considered a few parameters as design parameters and they didn't consider any geometrical constraint. However, they used AGMA standards to evaluate the bending stress and contact stress. As compared to [1] and [2], their results in terms of contact stress and bending stress were more accurate than the results of the others since the gear tooth geometry was included. Kapelevich and Shekhtman [5] examined the direct gear design. The direct gear design is a gear design which is not restricted by a choice of gear tooth profiles based on standard tool parameters. The method uses non-standard tooth shapes to cover the custom applications. They investigated fillet optimization of standard rack-generated gears by considering the bending stress. They tried to minimize the bending stress of the standard rack-generated gears by applying the fillet optimization. They proposed a method for balancing the bending stress of the pinion and the gear. They changed the tooth thickness ratio in FEA program to satisfy the bending stress balance requirement. They used FEA for bending stress evaluation because the Lewis equation and its related coefficients do not provide a reliable solution to the wide variety of non-standard gear tooth profiles. They concluded that optimization of the fillet profile allowed reducing the maximum bending stress in the gear tooth root area by 10-30 %. Padmanabhan et al. [6] investigated the optimization of spur gear pair by using Genetic Algorithm. They defined the objective functions of the problem as follows: maximization of power delivered by the gear pair, minimization of the overall weight, maximization of the efficiency of the gear pair, minimization of the center distance. They named the contact stress as the crushing stress. They took the crushing stress and the bending stress as the constraint functions. Module, face width, number of teeth in pinion and power were considered as design variables. They used the same formulas for the bending stress and for the contact stress proposed in [1]. They verified the

results by implementing FEA. By FEA analysis the maximum stress was less than the theoretical value. The weak side of the study is that bending stress and contact stress formula used in their study didn't include any information on the tooth geometry. They didn't consider the scuffing as a constraint function. Gopal et al. [7] investigated the optimization of helical gear design by using Genetic Algorithm. The minimum center distance was taken as objective function. They specified number of teeth on the pinion, diametral pitch and helix angle as design variables. They took involute interference, bending stress, contact stress, gear ratio and addendum to dedendum ratio as the design variables. They used AGMA standards to evaluate the bending stress and contact stress calculation. Their study didn't neglect the geometry of the gear tooth. However, they didn't use the arbitrary addendum and dedendum radii. Therefore, their study is limited to the gears which are restricted by the standard tool parameters. They didn't consider the scuffing evaluation. They didn't suggest any proposal how the possibility of converging a local optimum is vanished. Dr. Rajiv Suman et al. [8] investigated the optimization of helical gears by using the Genetic Algorithm. Face width, center distance and radius of the pinion were chosen as the parameters are to be optimized. They evaluated the contact stress, bending stress and the involute interference as the constraint functions. Pinion number of teeth, diametral pitch, helix angle, addendum ratio and dedendum ratio were specified as the design parameters. Since they considered the addendum and dedendum ratio as the design parameters, the proposed method in their study does not include the direct gear design. Rai et al. [9] investigated the optimization of spur gears by considering the center distance as the objective function. Contact ratio, involute interference, bending stress, contact stress and scuffing were considered as the constraint functions. They evaluated the optimization problem with scuffing evaluation and without scuffing evaluation and they tried to understand the effect of the scuffing into the optimized gear pair. They also used two different optimization techniques in their study. They used the simulated annealing and the real coded genetic algorithm for the same optimization problems. One of the main interests of the study is comparison between these two techniques. Summary of the some studies conducted in the literature is given in Table 1.1.

Table 1.1 *Summary of some studies*

Study	***Design Variables***	***Method***	***Constraints***	***Geometry Factor***
[1]	Module Mumber of teeth of pinion	Genetic Algorithm	Bending Stress Contact Stress	Not included
[2]	Module Number of teeth of pinion	Genetic Algorithm	Contact Ratio Gear Ratio Tip Interference	Not included
[6]	Module Number of teeth Power	Genetic Algorithm	Crushing stress Bending stress	Not included
[7]	Number of teeth, Diametral pitch Helix angle	Genetic Algorithm	Involute interference Bending stress Contact stress Gear ratio Addendum to dedendum ratio	Included
[8]	Module Radius of the pinion Diametral pitch Helix angle Addendum ratio Dedendum ratio	Genetic Algorithm	Contact Stress Bending Stress Involute interference	Included
[9]	Diametral pitch Number of teeth	Simulated annealing Real coded genetic algorithm	Contact Stress Involute interference Bending Stress Scuffing Temperature	Included

CHAPTER 2

CYLINDIRICAL EXTERNAL AND INTERNAL GEAR PAIR OPTIMIZATION PARAMETERS AND OPTIMIZION METHODOLOGY

2.1. Cylindrical External Gear Pair Optimization Parameters

The optimization parameters for external and internal gear pairs are given in this chapter. The optimization methodology is consisted of two constraint groups. The first constraint group is named as geometrical constraints and the second constraint group is named as material based constraints.

2.1.1. Geometrical Constraints

Geometrical constraints are investigated in this chapter. The geometrical constraints are root clearance, top land thickness, contact ratio, involute clearance and tiff clearance. The basic radii are given in Figure 2-1 and Figure 2-2.

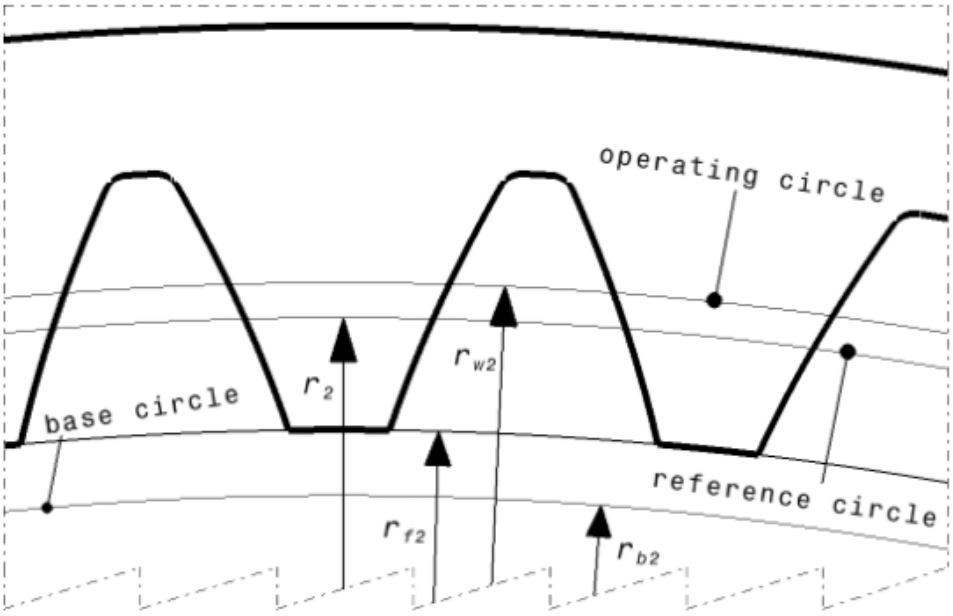

Figure 2-1 *Geometrical parameters of internal gear*

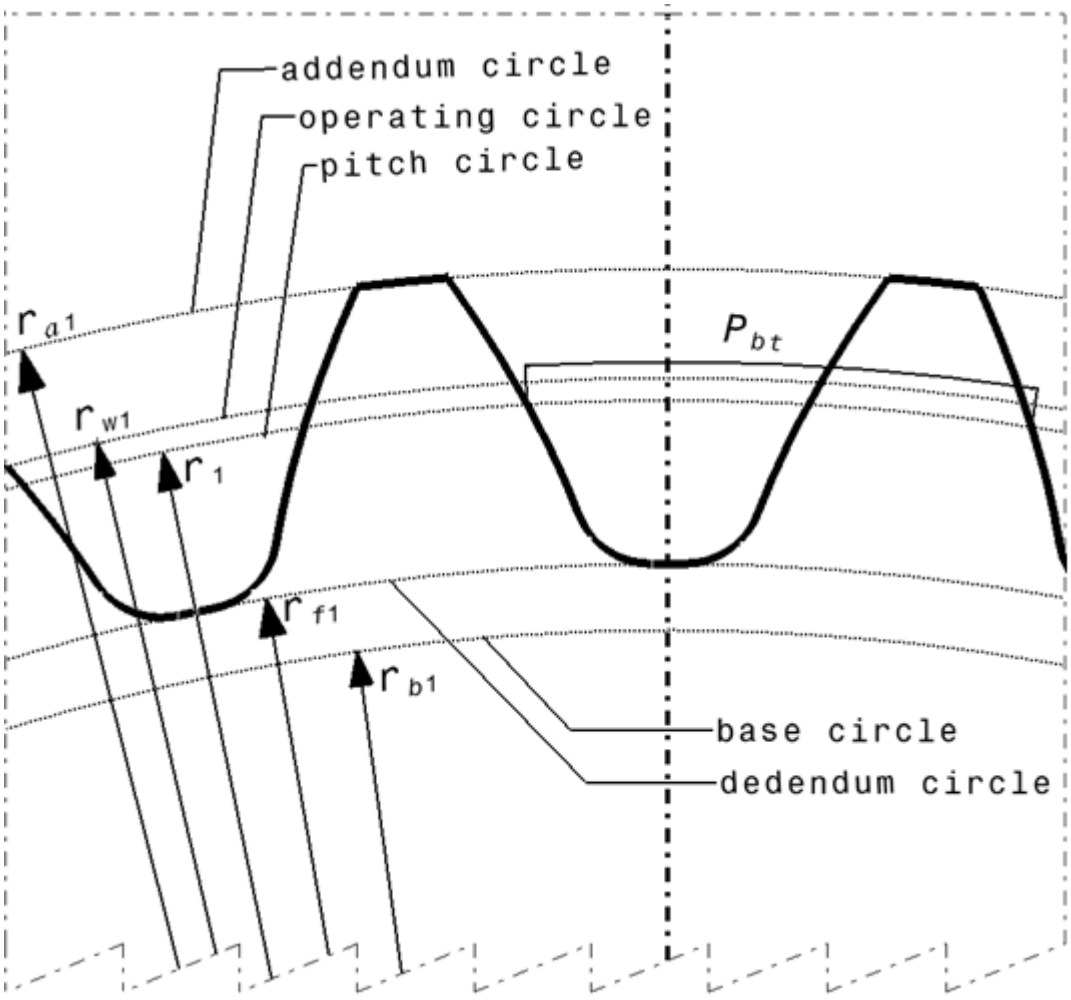

Figure 2-2 *Geometrical parameters of external gear*

2.1.1.1. Root Clearance

Root clearance for the cylindrical external gear pairs is given in [11]. As seen from Figure 2-3, the root clearance of the pinion and the gear is:

$$c_1 = a_w - r_{f1} - r_{a2} \tag{2.1}$$

$$c_2 = a_w - r_{f2} - r_{a1} \tag{2.2}$$

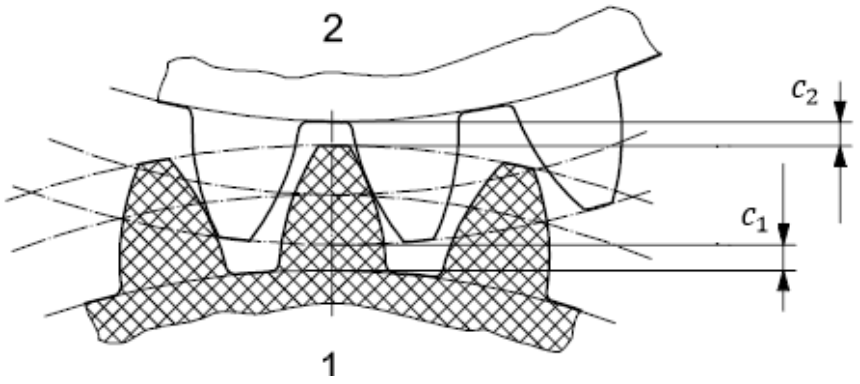

Figure 2-3 *Root clearances c_1 and c_2 of an external gear pair [11]*

Root clearance for the cylindrical internal gear pairs can be evaluated from Figure 2-4. As seen from Figure 2-4, the root clearance of the pinion and the gear is:

$$c_1 = r_{a2} - a_w - r_{f1} \tag{2.3}$$

$$c_2 = r_{f2} - a_w - r_{a1} \tag{2.4}$$

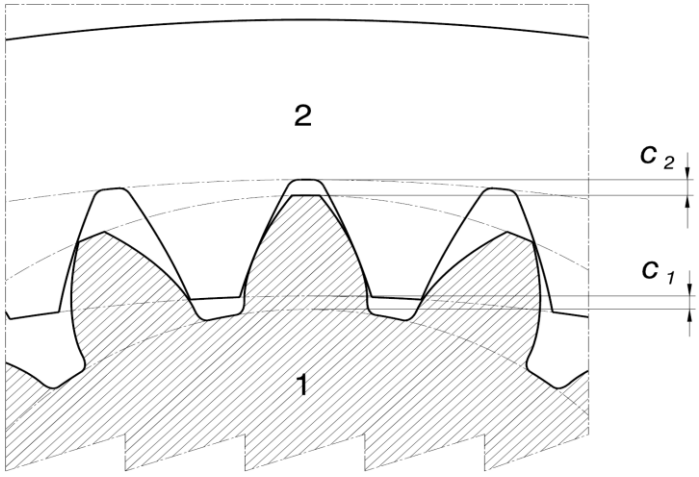

Figure 2-4 *Root clearances c_1 and c_2 of an internal gear pair*

2.1.1.2. Top Land Thickness Evaluation of External Gear Pairs

The basic geometric relations and top land thickness evaluation is outlined in this section. Basic geometric relations are given in Table 2.1.

Table 2.1 *Basic geometric relations*

Transverse circular pitch [12]	$p_t = \frac{p_n}{cos\beta}$	(2.5)
Transverse tooth thickness in reference circle [12]	$s_t = \frac{s_n}{cos\beta}$	(2.6)
Transverse module [12]	$m_t = \frac{m_n}{cos\beta}$	(2.7)
Diameter of the reference cylinder [12]	$d = \frac{zm_n}{cos\beta}$	(2.8)
Normal base pitch [13]	$P_{bn} = \pi m_n cos\alpha_n$	(2.9)
Transverse base pitch [13]	$P_{bt} = \frac{2\pi r_{b1t}}{z_1}$	(2.10)
Gear ratio [13]	$m_G = \frac{z_2}{z_1}$	(2.11)
Base helix angle [13]	$\beta_b = arccos\left(\frac{P_{bn}}{P_{bt}}\right)$	(2.12)
Reference center distance [12]	$a_{ref} = \frac{(d_1 + d_2)}{2}$	(2.13)
Profile shift coefficient [12]	$x = \frac{y}{m_n}$	(2.14)
Reference radius of the pinion [12]	$r_1 = \frac{z_1 m_n}{2cos\beta} = r_1 u$	(2.15)
Base radius of the pinion [12]	$r_{b1} = r_1 cos\alpha_t$	(2.16)
Base radius of the gear [12]	$r_{b2} = r_2 cos\alpha_t$	(2.17)
Transverse pressure angle [12]	$\alpha_t = arctan\left(\frac{tan\alpha_n}{cos\beta}\right)$	(2.18)

The normal circular tooth thickness of the zero backlash external gear at its reference cylinder is: [12]

$$S_n = \frac{1}{2}\pi m_n + 2ytan\alpha_n \tag{2.19}$$

The angle between the normal plane and the transverse plane is equal to helix angle. Therefore, tooth thickness at gear reference cylinder in transverse plane can be expressed as follows:

$$S_t = \frac{S_n}{cos\beta} \tag{2.20}$$

If two external gears are to mesh with no backlash, their profile shift values must satisfy: [12]

$$y_1 + y_2 = \frac{a_{ref}(inv\alpha_{wt} - inv\alpha_t)}{tan\alpha_t} \tag{2.21}$$

$$\alpha_{wt} = arccos\left(\frac{a_{ref}cos\alpha_t}{a_w}\right) \tag{2.22}$$

$$inv\alpha_t = tan\alpha_t - \alpha_t \tag{2.23}$$

$$inv\alpha_{wt} = tan\alpha_{wt} - \alpha_{wt} \tag{2.24}$$

Sum of profile shift coefficients for zero backlash is:

$$x_1 + x_2 = \frac{a_{ref}(inv\alpha_{wt} - inv\alpha_t)}{m_n tan\alpha_t} \tag{2.25}$$

Pinion operating radius is:

$$r_{w1} = \frac{r_{b1}}{cos\alpha_{wt}} \tag{2.26}$$

Gear operating radius is:

$$r_{w2} = \frac{r_{b2}}{cos\alpha_{wt}} \tag{2.27}$$

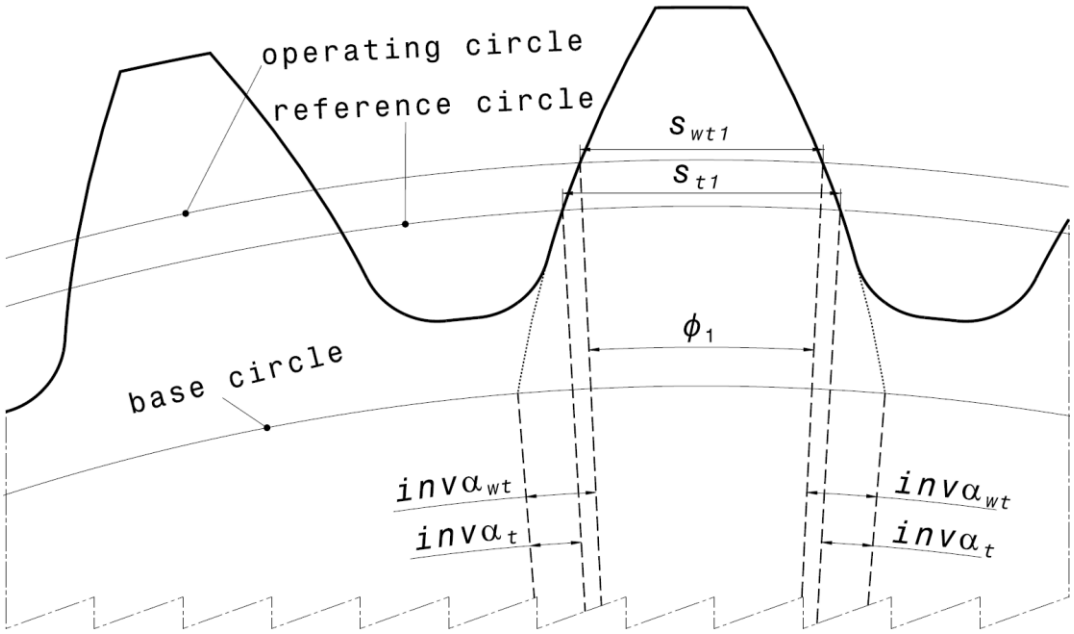

Figure 2-5 *Tooth thickness of external gear pair pinion at reference and operating circles*

$$\phi_1 = \frac{S_{t1}}{r_1} - 2(inv\alpha_{wt} - inv\alpha_t) \tag{2.28}$$

$$S_{wt1} = r_{w1}\phi_1 \tag{2.29}$$

Backlash at operating circle in traverse section is given as:

$$J_{twr} = \frac{J_{nwr}}{cos\beta} \tag{2.30}$$

Tooth thickness at operating circle with backlash in transverse section is given as:

$$S_{wt1b} = S_{wt1} - \frac{J_{twr}}{2} \tag{2.31}$$

Tooth thickness at reference circle with backlash in transverse section and in normal section is given as:

$$\theta_1 = \left(\frac{S_{wt1b}}{r_{w1}}\right) + 2(inv\alpha_{wt} - inv\alpha_t) \tag{2.32}$$

$$S_{t1b} = r_1\theta_1 = r_1\left(\left(\frac{S_{wt1b}}{r_{w1}}\right) + 2(inv\alpha_{wt} - inv\alpha_t)\right) \tag{2.33}$$

$$S_{n1b} = S_{t1b}cos\beta \tag{2.34}$$

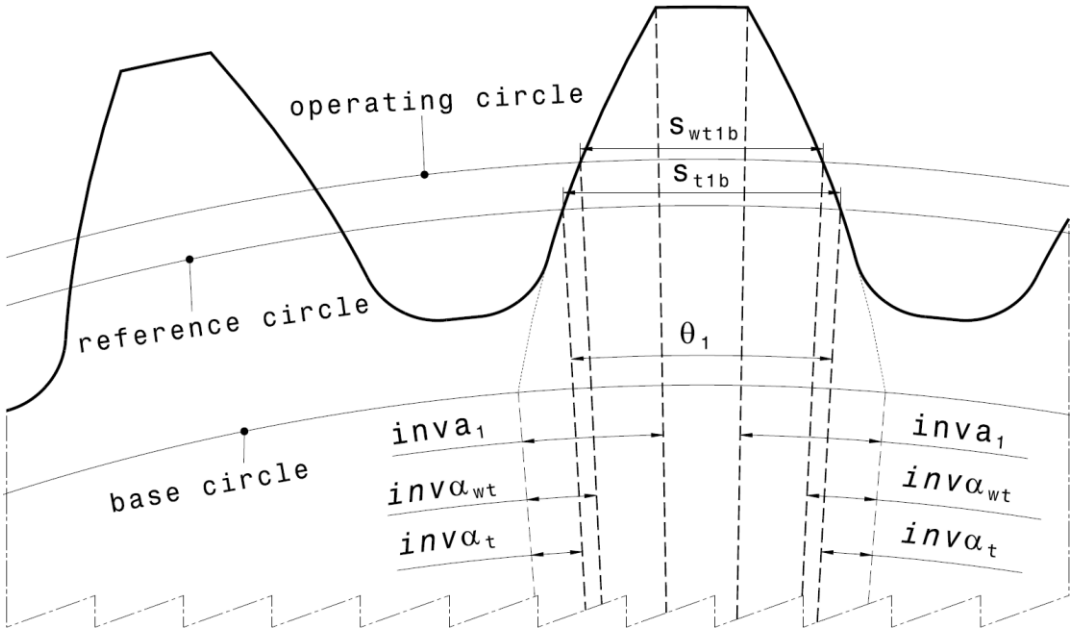

Figure 2-6 *Top land thickness evaluation of external gear pair pinion*

Top land thickness of the pinion in the transverse section is expressed as:

$$s_{nat1} = r_{a1}\left(\theta_1 - 2(inva_1 - inv\alpha_t)\right) \tag{2.35}$$

Top land thickness of the pinion in the normal section is expressed as:

$$s_{nan1=}s_{nat1}cos\left(arctan\left(tan\beta\,\frac{r_{a1}}{r_1}\right)\right) \tag{2.36}$$

Similarly for the gear:

$$\phi_2 = \frac{S_{t2}}{r_2} - 2(inv\alpha_{wt} - inv\alpha_t) \tag{2.37}$$

$$S_{wt2} = r_{w2}\psi_2 \tag{2.38}$$

Tooth thickness at operating circle with backlash in transverse section is given as:

$$S_{wt2b} = S_{wt2} - \frac{J_{twr}}{2} \tag{2.39}$$

Tooth thickness at reference circle with backlash in transverse section is given as:

$$\theta_2 = \left(\frac{S_{wt2b}}{r_{w2}}\right) + 2(inv\alpha_{wt} - inv\alpha_t) \tag{2.40}$$

$$S_{t2b} = r_2\theta_2 = r_2\left(\left(\frac{S_{wt2b}}{r_{w2}}\right) + 2(inv\alpha_{wt} - inv\alpha_t)\right) \tag{2.41}$$

Top land thickness of the gear in the transverse section is expressed as:

$$s_{nat2} = r_{a2}\left(\theta_2 - 2(inva_2 - inv\alpha_t)\right) \tag{2.42}$$

Top land thickness of the gear in the normal section is expressed as:

$$s_{nan2} = s_{nat2}cos\left(arctan\left(tan\beta\,\frac{r_{a2}}{r_2}\right)\right) \tag{2.43}$$

2.1.1.3. Top Land Thickness Evaluation of Internal Gear Pairs

The normal circular tooth thickness of the zero backlash internal gear at its reference cylinder is: [12]

$$S_n = \frac{1}{2}\pi m_n \pm 2ytan\alpha_n \tag{2.44}$$

If an external pinion and an internal gear are to mesh with no backlash, their profile shift values must satisfy: [12]

$$y_2 - y_1 = \frac{a_{ref}(inv\alpha_{wt} - inv\alpha_t)}{tan\alpha_t} \tag{2.45}$$

Reference center distance for an internal gear pair is:

$$a_{ref} = \frac{(d_2 - d_1)}{2} = r_2 - r_1 \tag{2.46}$$

Profile shift coefficients for zero backlash have the following relation:

$$x_2 - x_1 = \frac{a_{ref}(inv\alpha_{wt} - inv\alpha_t)}{m_n tan\alpha_t} \tag{2.47}$$

From Figure 2-7,

$$\phi_2 = \frac{S_{t2}}{r_2} - 2(inv\alpha_t - inv\alpha_{wt}) \tag{2.48}$$

$$S_{wt2} = r_{w2}\phi_2 \tag{2.49}$$

$$S_{wt2b} = S_{wt2} - \frac{J_{twr}}{2} \tag{2.50}$$

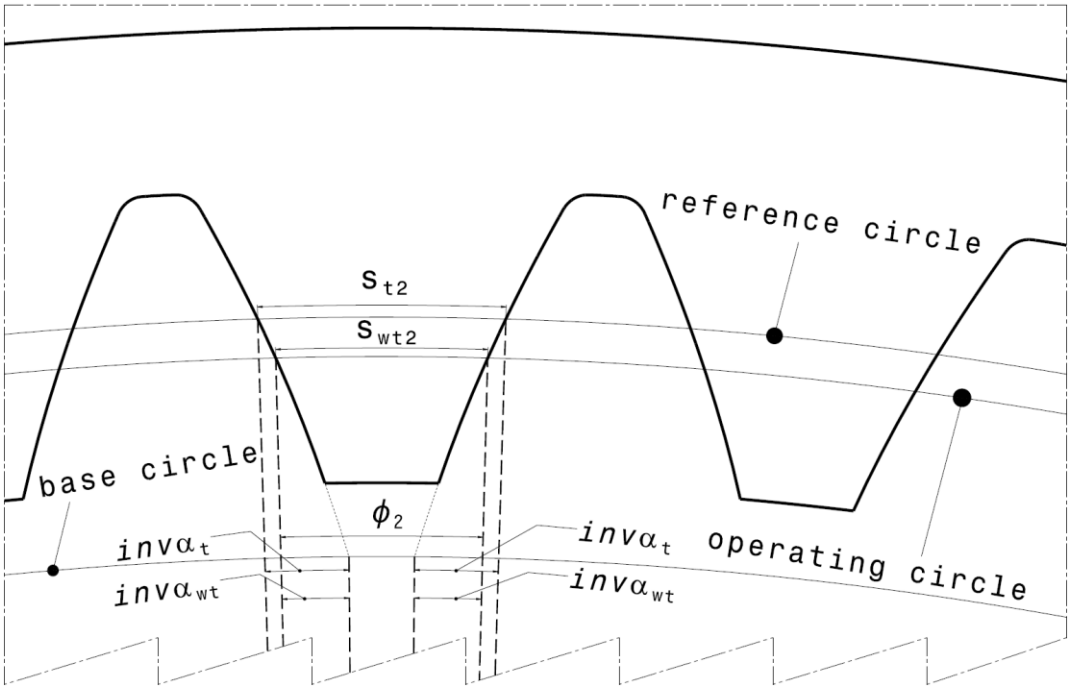

Figure 2-7 *Tooth thickness of internal gear at reference and operating circles*

Tooth thickness at reference circle with backlash in transverse section is given as:

$$\theta_2 = \left(\frac{S_{wt2b}}{r_{w2}}\right) + 2(inv\alpha_t - inv\alpha_{wt}) \tag{2.51}$$

$$S_{t2b} = r_2\left(\left(\frac{S_{wt2b}}{r_{w2}}\right) + 2(inv\alpha_t - inv\alpha_{wt})\right) \tag{2.52}$$

$$S_{n2b} = S_{t2b}cos\beta \tag{2.53}$$

Top land thickness of the gear in the transverse section is expressed as:

$$s_{nat2} = r_{a2}(\theta_2 - 2(inv\alpha_t - inv\mathrm{a}_2)) \tag{2.54}$$

Top land thickness of the gear in the normal section is expressed as:

$$s_{nan2} = s_{toplandt2}cos\left(arctan\left(tan\beta\frac{r_{a2}}{r_2}\right)\right) \tag{2.55}$$

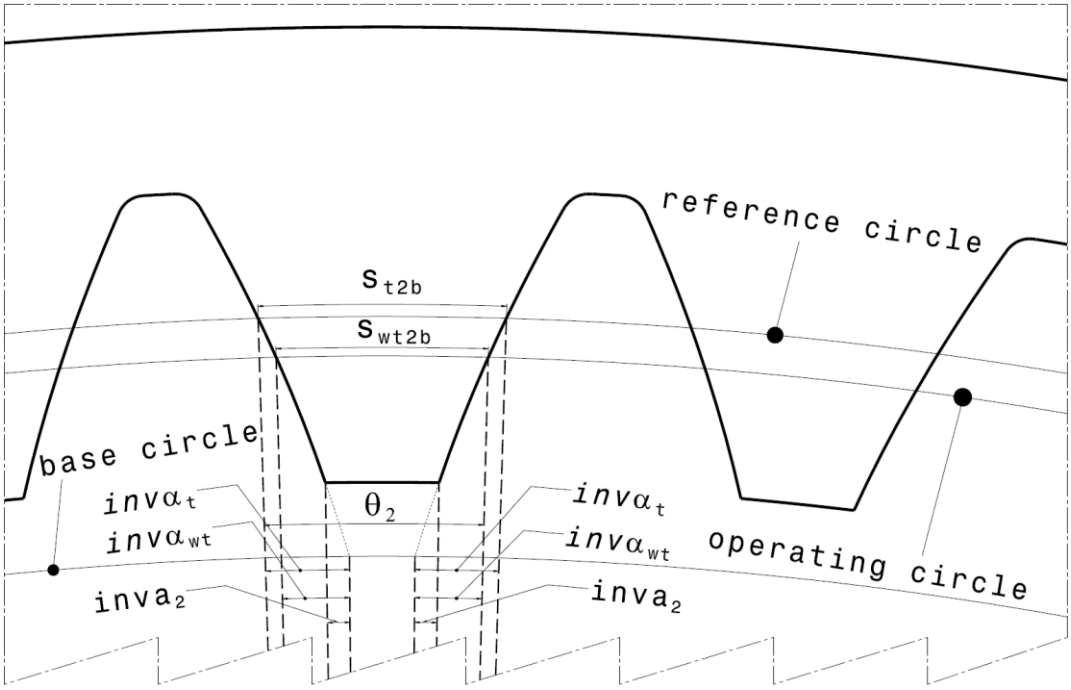

Figure 2-8 *Top land thickness evaluation of internal gear pair*

2.1.1.4. Contact Ratio Evaluation of External Gear Pairs

Tip form radius of the pinion of external gear pair is given as:

$$r_{tf1} = r_{a1} - tc \tag{2.56}$$

Tip form radius of the gear of external gear pair is given as:

$$r_{tf2} = r_{a2} - tc \tag{2.57}$$

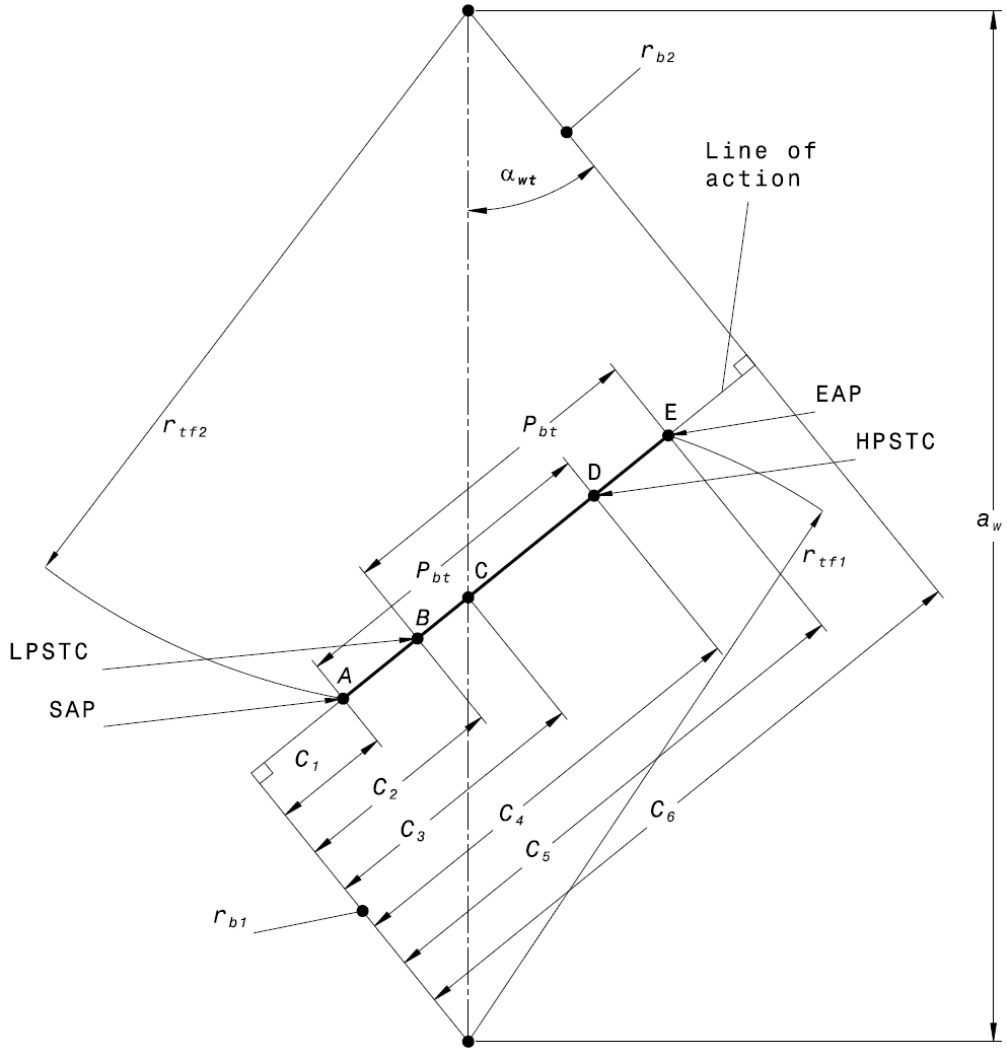

Figure 2-9 *Transverse plane view of the line of action of an external gear pair*

$$C_6 = (r_{b1} + r_{b2})tan\alpha_{wt} = a_w sin\alpha_{wt} \tag{2.58}$$

$$C_1 = C_6 - \sqrt{{r_{tf2}}^2 - {r_{b2}}^2} \tag{2.59}$$

$$C_5 = \sqrt{{r_{tf1}}^2 - {r_{b1}}^2} \tag{2.60}$$

$$C_2 = C_5 - P_{bt} \tag{2.61}$$

$$C_3 = r_{b1} tan\alpha_{wt} \tag{2.62}$$

$$C_4 = C_1 + P_{bt} \tag{2.63}$$

$$r_{SAP_1} = \sqrt{{r_{b1}}^2 + {C_1}^2} \tag{2.64}$$

$$r_{SAP_2} = \sqrt{{r_{b2}}^2 + (C_6 - C_5)^2} \tag{2.65}$$

Active length of line of action is expressed as:

$$Z = C_5 - C_1 \tag{2.66}$$

Transverse contact ratio is given as: [13]

$$m_p = \frac{Z}{P_{bt}} \tag{2.67}$$

2.1.1.5. Contact Ratio Evaluation of Internal Gear Pairs

Contact ratio evaluation of the internal gear pair is conducted as follows:

Tip form radius of the pinion of internal gear pair is given as:

$$r_{tf1} = r_{a1} - tc \tag{2.68}$$

Tip form radius of the gear of internal gear pair is given as:

$$r_{tf2} = r_{a2} + tc \tag{2.69}$$

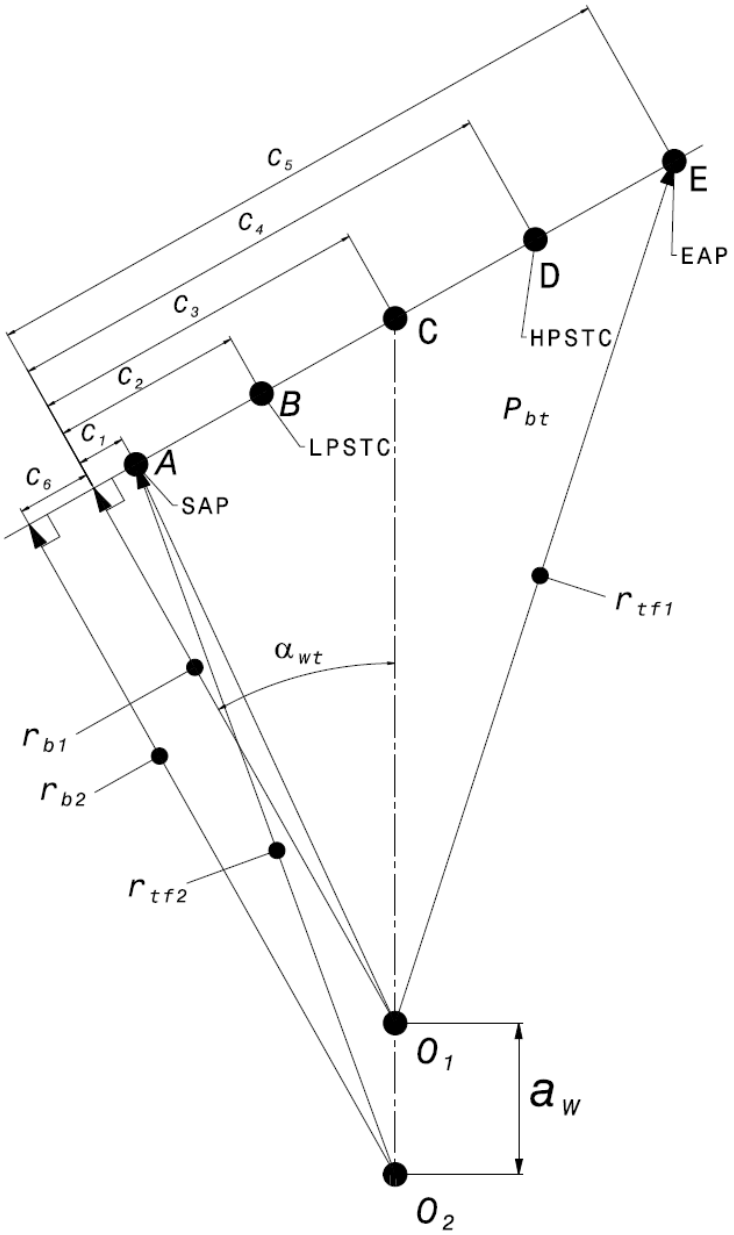

Figure 2-10 *Transverse plane view of the line of action of an internal gear pair*

$$C_6 = (r_{b2} - r_{b1})tan\alpha_{wt} = a_w sin\alpha_{wt} \tag{2.70}$$

$$C_1 = \sqrt{{r_{tf2}}^2 - {r_{b2}}^2} - C_6 \tag{2.71}$$

$$C_5 = \sqrt{{r_{tf1}}^2 - {r_{b1}}^2} \tag{2.72}$$

$$C_2 = C_5 - P_{bt} \tag{2.73}$$

$$C_3 = r_{b1} tan\alpha_{wt} \tag{2.74}$$

$$C_4 = C_1 + P_{bt} \tag{2.75}$$

Active length of line of action is expressed as:

$$Z = C_5 - C_1 \tag{2.76}$$

Transverse contact ratio is given as: [13]

$$m_p = \frac{Z}{P_{bt}} \tag{2.77}$$

2.1.1.6. Gear Root Evaluation of External Gear Pairs

Gear root evaluation of the external gear pairs is conducted in this section. Helical gears have rounded gear root in normal section. Therefore, gear root evaluation is evaluated in transverse section and then it is transmitted into the normal section. As seen from Figure 2-11,

$$\zeta_1 = \left[\frac{\left(\frac{p_t - S_{t1b}}{2}\right)}{r_1} - \left(inv\alpha_t - inv\alpha_{R_{f1t}}\right)\right] \tag{2.78}$$

$$R_{f1tx} = R_{f1t} sin\zeta_1 \tag{2.79}$$

$$R_{f1ty} = R_{f1t} cos\zeta_1 \tag{2.80}$$

Conversion of the R_{f1t} into the normal plane is given as

$$R_{f1nx} = R_{f1t} sin\zeta_1 cos\beta_{R_{f1t}} \tag{2.81}$$

$$R_{f1ny} = R_{f1t} cos\xi_1 \tag{2.82}$$

$$R_{f1n} = \sqrt{{R_{f1nx}}^2 + {R_{f1ny}}^2} \tag{2.83}$$

As seen from Figure 2-11,

$$r_{b1tx} = r_{b1} sin\left(\zeta_1 + \alpha_{R_{f1t}}\right) \tag{2.84}$$

$$r_{b1ty} = r_{b1} cos\left(\zeta_1 + \alpha_{R_{f1t}}\right) \tag{2.85}$$

Conversion into the normal section

$$r_{b1nx} = r_{b1} sin\left(\zeta_1 + \alpha_{R_{f1t}}\right) cos\beta_{rf1t} \tag{2.86}$$

$$r_{b1ny} = r_{b1} cos\left(\zeta_1 + \alpha_{R_{f1t}}\right) \tag{2.87}$$

$$r_{b1n} = \sqrt{{r_{b1nx}}^2 + {r_{b1ny}}^2} \tag{2.88}$$

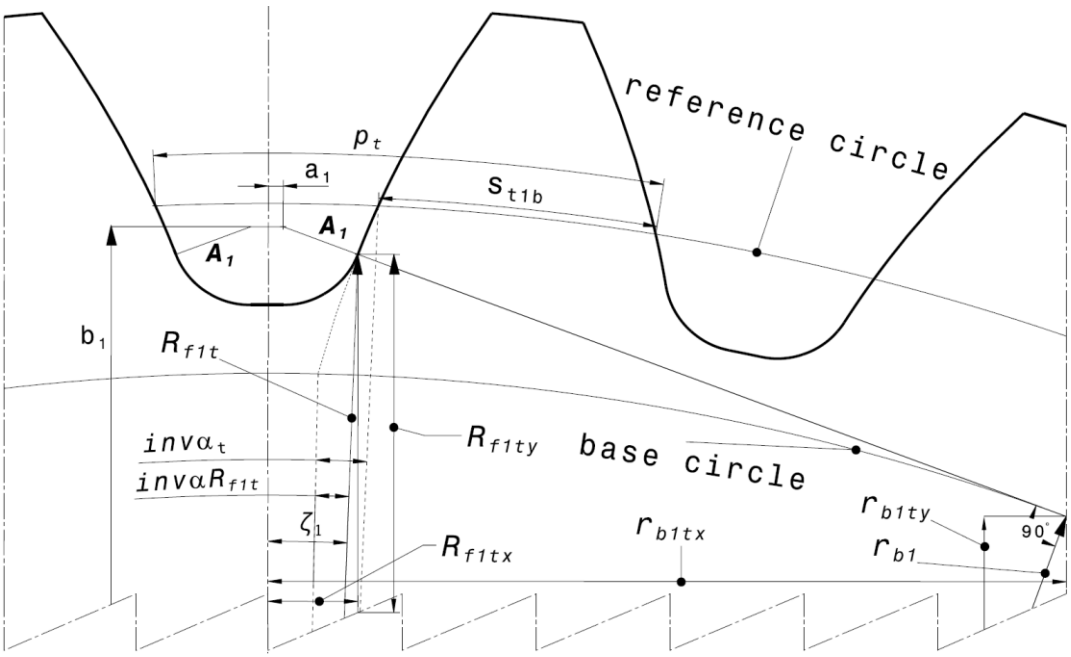

Figure 2-11 *Transverse plane view of external gear pair pinion tooth*

As seen from Figure 2-12, set of equation of the gear root is given as:

$$\theta_{x1} = arctan\left(\frac{a_1}{b_1}\right) \tag{2.89}$$

$$R_{f1ny} + A_1 cos(\theta_1 - \theta_{x1}) - b_1 = 0 \tag{2.90}$$

$$a_1 + A_1 sin(\theta_1 - \theta_{x1}) - R_{f1nx} = 0 \tag{2.91}$$

$$a_1{}^2 + b_1{}^2 - \left(r_{f1} + A_1\right)^2 = 0 \tag{2.92}$$

$$\sqrt{\left(r_{f1} + A_1\right)^2 - r_{b1n}{}^2} - A_1 - \sqrt{R_{f1n}{}^2 - r_{b1n}{}^2} = 0 \tag{2.93}$$

$A_1, \theta_1, R_{f1n}, b_1$ are unknown parameters which are to be determined by solving the nonlinear equations given above. Initial values are assigned for these unknown parameters and the set of equation is solved by using an iterative method. In this study, the gear root equations are solved by using fsolve method in MATLAB.

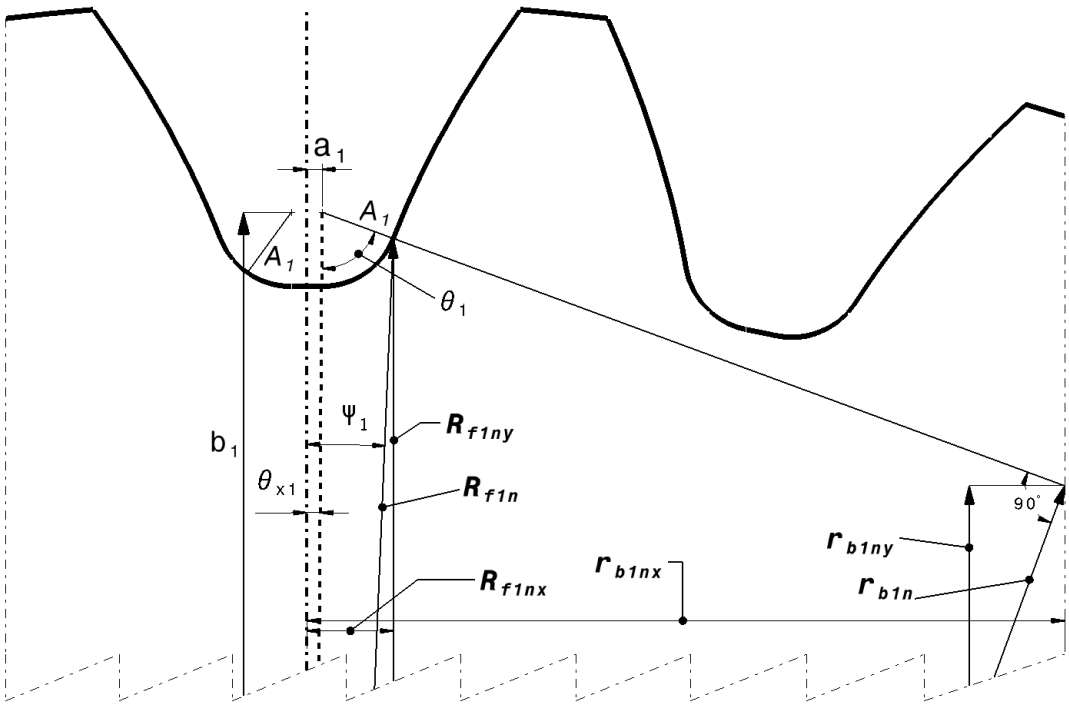

Figure 2-12 *Normal plane view of external gear pair pinion tooth*

The gear root evaluation for the external gear is conducted by using the same methodology given previously for external pinion.

2.1.1.7. Gear Root Evaluation of Internal Gear Pairs

Gear root evaluation of the internal gear pairs is conducted in this section. Gear root evaluation of the external gear pairs are given in the previous section. The same methodology given in Chapter 2.1.1.6 is used for the gear root evaluation of the pinion of internal gear pairs. Helical gears have rounded gear root in normal section. Therefore, gear root evaluation is evaluated in transverse section and then it is transmitted into the normal section. As seen from Figure 2-13,

$$\zeta_2 = \left[\frac{\left(\frac{p_t - S_{t2b}}{2}\right)}{r_2} - \left(inv\alpha_{R_{f2t}} - inv\alpha_t\right)\right] \tag{2.94}$$

$$R_{f2tx} = R_{f2t} sin\zeta_2 \tag{2.95}$$

$$R_{f2ty} = R_{f2t} cos\zeta_2 \tag{2.96}$$

Conversion of the R_{f2t} into the normal plane is given as

$$R_{f2nx} = R_{f2t} sin\zeta_2 cos\beta_{R_{f2t}} \tag{2.97}$$

$$R_{f2ny} = R_{f2t} cos\xi_2 \tag{2.98}$$

$$R_{f2n} = \sqrt{{R_{f2nx}}^2 + {R_{f2ny}}^2} \tag{2.99}$$

As seen from Figure 2-13,

$$r_{b2tx} = r_{b2} sin\left(\alpha_{R_{f2t}} - \zeta_2\right) \tag{2.100}$$

$$r_{b2ty} = r_{b2} cos\left(\alpha_{R_{f2t}} - \zeta_2\right) \tag{2.101}$$

Conversion into the normal section

$$r_{b2nx} = r_{b2} sin\left(\alpha_{R_{f2t}} - \zeta_2\right) cos\beta_{R_{f2t}} \tag{2.102}$$

$$r_{b2nx} = r_{b2} cos\left(\alpha_{R_{f2t}} - \zeta_2\right) \tag{2.103}$$

$$r_{b2n} = \sqrt{{r_{b2nx}}^2 + {r_{b2ny}}^2} \tag{2.104}$$

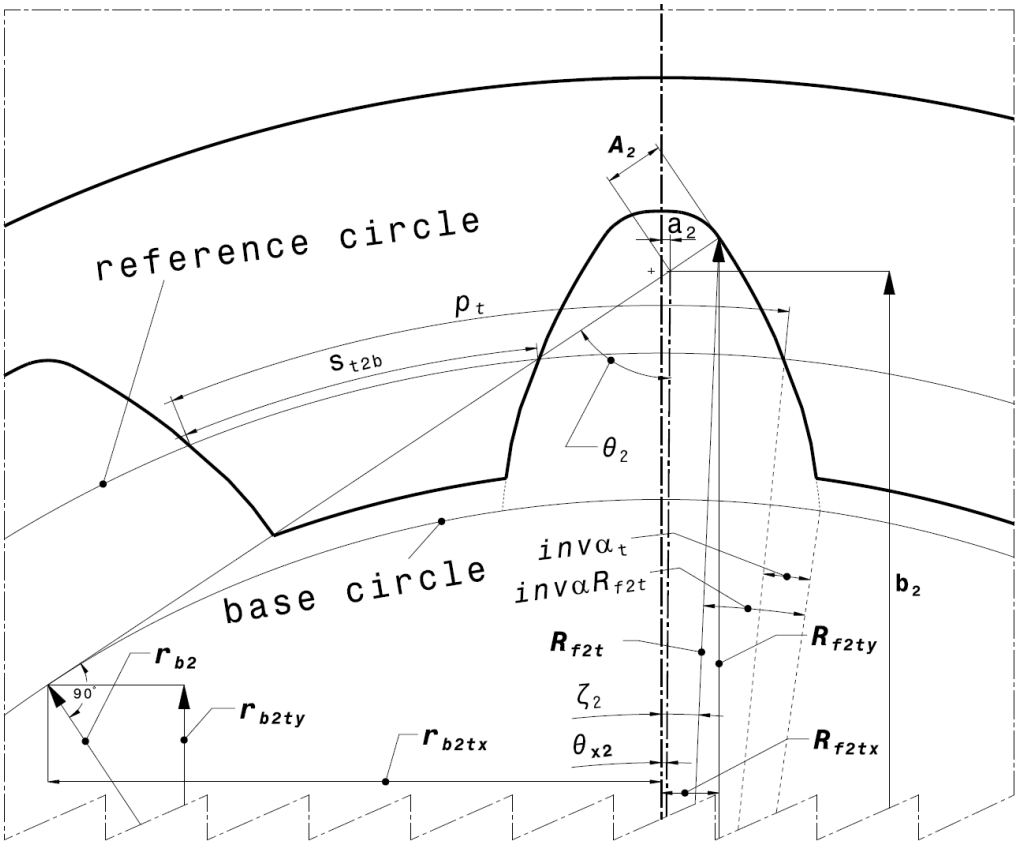

Figure 2-13 *Transverse plane view of internal gear pair gear tooth*

As seen from Figure 2-14, the set of equation of the gear root is given as:

$$\theta_{x2} = arctan\left(\frac{a_2}{b_2}\right) \tag{2.105}$$

$$R_{f2ny} - A_2 cos(\theta_2 + \theta_{x2}) - b_2 = 0 \tag{2.106}$$

$$a_2 + A_2 sin(\theta_2 + \theta_{x2}) - R_{f2nx} = 0 \tag{2.107}$$

$$a_2{}^2 + b_2{}^2 - (r_{d2} - A_2)^2 = 0 \tag{2.108}$$

$$\sqrt{\left(r_{b2n} tan\left(\frac{\pi}{2} - (\theta_2 + \theta_{x2})\right) + \frac{a_2}{sin(\theta_2 + \theta_{x2})} + A_2\right)^2 + r_{b2n}{}^2} - \sqrt{R_{f2nx}{}^2 + R_{f2ny}{}^2} = 0 \tag{2.109}$$

$A_2, \theta_2, R_{f2n}, b_2$ are unknown parameters which are to be determined by solving the nonlinear equations given above. Initial values are assigned for these unknown parameters and the set of equation is solved by using an iterative method. In this study, the gear root equations are solved by using fsolve method in MATLAB.

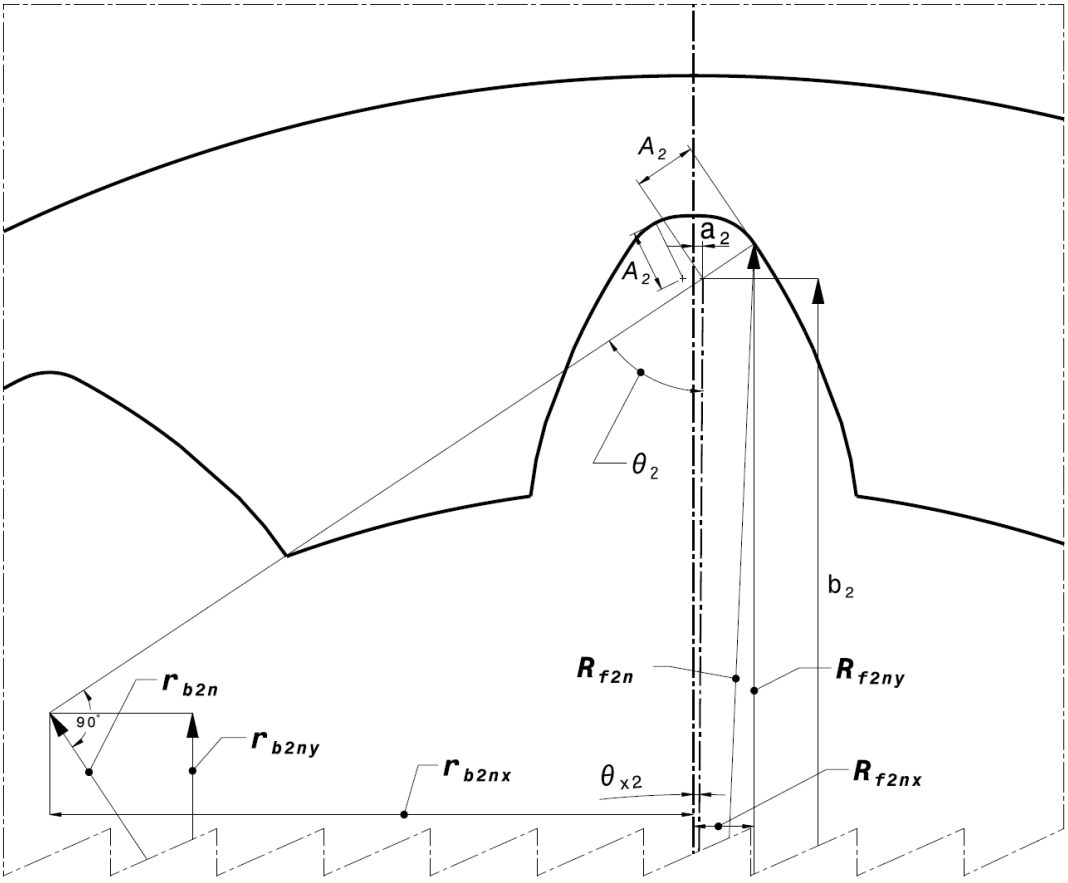

Figure 2-14 *Normal plane view of internal gear pair gear tooth*

2.1.1.8. Involute Clearance

The gear tooth should have a clearance between the starting radius of the involute and the base radius to eliminate the mounting and manufacturing errors. Root form radius which is lower than the base radius causes the undercutting of the gear root. The clearance is mathematically expressed for the pinion of external and the internal gear pairs as:

$$Ic_1 = R_{f1} - r_{b1} \tag{2.110}$$

For the gear of external gear as:

$$Ic_2 = R_{f2} - r_{b2} \tag{2.111}$$

For internal gears the clearance between the starting radius of the involute and the base radius is expressed as:

$$Ic_2 = r_{a2} - r_{b2} \tag{2.112}$$

2.1.1.9. Tiff Clearance

Clearance between the start of active profile radius and the root form radius is defined as the tiff clearance. Tiff clearance is a required clearance to satisfy the operating condition of the gear pair. The start of active profile radius which is lower than the root form radius causes the crashing of the pinion and gear teeth and the gear pair could not operate. The clearance for the pinion of the external and the internal gear pairs is mathematically expressed as:

$$Tiff_1 = r_{SAP_1} - R_{f1} \tag{2.113}$$

Tiff clearance for the gear of external gear pairs is:

$$Tiff_2 = r_{SAP_2} - R_{f2} \tag{2.114}$$

Tiff clearance for the gear of internal gear pairs is:

$$Tiff_2 = R_{f2} - r_{SAP_2} \tag{2.115}$$

2.1.2. Material Based Constraints

Material based constraints are investigated in this chapter. The material based constraints are consisted of three groups. These are conducted as follow:

Contact stress number evaluation, bending stress number evaluation and scuffing risk evaluation.

2.1.2.1. Contact Stress Number Evaluation of External Gear Pairs

The contact stress number formula for gear teeth is: [14]

$$s_c = C_p \sqrt{W_t K_o K_v K_s \frac{K_m}{d_{w1} F} \frac{C_f}{I}} \tag{2.116}$$

Contact strength geometry factor is given as: [13]

$$I = \frac{cos\alpha_t {C_\psi}^2}{\left(\frac{1}{\rho_1} \pm \frac{1}{\rho_2}\right) d_{w1} m_N} \tag{2.117}$$

Helical overlap factor, C_ψ is given as follows: [13]

For LACR helical gears ($m_F \leq 1.0$)

$$C_\psi = \left[1 - m_F \left(1 - \frac{\rho_{m1}\rho_{m2} Z}{\rho_1 \rho_2 P_{bn}}\right)\right]^{0.5} \tag{2.118}$$

Radius of curvature of the pinion profile at the mean radius of the pinion, ρ_{m1}

$$\rho_{m1} = (R_{m1} - r_{b1})^{0.5} \tag{2.119}$$

Radius of curvature of the gear profile at the mean radius of the gear, ρ_{m2}

$$\rho_{m2} = C_6 \mp \rho_{m1} \tag{2.120}$$

For spurs and conventional helical gears ($m_F > 1.0$)

$$C_\psi = 1.0 \tag{2.121}$$

Load sharing ratio, m_n is given as follows:

For helical gears:

$$m_N = \frac{F}{L_{min}} \tag{2.122}$$

For spur gears with $m_P < 2.0$, gives $L_{min} = F$, therefore:

$$m_N = 1.0 \tag{2.123}$$

For LACR helicals, ($m_F \leq 1.0$), load sharing is accommodated by C_ψ, therefore load sharing factor is taken as unity.

Face width ratio is given in Table 2.2 according to gear mounting relative to bearings.

Table 2.2 *Maximum Face width Ratio [15]*

Type of Gear	*Face width ratio, $c = b/d_1$* *Gear mounting relative to bearings*		
	Symmetric	Asymmetric	Overhung
Spur and Single Helical	< 1.6	< 1.2	< 0.8
1. Hardness < 180 HB	< 1.4	< 1.1	< 0.7
2. Hardness > 180 HB	< 1.1	< 0.9	< 0.6
3. Induction hardened, case carburised	< 0.8	< 0.6	< 0.5
4. Nitrided			
Spur and Single Helical, with lead correction			
5. Case carburised	< 1.4	< 1.2	
6. Nitrided	< 1.2	< 1.0	
Double Helical Gears			
7. Induction hardened, case carburised	< 2.0	< 1.6	
8. Nitrided	< 1.4	< 1.1	

In the current study face width ratio is taken as ‘’0.7’’. Therefore, the face width ratio considered in this study is applicable for spur and helical gears which are induction hardened or case carburized with lead correction or without lead correction. The face width is given as:

$$F = 0.7 \cdot m_t \cdot N_1 \tag{2.124}$$

Axial contact ratio is given as:

$$m_F = \frac{F}{P_x} \tag{2.125}$$

where axial pitch, P_x , is

$$P_x = \frac{\pi}{sin\beta} \tag{2.126}$$

Minimum length of the lines of contact is given as follows:

For spur gears with $m_P < 2.0$ the minimum length of contact lines, L_{min} , is

$$L_{min} = F \tag{2.127}$$

For helical gears, two cases must be considered:

Case I, for $n_a \leq 1 - n_r$

$$L_{min} = \frac{m_P F - n_a n_r P_x}{cos\beta_b} \tag{2.128}$$

Case II, for $n_a > 1 - n_r$

$$L_{min} = \frac{m_P F - (1 - n_a)(1 - n_r) P_x}{cos\beta_b} \tag{2.129}$$

where n_r is the fractional part of m_P and n_a is the fractional part of m_F.

Normal base pitch is given as:

$$P_{bn} = \pi m_n cos\alpha_n \tag{2.130}$$

Transverse base pitch

$$P_{bt} = \frac{2\pi r_{b1t}}{z_1} \tag{2.131}$$

Base helix angle

$$\beta_b = arccos\left(\frac{P_{bn}}{P_{bt}}\right) \tag{2.132}$$

Radii of curvature of profiles at stress calculation point are given as follows:

For conventional helical gears ($m_F > 1.0$) the radii of curvature are calculated at the mean radius or middle of the working profile of the pinion where:

Mean radius of pinion, R_{m1}

$$R_{m1} = \frac{1}{2}[r_{a1} \pm (a_w - r_{a2})] \tag{2.133}$$

Radius of curvature of the pinion profile at the point of contact stress calculation, ρ_1

$$\rho_1 = \sqrt{{R_{m1}}^2 - {r_{b1}}^2} \tag{2.134}$$

Radius of curvature of the gear profile at the point of contact stress calculation, ρ_2

$$\rho_2 = C_6 \mp \rho_1 \tag{2.135}$$

For spurs and LACR helical gears ($m_F \leq 1.0$) the radii of curvature are calculated at the LPSTC

$$\rho_1 = C_2 \tag{2.136}$$

$$\rho_2 = C_6 \mp \rho_1 \tag{2.137}$$

2.1.2.2. Bending Strength Geometry Factor and Bending Stress Number Evaluation

The fundamental formula for bending stress number is given in [14]

$$s_t = W_t K_o K_v K_s \frac{P_d}{F} \frac{K_m K_B}{J} \tag{2.138}$$

Bending stress geometry factor is evaluated as follows:

Bending stress geometry factor is given as: [13]

$$J = \frac{Y C_\psi}{K_f m_N} \tag{2.139}$$

Tooth form factor is given in [13].

$$Y = \frac{K_{\psi}}{\frac{cos\alpha_{nL}}{cos\alpha_{w}}\left[\frac{6h_f}{{S_F}^2 C_h} - \frac{tan\alpha_{nL}}{S_F}\right] m_n} \tag{2.140}$$

Helical factor is given as follows: [13]

For Spur and LACR Helical Gears ($m_F \leq 1.0$), a unity value is used,

$$C_h = 1.0 \tag{2.141}$$

For Conventional Helical Gears, when $m_F > 1.0$

$$C_h = \frac{1}{1 - \left[\frac{w}{100}\left(1 - \frac{w}{100}\right)\right]^{0.5}} \tag{2.142}$$

$$w = arctan(tan\beta sin\alpha_n) \tag{2.143}$$

The helix angle factor given in [13] depends on the type of gear. For Spur and LACR Helical Gears ($m_F \leq 1.0$), a unity value is used. For Conventional Helical Gears, when $m_F > 1.0$

$$K_{\psi} = cos\beta_w cos\beta \tag{2.144}$$

Stress correction factor for the pinion is given as:

$$K_{f1} = H + \left(\frac{S_{F1}}{A_{1v}}\right)^L \left(\frac{S_{F1}}{h_{f1}}\right)^M \tag{2.145}$$

Similarly for the gear

$$K_{f2} = H + \left(\frac{S_{F2}}{A_{2v}}\right)^L \left(\frac{S_{F2}}{h_{f2}}\right)^M \tag{2.146}$$

where $H = 0.331 - 0.436\alpha_n \quad L = 0.324 - 0.492\alpha_n \quad M = 0.261 + 0.545\alpha_n$

2.1.2.2.1. Virtual Spur Gear Evaluation

Helical gears are considered as virtual spur gears with the following virtual geometry while for the spur gear the actual geometry is used. The following geometrical relations given in Table 2.3 are used for virtual gear root evaluation.

Table 2.3 *Basic geometric relations of virtual gear*

Virtual tooth number of the pinion [13]	$z_{1v} = \frac{z_1}{cos^3\beta}$	(2.147)
Virtual tooth number of the gear [13]	$z_{2v} = \frac{z_2}{cos^3\beta}$	(2.148)
Virtual reference radius of the pinion [13]	$r_{1v} = m_n \frac{z_{1v}}{2}$	(2.149)
Virtual reference radius of the gear [13]	$r_{2v} = m_n \frac{z_{2v}}{2}$	(2.150)
Virtual base radius of the pinion [13]	$r_{b1v} = r_{1v} cos\alpha_n$	(2.151)
Virtual base radius of the gear [13]	$r_{b2v} = r_{2v} cos\alpha_n$	(2.152)
Virtual outside radius of the pinion [13]	$r_{a1v} = r_{1v} + r_{a1} - r_1$	(2.153)
Virtual outside radius of the gear [13]	$r_{a2v} = r_{2v} + r_{a2} - r_2$	(2.154)
Virtual root radius of the pinion [13]	$r_{f1v} = r_{1v} - r_1 + r_{f1}$	(2.155)
Virtual root radius of the gear [13]	$r_{f2v} = r_{2v} - r_2 + r_{f2}$	(2.156)

Tip form radii of the pinion and the gear can be expressed in a similar way used in evaluating the outside radii. Virtual tip form radius of the pinion:

$$r_{tf1v} = r_{1v} + r_{tf1} - r_1 \tag{2.157}$$

Virtual tip form radius of the gear:

$$r_{tf2v} = r_{2v} + r_{tf2} - r_2 \tag{2.158}$$

Sixth distance along line of action of virtual spur gear is:

$$C_{6v} = (r_{b2v} \pm r_{b1v}) tan\alpha_{wn} \tag{2.159}$$

First distance along line of action of virtual spur gear is:

$$C_{1v} = \pm\left[C_{6v} - \left({r_{tf2v}}^2 - {r_{b2v}}^2\right)^{0.5}\right] \tag{2.160}$$

Fourth distance along line of action of virtual spur gear is:

$$C_{4v} = C_{1v} + P_{bn} \tag{2.161}$$

2.1.2.2.2. Load Angle and Load Radius for External Gear Pairs

For helical gears and spur gears that are analyzed where the load is applied at the tip of the tooth, the pressure angle at load application point for the pinion is given in [13].

$$tan\alpha_{nW1} = \left[\left(\frac{r_{tf1v}}{r_{b1v}}\right)^2 - 1\right]^{0.5} \tag{2.162}$$

For spur gears, where the highest bending stress occurs when the load is at the highest point of single tooth contact (HPSTC), the pressure angle for the pinion is given in [13].

$$tan\alpha_{nW1} = \frac{C_4}{r_{b1v}} \tag{2.163}$$

Equation (2.163) may also be used for LACR helical gears ($m_F \leq 1.0$), but distance C_4 must be based on the virtual spur gear.

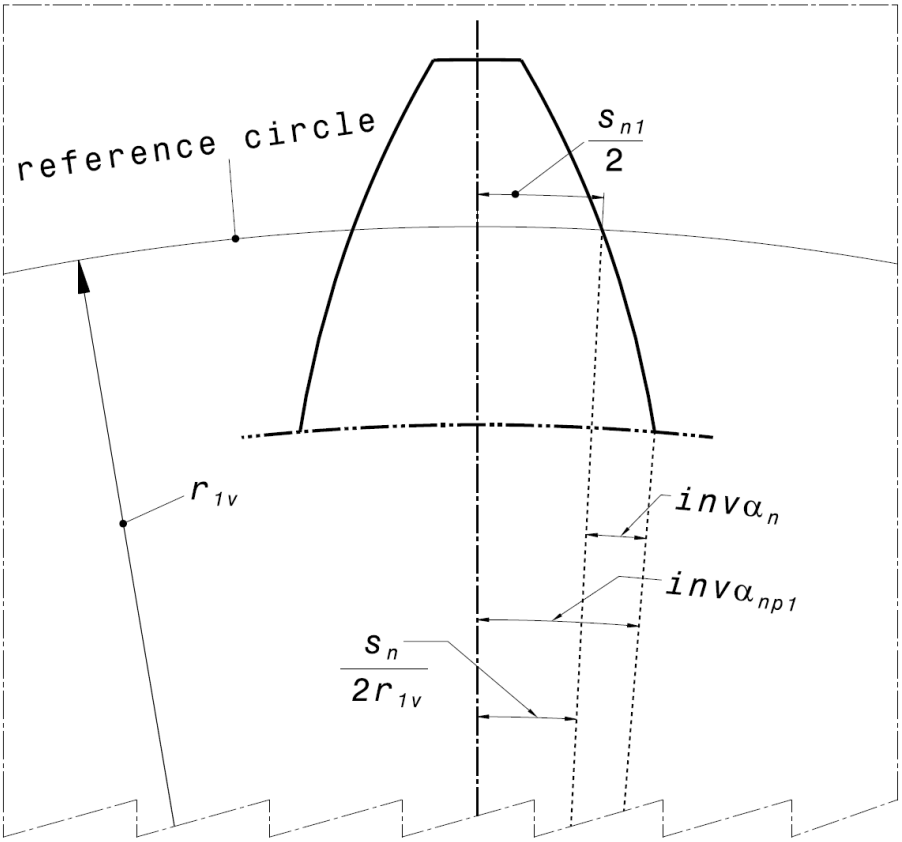

Figure 2-15 *Pressure angle where external gear tooth comes to point*

As seen from Figure 2-15.

$$inv\alpha_{np1} = inv\alpha_n + \frac{s_{n1}}{2r_{1v}} \tag{2.164}$$

$$inv\alpha_n = tan\alpha_n - \alpha_n \tag{2.165}$$

By subs.

$$inv\alpha_{np1} = tan\alpha_n - \alpha_n + \frac{s_{n1}}{2r_{1v}} \tag{2.166}$$

As seen from Figure 2-16,

$$\alpha_{nL1} = tan\alpha_{nw1} - inv\alpha_{np1} \tag{2.167}$$

$$\alpha_{nL1} = tan\alpha_{nw1} - tan\alpha_n + \alpha_n - \frac{s_{n1}}{2r_{1v}} \tag{2.168}$$

$$r_{nL1} = \frac{r_{b1v}}{cos\alpha_{nL1}} \tag{2.169}$$

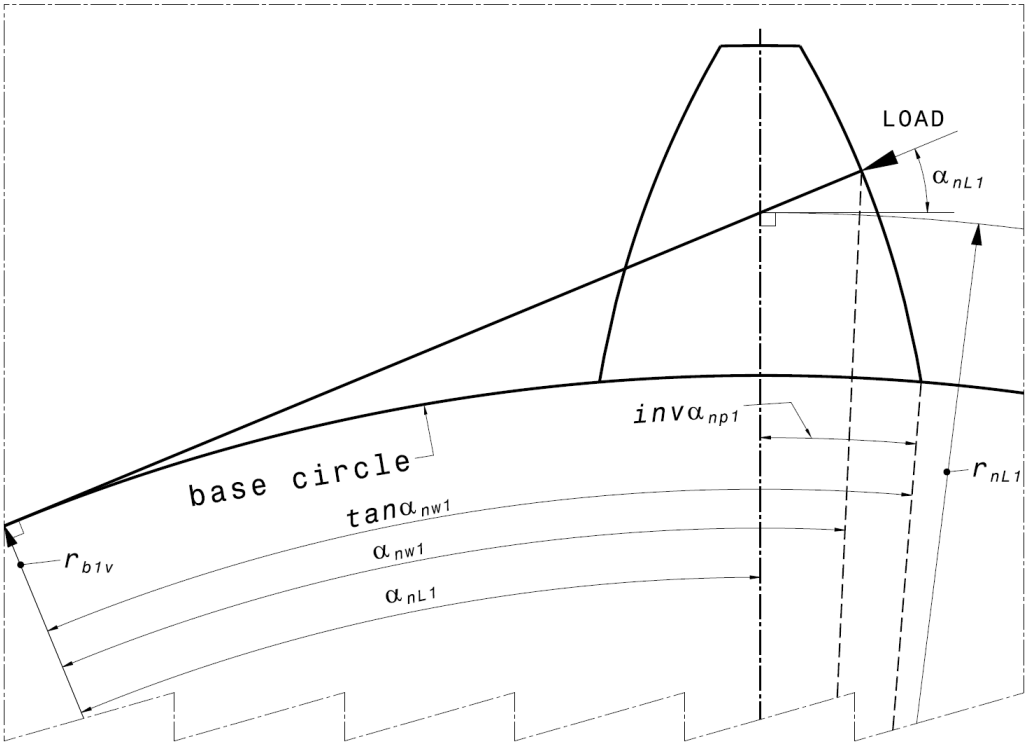

Figure 2-16 *Load angle and load radius of an external gear*

2.1.2.2.3. Virtual Gear Root Evaluation for External Gear Pairs

Virtual gear root evaluation is outlined in this chapter. As seen from Figure 2-17,

$$R_{f1v} = \sqrt{\left(\sqrt{\left(r_{f1v} + A_{1v}\right)^2 - {r_{b1v}}^2} - A_{1v}\right)^2 + {r_{b1v}}^2} \tag{2.170}$$

$$\gamma_{1v} = arccos\left(\frac{r_{b1v}}{r_{f1v} + A_{1v}}\right) \tag{2.171}$$

$$\alpha_{R_{f1v}} = arccos\left(\frac{r_{b1v}}{R_{f1v}}\right) \tag{2.172}$$

$$inv\alpha_{R_{f1v}} = tan\alpha_{R_{f1v}} - \alpha_{R_{f1v}} \tag{2.173}$$

$$\theta_{1v} = arcsin\left(\frac{r_{b1v}}{r_{f1v} + A_{1v}}\right) \tag{2.174}$$

$$b_{1v} = \left(r_{f1v} + A_{1v}\right)cos\left(\theta_{p1v} - \left(inv\alpha_n - inv\alpha_{R_{f1v}}\right) - \left(\gamma_{1v} - \alpha_{R_{f1v}}\right)\right) \tag{2.175}$$

$$\theta_{x1v} = arctan\left(\frac{a_{1v}}{b_{1v}}\right) \tag{2.176}$$

$$\theta_{p1v} = \frac{(p_n - s_{n1b})}{2r_{1v}} \tag{2.177}$$

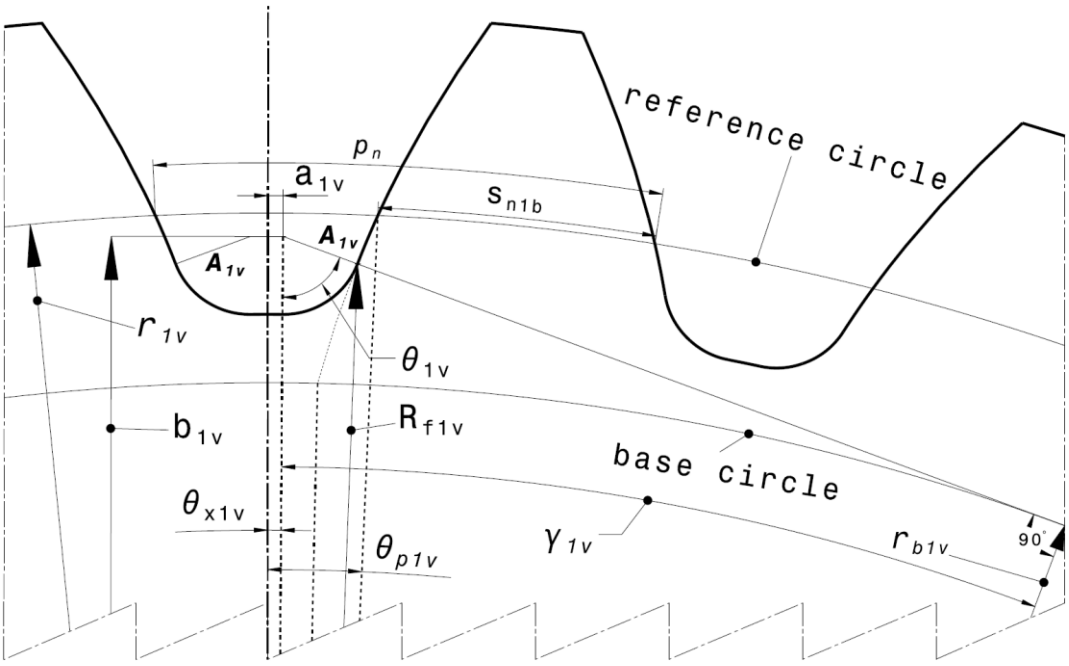

Figure 2-17 *Normal plane view of virtual spur gear*

The eqution of the virtual gear root of the pinion is expressed as:

$$a_{1v} + A_{1v}sin(\theta_{1v} - \theta_{x1v}) - R_{f1v}sin\left(\theta_{p1v} - \left(inv\alpha_n - inv\alpha_{R_{f1v}}\right)\right) = 0 \quad (2.178)$$

This nonlinear equation is solved by implementing an iterative method. The equation is solved by using fsolve in MATLAB in this study. The virtual gear root evaluation of the gear of external gear pair is conducted by using the same methodology which is outlined in the current section.

2.1.2.2.4. Critical Section Determination for External Gear Pairs

The related equations for evaluation of the critical section are outlined in this section. As seen from Figure 2-18,

$$\alpha_{crv1} = \arctan\left(\frac{a_{1v}}{b_{1v}}\right) + arccos\left(\frac{{a_{1v}}^2 + {b_{1v}}^2 + {r_{crv1}}^2 - {A_{1v}}^2}{2r_{crv1}\sqrt{{a_{1v}}^2 + {b_{1v}}^2}}\right) \quad (2.179)$$

$$L_{hv1} = \frac{r_{b1v}}{\cos(\alpha_{nL1})} \quad (2.180)$$

$$h_{f1} = L_{hv1} - r_{crv1}cos\left(\frac{\pi}{z_{1v}} - \alpha_{crv1}\right) \quad (2.181)$$

$$S_{F1} = 2r_{crv1}sin\left(\frac{\pi}{z_{1v}} - \alpha_{crv1}\right) \quad (2.182)$$

Similarly for virtual gear root

$$\alpha_{crv2} = \arctan\left(\frac{a_{2v}}{b_{2v}}\right) + arccos\left(\frac{{a_{2v}}^2 + {b_{2v}}^2 + {r_{crv2}}^2 - {A_{2v}}^2}{2r_{crv2}\sqrt{{a_{2v}}^2 + {b_{2v}}^2}}\right) \quad (2.183)$$

$$h_{f2} = L_{hv2} - r_{crv2}cos\left(\frac{\pi}{z_{2v}} - \alpha_{crv2}\right) \quad (2.184)$$

$$S_{F2} = 2r_{crv2}sin\left(\frac{\pi}{z_{2v}} - \alpha_{crv2}\right) \quad (2.185)$$

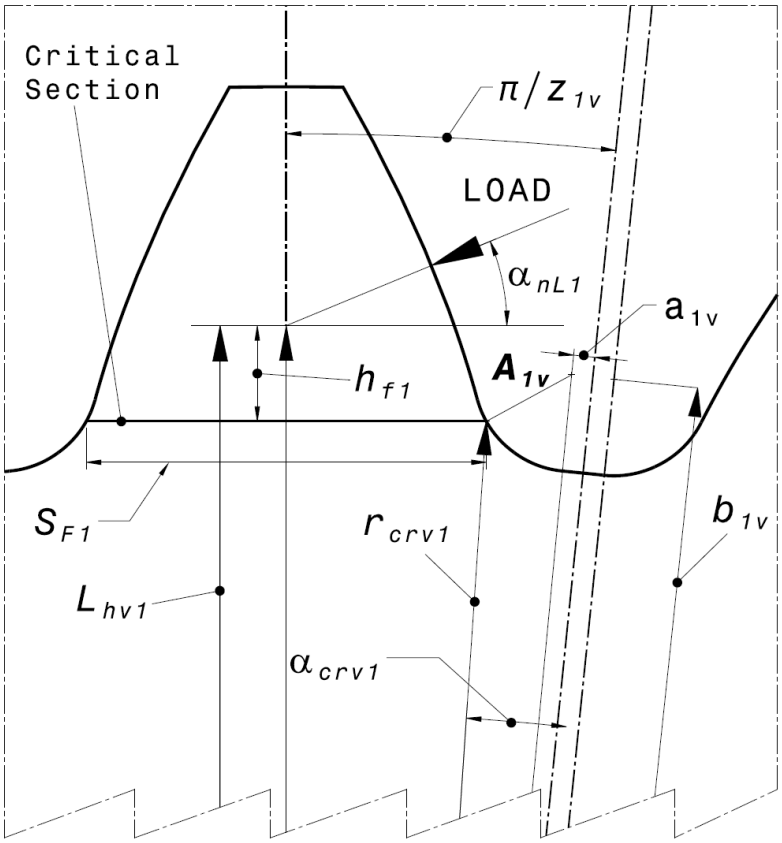

Figure 2-18 *Critical section evaluation of virtual spur gear*

2.1.2.2.5. Evaluation of the Critical Radius for External Gear Pairs

Critical radius is determined by using the following methodology outlined in this section.

Table 2.4 *Critical radius algorithm for the pinion*

$$\boldsymbol{for\ i = 1{:}50}$$

$$r_{crv1}(1) = r_{f1v}$$

$$r_{crv1}(i+1) = r_{crv1}(i) + \frac{\left(R_{f1v} - r_{f1v}\right)}{itr}$$

$$\boldsymbol{end}$$

The same algorithm given in Table 2.4 is used to evaluate the critical radius of the gear. The consisted radii are substituted into the formulas of α_{crv1}, h_{f1} and S_{F1}. Then, the related Y_1, K_{f1} values are obtained for each different α_{crv1}, h_{f1} and S_{F1}. For each different Y_1, K_{f1} values, the different geometry factor values of the pinion (J_1) are evaluated. Mathematically it is expressed as:

Table 2.5 *Algorithm of bending strength geometry factor for the pinion*

$$\boldsymbol{for\ i = 1{:}50}$$

$$\alpha_{crv1}(i) = \arctan\left(\frac{a_{1v}}{b_{1v}}\right) + arccos\left(\frac{{a_{1v}}^2 + {b_{1v}}^2 + \left(r_{crv1}(i)\right)^2 - {A_{1v}}^2}{2r_{crv1}(i)\sqrt{{a_{1v}}^2 + {b_{1v}}^2}}\right)$$

$$h_{f1}(i) = L_{hv1} - r_{crv1}(i)cos\left(\frac{\pi}{z_{1v}} - \alpha_{crv1}(i)\right)$$

$$Y_1(i) = \frac{K_\psi}{\frac{cos\alpha_{nL1}}{cos\alpha_{w1}}\left[\frac{6h_{f1}(i)}{\left(S_{F1}(i)\right)^2 C_h} - \frac{tan\alpha_{nL1}}{S_{F1}(i)}\right]}$$

$$S_{F1}(i) = 2r_{crv1}(i)sin\left(\frac{\pi}{z_{1v}} - \alpha_{crv1}(i)\right)$$

$$Y_1(i) = \frac{K_\psi}{\frac{cos\alpha_{nL1}}{cos\alpha_{w1}}\left[\frac{6h_{f1}(i)}{\left(S_{F1}(i)\right)^2 C_h} - \frac{tan\alpha_{nL1}}{S_{F1}(i)}\right]}$$

$$K_{f1}(i) = H + \left(\frac{S_{F1}(i)}{A_{1v}}\right)^L \left(\frac{S_{F1}(i)}{h_{f1}(i)}\right)^M$$

$$J_1(i) = \frac{Y_1(i)C_\psi}{K_{f1}(i)m_N}$$

$$\boldsymbol{end}$$

The same algorithm given in Table 2.5 is used for the bending stress calculation of the gear.The minimum ones of the J_1 and J_2 are taken as the geometry factor and implemented into the bending stress equation.

2.1.2.2.6. Load Angle and Load Radius for Internal Gear Pairs

The pressure angle at load application point for the pinion is given by:

$$tan\alpha_{nW1} = \left[\left(\frac{r_{tf1v}}{r_{b1v}}\right)^2 - 1\right]^{0.5} \tag{2.186}$$

The pressure angle at load application for the gear is given by:

$$tan\alpha_{nW2} = \left[\left(\frac{r_{tf2v}}{r_{b2v}}\right)^2 - 1\right]^{0.5} \tag{2.187}$$

For spur gears, where the highest bending stress occurs when the load is at the highest point of single tooth contact (HPSTC), the pressure angle for the pinion is given by:

$$tan\alpha_{nW1} = \frac{C_4}{r_{b1v}} \tag{2.188}$$

Pressure angle for the gear is given by:

$$tan\alpha_{nW2} = \frac{C_4}{r_{b2v}} \tag{2.189}$$

Equation (2.188) and equation (2.189) May also be used for LACR helical gears $(m_F \leq 1.0)$, but distance C_4 must be based on the virtual spur gear.

The pressure angle for the pinion is:

$$tan\alpha_{nW1} = \frac{C_{4v}}{r_{b1v}} \tag{2.190}$$

The pressure angle for the gear is:

$$tan\alpha_{nW2} = \frac{C_{4v}}{r_{b2v}} \tag{2.191}$$

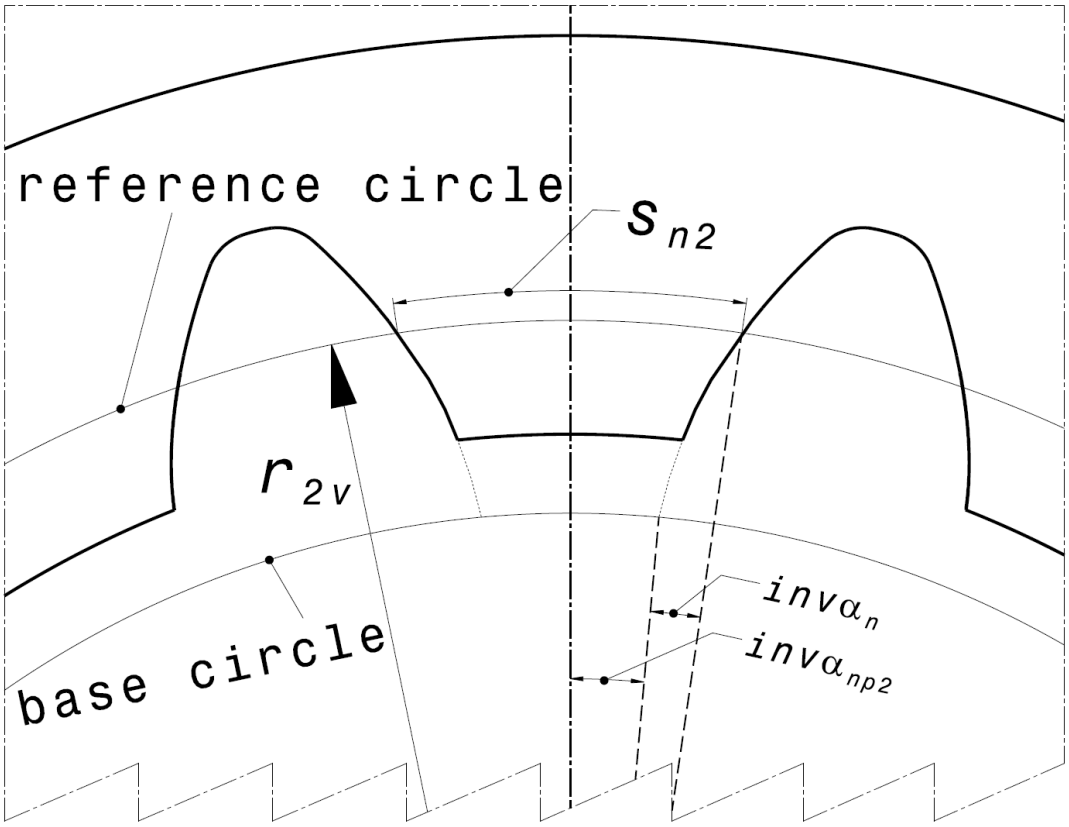

Figure 2-19 *Pressure angle where internal gear tooth comes to point*

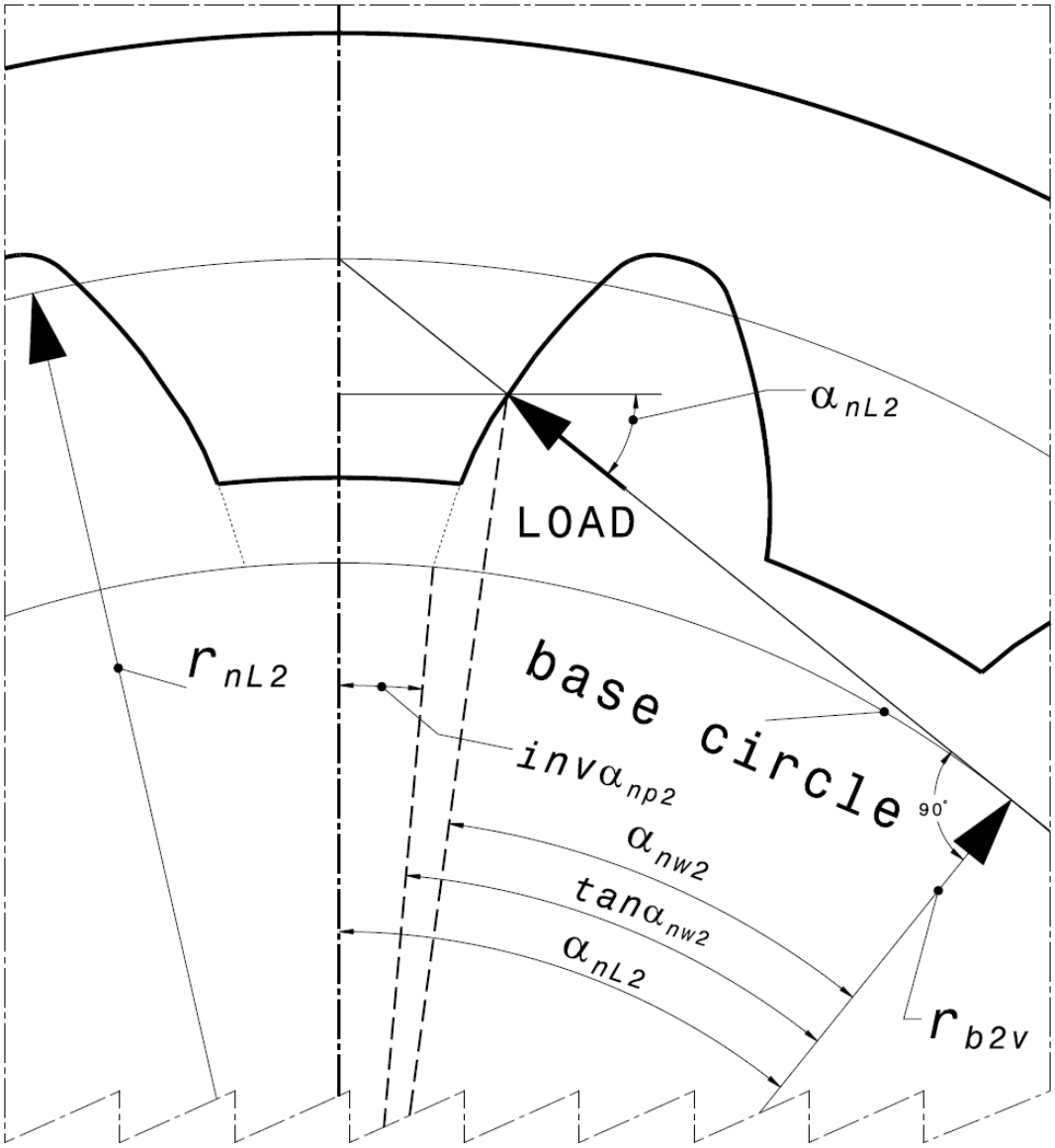

Figure 2-20 *Load angle and load radius of an internal gear*

As seen from Figure 2-19,

$$inv\alpha_{np2} = \frac{s_{n2}}{2r_{2v}} - inv\alpha_n \tag{2.192}$$

$$inv\alpha_n = tan\alpha_n - \alpha_n \tag{2.193}$$

By subs.

$$inv\alpha_{np2} = \frac{s_{n2}}{2r_{2v}} - tan\alpha_n + \alpha_n \tag{2.194}$$

$$\alpha_{nL2} = tan\alpha_{nw2} + inv\alpha_{np2} \tag{2.195}$$

$$\alpha_{nL2} = tan\alpha_{nw2} - tan\alpha_n + \alpha_n + \frac{s_{n2}}{2r_{2v}} \tag{2.196}$$

$$r_{nL2} = \frac{r_{b2v}}{cos\alpha_{nL2}} \tag{2.197}$$

2.1.2.2.7. Virtual Gear Root Evaluation for Internal Gear Pairs

Virtual gear root evaluation of the internal gears is outlined in this chapter. The following equations are derived from Figure 2-21.

$$R_{f2v} = \sqrt{\left(\sqrt{\left(r_{f2v} - A_{2v}\right)^2 - {r_{b2v}}^2} + A_{2v}\right)^2 + {r_{b2v}}^2} \tag{2.198}$$

$$\gamma_{2v} = arccos\left(\frac{r_{b2v}}{r_{f2v} - A_{2v}}\right) \tag{2.199}$$

$$\alpha_{R_{f2v}} = arccos\left(\frac{r_{b2v}}{R_{f2v}}\right) \tag{2.200}$$

$$inv\alpha_{R_{f2v}} = tan\alpha_{R_{f2v}} - \alpha_{R_{f2v}} \tag{2.201}$$

$$\theta_{2v} = arcsin\left(\frac{r_{b2v}}{r_{f2v} - A_{2v}}\right) \tag{2.202}$$

$$b_{2v} = \left(r_{f2v} - A_{2v}\right)cos\left(\theta_{p2v} - \left(inv\alpha_{R_{f2v}} - inv\alpha_n\right) - \left(\alpha_{R_{f2v}} - \gamma_{2v}\right)\right) \tag{2.203}$$

$$\theta_{x2v} = arctan\left(\frac{a_{2v}}{b_{2v}}\right) \tag{2.204}$$

The equation of the virtual gear root of the gear is expressed as:

$$a_{2v} + A_{2v}sin(\theta_{2v} + \theta_{x2v}) - R_{f2v}sin\left(\theta_{p2v} - \left(inv\alpha_{R_{f2v}} - inv\alpha_n\right)\right) = 0 \tag{2.205}$$

This nonlinear equation is solved by implementing an iterative method. The equation is solved by using fsolve in MATLAB in this study.

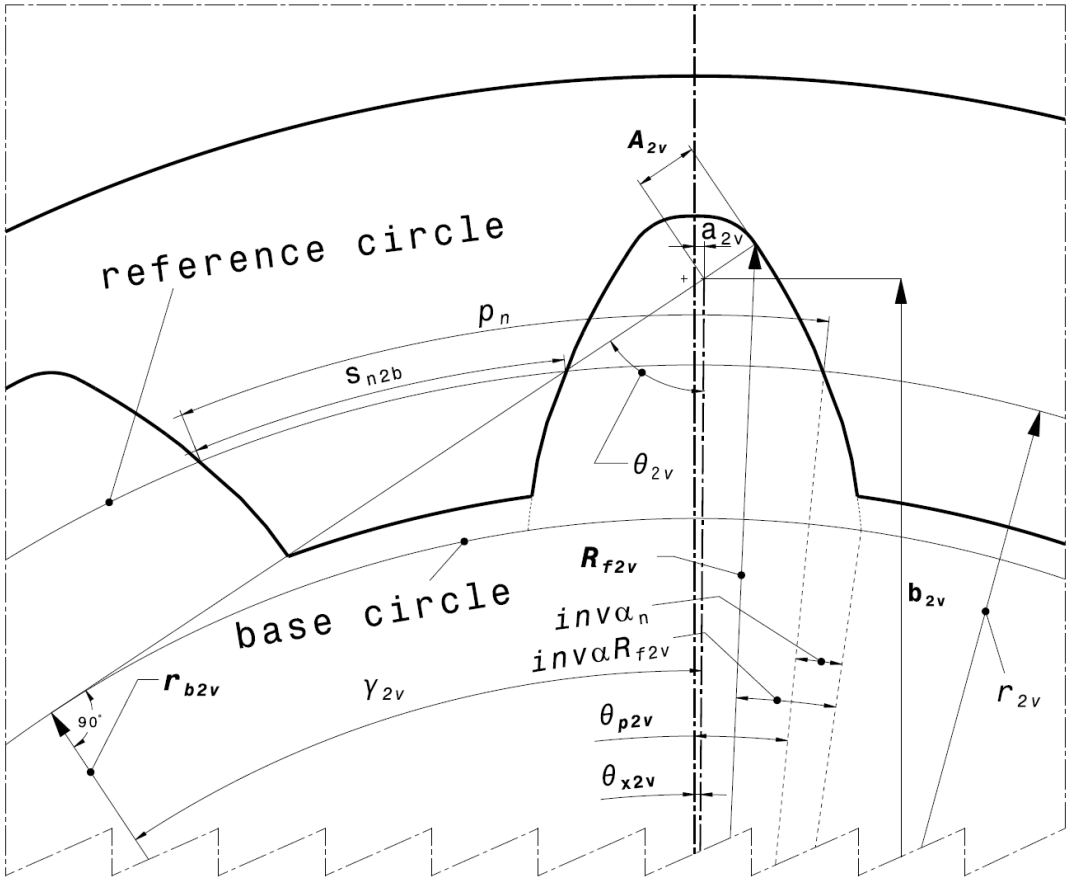

Figure 2-21 *Normal plane view of virtual spur gear*

2.1.2.2.8. Critical Section Determination for Internal Gear Pairs

The related equations for critical section evaluation of internal gear are outlined in this chapter. As seen from Figure 2-22,

$$\alpha_{crv2} = \arctan\left(\frac{a_{2v}}{b_{2v}}\right) + arccos\left(\frac{{a_{2v}}^2 + {b_{2v}}^2 + {r_{crv2}}^2 - {A_{2v}}^2}{2r_{crv2}\sqrt{{a_{2v}}^2 + {b_{2v}}^2}}\right) \quad (2.206)$$

$$L_{hv2} = \frac{r_{b2v}}{\cos(\alpha_{nL2})} \quad (2.207)$$

$$h_{f2} = r_{crv2}cos\left(\frac{\pi}{z_{2v}} - \alpha_{crv2}\right) - L_{hv2} \quad (2.208)$$

$$S_{F2} = 2r_{crv1} sin\left(\frac{\pi}{z_{2v}} - \alpha_{crv2}\right) \tag{2.209}$$

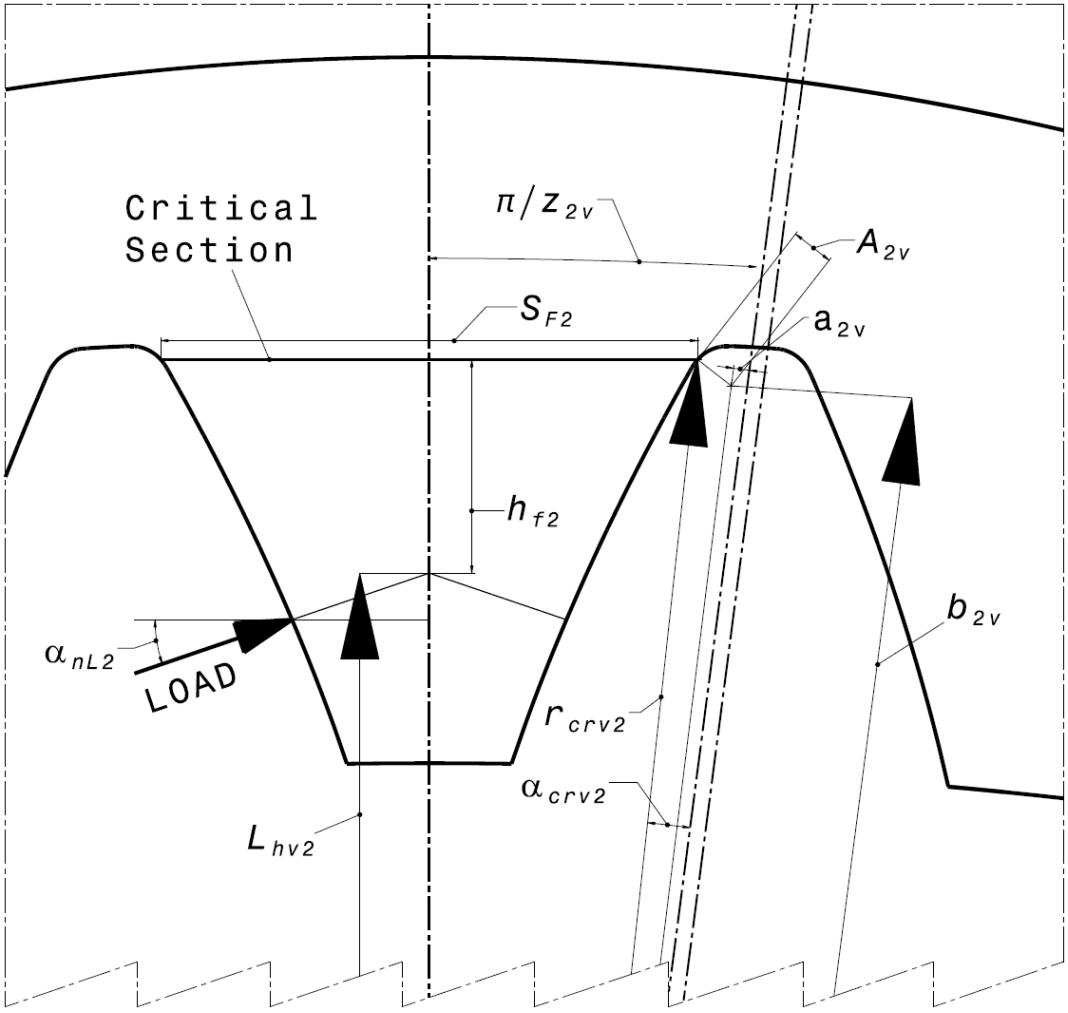

Figure 2-22 *Critical section evaluation of virtual spur gear*

2.1.2.2.9. Evaluation of the Critical Radius for Internal Gear Pairs

Evaluation of critical radius for internal gear is outlined in this section.

$$r_{crv2}(1) = R_{f2v} \tag{2.210}$$

$$r_{crv2}(i+1) = r_{crv2}(i) + \frac{\left(r_{f2v} - R_{f2v}\right)}{itr} \tag{2.211}$$

The consisted radii are substituted into the formulas of α_{crv2}, h_{f2} and S_{F2}. Then, the related Y_2, K_{f2} values are obtained for each different α_{crv2}, h_{f2} and S_{F2}. For each different Y_2, K_{f2} values, the different geometry factor values of the pinion (J_2) are evaluated. Mathematically it is expressed as:

for i = 1: itr

$$\alpha_{crv2}(i) = \arctan\left(\frac{a_{2v}}{b_{2v}}\right) + arccos\left(\frac{{a_{2v}}^2 + {b_{2v}}^2 + \left(r_{crv2}(i)\right)^2 - {A_{2v}}^2}{2r_{crv2}(i)\sqrt{{a_{2v}}^2 + {b_{2v}}^2}}\right)$$

$$h_{f2}(i) = r_{crv2}(i)cos\left(\frac{\pi}{z_{2v}} - \alpha_{crv2}(i)\right) - L_{hv2}$$

$$S_{F2}(i) = 2r_{crv2}(i)sin\left(\frac{\pi}{z_{2v}} - \alpha_{crv2}(i)\right)$$

$$Y_2(i) = \frac{K_\psi}{\frac{cos\alpha_{nL2}}{cos\alpha_{w2}}\left[\frac{6h_{f2}(i)}{\left(S_{F2}(i)\right)^2 C_h} - \frac{tan\alpha_{nL2}}{S_{F2}(i)}\right]}$$

$$K_{f2}(i) = H + \left(\frac{S_{F2}(i)}{A_{2v}}\right)^L \left(\frac{S_{F2}(i)}{h_{f2}(i)}\right)^M$$

$$J_2(i) = \frac{Y_2(i)C_\psi}{K_{f2}(i)m_N}$$

end

The minimum one of the J_2 is taken as the geometry factor and implemented into the bending stress equation.

2.1.2.3. Scuffing Evaluation

The term scuffing is defined as localized damage caused by solid-phase welding between surfaces in relative motion. It is accompanied by transfer of metal from one surface to another due to welding and subsequent tearing, and may occur in any highly loaded contact where the oil film is too thin to adequately spate the surfaces. Scuffing appears as a matte, rough finish due to the microscopic tearing at the surface. It occurs most commonly at extreme end regions of the contact path or near points of single tooth contact. Scuffing is also known generically as severe adhesive wear.

Scuffing risk is considered as the main criteria for scuffing elimination in optimization process.

Table 2.6 *Scuffing Risk [16]*

Probability of scuffing	Scuffing risk
<10%	Low
10 to 30%	Moderate
>30%	High

Maximum contact temperature is given as:

$$\theta_{B\,max} = \theta_M + \theta_{fl_{max}} \tag{2.212}$$

Tooth temperature is given as:

$$\theta_M = k_{sump}\theta_{oil} + 0.56\theta_{fl_{max}} \tag{2.213}$$

where

k_{sump} = 1.0 if splash lube; 1.2 if spray lube;

In the current study, temperature of the oil is considered as 100 ℃.

$$\theta_{oil} = 100\ ℃$$

Flash temperature is given as:

$$\theta_{fl_{(i)}} = 31.62K\mu_{m_{(i)}} \frac{X_{\Gamma_{(i)}} w_n}{\left(b_{H_{(i)}}\right)^{0.5}} \frac{\left|v_{r1_{(i)}} - v_{r2_{(i)}}\right|}{B_{M1}\left(v_{r1_{(i)}}\right)^{0.5} + B_{M2}\left(v_{r2_{(i)}}\right)^{0.5}} \quad (2.214)$$

Mean coefficient of friction, $\mu_{m_{(i)}}$ is given as:

$$\mu_{m_{(i)}} = \mu_{m_{const}} = 0.06C_{R_{avg_x}} \quad (2.215)$$

The surface roughness constant, $C_{R_{avg_x}}$, is limited to a maximum value of 3.0:

$$1.0 \leq C_{R_{avg_x}} = \frac{1.13}{1.13 - R_{avg_x}} \leq 3.0 \quad (2.216)$$

$$R_{avg_x} = \frac{R_{a_{1x}} + R_{a_{2x}}}{2} \quad (2.217)$$

The thermal contact coefficient accounts for the influence of the material properties of pinion and gear:

$$B_{M1} = (\lambda_{M1}\rho_{M1}c_{m1})^{0.5} \quad (2.218)$$

$$B_{M2} = (\lambda_{M2}\rho_{M2}c_{m2})^{0.5} \quad (2.219)$$

For martensitic steels the range of heat conductivity, λ_M, is 41 to 52 $N/[s\ K]$ and the product of density times the specific heat per unit mass, $\rho_m c_m$ is about 3.8 $N/[mm^2K]$, so that the use of the average value $B_M = 13.6\ N/[mms^{0.5}K]$ for such steels will not introduce a large error when the thermal contact coefficient is unknown.

Hertzian contact band is given as:

The semi-width of the rectangular contact band is given by:

$$b_{H_{(i)}} = \left(\frac{8X_{\Gamma_{(i)}} w_n \rho_{n_{(i)}}}{\pi E_r}\right)^{0.5} \quad (2.220)$$

E_r is reduced modulus of elasticity given by:

$$E_r = 2\left(\frac{1-{v_1}^2}{E_1}+\frac{1-{v_2}^2}{E_2}\right)^{-1} \tag{2.221}$$

Evaluating the roll angles is necessary to implement the load sharing factor. Pinion roll angles corresponding to the five specific points along the line of action shown in Figure 2-23 are given by:

$$\xi_j = \frac{C_i}{r_{b1}} \tag{2.222}$$

where

$$j = A, B, C, D, E$$

$$i = 1,2,3,4,5$$

2.1.2.3.1. Profile Radii of Curvature

Figure 2-23 shows the transverse radii of curvature, $\rho_{1_{(i)}}$ and $\rho_{2_{(i)}}$, of the gear tooth profiles at a general contact point defined by the roll angle $\xi_{(i)}$, where (i) is any point on the line of action from A to E.

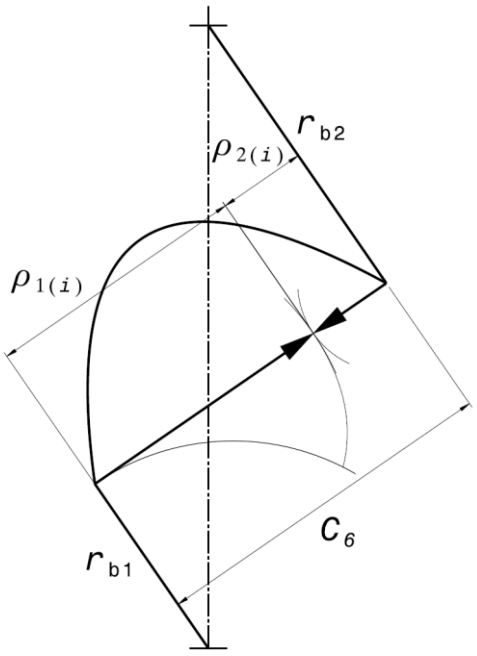

Figure 2-23 *Transverse relative radius of curvature for external gears [16]*

$$\rho_{1_{(i)}} = r_{b1}\xi_{(i)} \tag{2.223}$$

where

$$\xi_A \leq \xi_{(i)} \leq \xi_E$$

$$\rho_{2_{(i)}} = C_6 \mp \rho_{1_{(i)}} \tag{2.224}$$

Transverse relative radius of curvature

$$\rho_{r_{(i)}} = \frac{\rho_{1_{(i)}}\rho_{2_{(i)}}}{\rho_{2_{(i)}} \pm \rho_{1_{(i)}}} \tag{2.225}$$

Normal relative radius of curvature

$$\rho_{n_{(i)}} = \frac{\rho_{r_{(i)}}}{cos\beta_b} \tag{2.226}$$

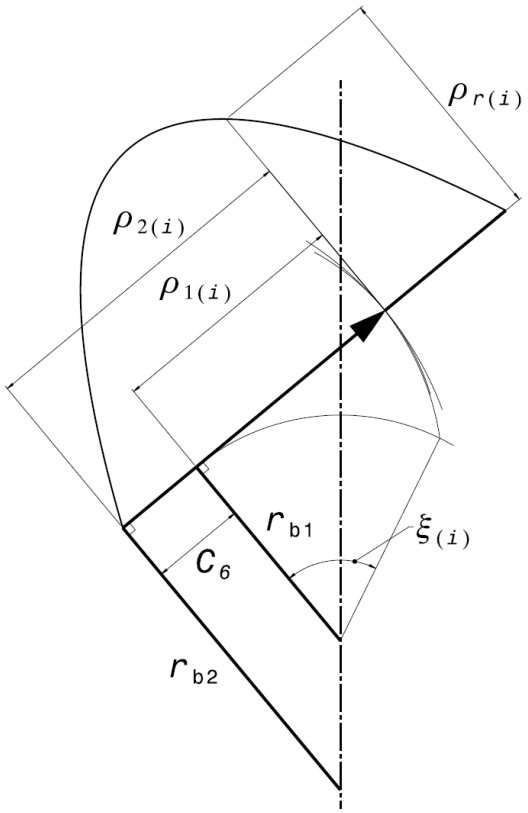

Figure 2-24 *Transverse relative radius of curvature for internal gears*

2.1.2.3.2. Gear Tooth Velocities and Loads

Rotational (angular) velocities

$$w_1 = \frac{\pi n_1}{30} \tag{2.227}$$

$$w_2 = \frac{w_1}{m_G} \tag{2.228}$$

Operating pitch line velocity

$$v_t = \frac{w_1 r_{w1}}{1000} \tag{2.229}$$

Rolling (tangential) velocities

$$v_{r1_{(i)}} = \frac{w_1 \rho_{1_{(i)}}}{1000} \tag{2.230}$$

$$v_{r2_{(i)}} = \frac{w_2 \rho_{2_{(i)}}}{1000} \tag{2.231}$$

Sliding velocity (absolute value)

$$v_{s_{(i)}} = \left| v_{r1_{(i)}} - v_{r2_{(i)}} \right| \tag{2.232}$$

Entraining velocity (absolute value)

$$v_{e_{(i)}} = \left| v_{r1_{(i)}} + v_{r2_{(i)}} \right| \tag{2.233}$$

Nominal tangential load

$$(F_t)_{nom} = \frac{1000P}{v_t} \tag{2.234}$$

Combined derating factor

$$K_D = K_o K_m K_v \tag{2.235}$$

where

$$F_t = (F_t)_{nom} K_D \tag{2.236}$$

Normal operating load

$$F_{wn} = \frac{F_t}{cos\alpha_{wn} cos\beta_w} \tag{2.237}$$

Normal unit load

$$w_n = \frac{F_{wn}}{L_{min}} \tag{2.238}$$

2.1.2.3.3. Load Sharing Factor

For unmodified tooth profiles

If there is no tip or root relief

For $\xi_A \leq \xi_{(i)} < \xi_B$

$$X_{\Gamma_{(i)}} = \frac{1}{3} + \frac{1}{3}\left(\frac{\xi_{(i)} - \xi_A}{\xi_B - \xi_A}\right) \tag{2.239}$$

For $\xi_B \leq \xi_{(i)} \leq \xi_D$

$$X_{\Gamma_{(i)}} = 1 \tag{2.240}$$

For $\xi_D < \xi_{(i)} \leq \xi_E$

$$X_{\Gamma_{(i)}} = \frac{1}{3} + \frac{1}{3}\left(\frac{\xi_E - \xi_{(i)}}{\xi_E - \xi_D}\right) \tag{2.241}$$

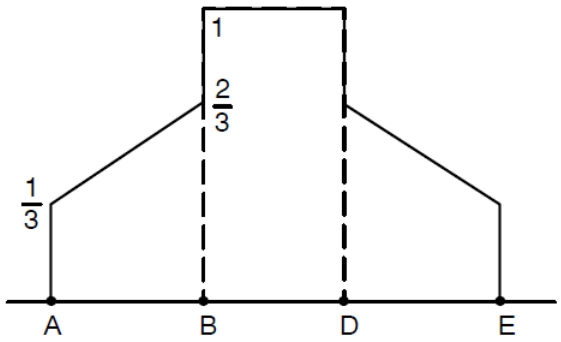

Figure 2-25 *Load sharing factor – unmodified profiles [16]*

2.1.2.3.4. Evaluation of Maximum Flash Temperature

The roll angles are evaluated to find the maximum flash temperature.

$$\boldsymbol{for\ i = 1{:}48}$$

$$\xi_1 = \xi_A$$

$$\boldsymbol{if}\quad i < \frac{itp}{4}$$

$$\xi_{i+1} = \xi_i + \frac{\xi_B - \xi_A}{\frac{itp}{4} - 1}$$

$$\boldsymbol{if}\quad i \geq \frac{itp}{4}\ \ \&\&\ \ i < 2\frac{itp}{4}$$

$$\xi_{i+1} = \xi_i + \frac{\xi_C - \xi_B}{\frac{itp}{4}}$$

$$\boldsymbol{if}\quad i \geq 2\frac{itp}{4}\ \ \&\&\ \ i < 3\frac{itp}{4}$$

$$\xi_{i+1} = \xi_i + \frac{\xi_D - \xi_C}{\frac{itp}{4}}$$

$$\boldsymbol{if}\quad i \geq 3\frac{itp}{4}\ \ \&\&\ \ i < itp$$

$$\xi_{i+1} = \xi_i + \frac{\xi_E - \xi_D}{\frac{itp}{4}}$$

$$\boldsymbol{end}$$

$\rho_{1_{(i)}}, \rho_{2_{(i)}}, \rho_{r_{(i)}}, \rho_{n_{(i)}}, v_{r1_{(i)}}, v_{r2_{(i)}}, X_{\Gamma_{(i)}}$ and $b_{H_{(i)}}$ are obtained by implementing the all different roll angles. Therefore, different flash temperatures values, $\theta_{fl_{(i)}}$, for each roll angle are obtained. The maximum one of the different flash temperature values is

implemented into the equation (2.213*)* to find the tooth temperature. Tooth temperature is implemented into eq (2.212) to evaluate the contact temperature.

Speed parameter,

$$U_{(i)} = \frac{\eta_M v_{e_{(i)}}}{2E_r \rho_{n_{(i)}}} x\ 10^{-6} \tag{2.242}$$

Load parameter,

$$W_{(i)} = \frac{X_{\Gamma_{(i)}} w_n}{E_r \rho_{n_{(i)}}} \tag{2.243}$$

Dimensionless central film thickness,

$$H_{c_{(i)}} = 3.06 \frac{G^{0.56} U_{(i)}^{0.69}}{W_{(i)}^{0.10}} \tag{2.244}$$

The central film thickness at a given point is:

$$h_{c_{(i)}} = H_{c_{(i)}} \rho_{n_{(i)}}\ x\ 10^3 \tag{2.245}$$

The specific film thickness is:

$$\lambda_{2b_{H_{(i)}}} = \frac{h_{c_{(i)}}}{\sigma_{0.8}} \left[\frac{L_{0.8}}{2b_{H_{(i)}}} \right]^{0.5} \tag{2.246}$$

where

$$\sigma_x = [Ra_{1x}^2 + Ra_{2x}^2]^{0.5}$$

$$L_{0.8} = 0.8\ mm$$

CHAPTER 3

OPTIMIZATION METHODOLOGY

3.1. Root Clearance Criteria

Addendum and dedendum coefficient of the standard cutters are given in Table 3.1. Coefficients are given for standard center distance.

Table 3.1 *Addendum and dedendum coefficient of standard cutters*

Standard	Profil Type	Dedendum coefficient	Addendum coefficient
ISO 53.2:1997	Profil A	1.25	1.00
ISO 53.2:1997	Profil B	1.25	1.00
ISO 53.2:1997	Profil C	1.25	1.00
ISO 53.2:1997	Profil D	1.40	1.00
DIN 867:1986	-	1.25	1.00
DIN 3972:1952 I	-	1.1670	1.00
DIN 3972:1952 II	-	1.25	1.00
DIN 58400:1984	(m_n 0.1 − 0.6)	1.50	1.10
DIN 58400:1984	(m_n > 0.1 − 0.6)	1.35	1.00
DIN 58412:1984	(m_n 0.1 − 0.6)	1.50	1.10
DIN 58412:1984	(m_n > 0.1 − 0.6)	1.35	1.10
DIN 58412:1987	-	1.25	1.00
DIN 867:1986	-	1.20	1.00
DIN 867:1986	-	1.16	1.00
DIN 867:1986	-	1.30	1.00
DIN 867:1986	-	1.40	1.00

As seen from Table 3.1, the standard cutters generally satisfy $0.25 \cdot m_t$ root clearance. The minimum standard root clearance is $0.16 \cdot m_t$. The maximum standard root clearance is $0.4 \cdot m_t$. Therefore, the minimum root clearance is specified as $0.16 \cdot m_t$ and the maximum root clearance is specified as $0.4 \cdot m_t$

3.2. Top Land Thickness Criteria

Surface hardened gear teeth require adequate case depth to resist the subsurface shear stresses developed by tooth contact loads and the tooth root fillet tensile stresses, but depths must not be so great as to result in brittle teeth and high residual tensile stress in the core.

Correlation between the normal diametral pitch and the effective case depth is given in Figure 3-1.

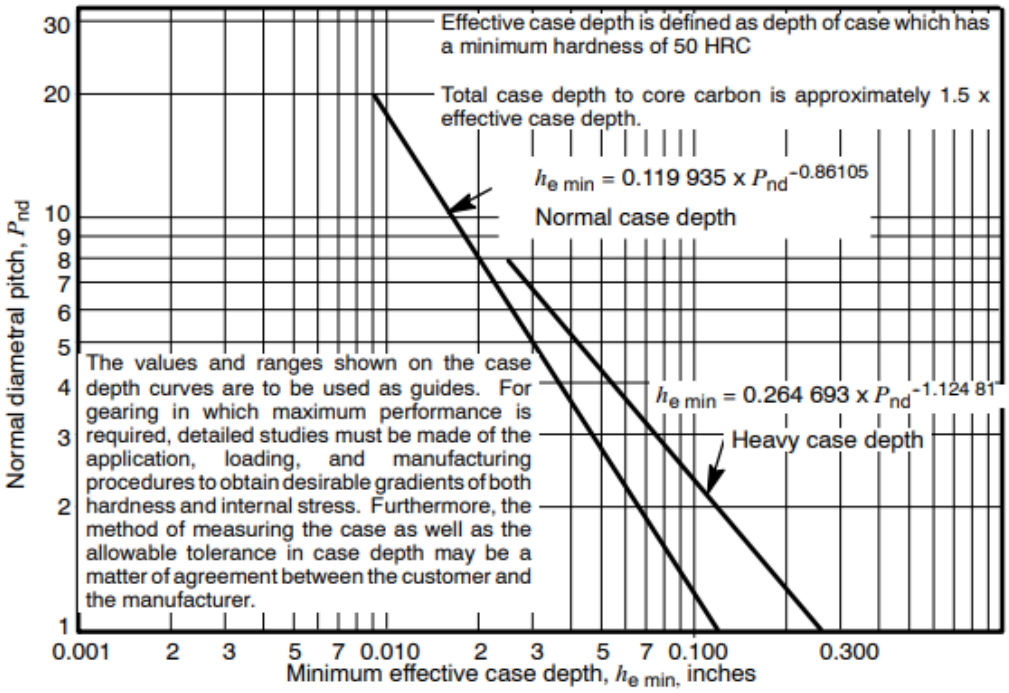

Figure 3-1 *Minimum effective case depth for carburized gears, $h_{e\ min}$ [14]*

For heavy case depth,

$$h_{e\ min} = 0.264693 P_{nd}{}^{-1.12481} \tag{3.1}$$

The unit is converted into mm , the equation becomes

$$h_{e\,min} = 0.264693\left(\frac{25.4}{m_n}\right)^{-1.12481} \cdot 25.4 \tag{3.2}$$

The tolerance of the carburizing depth can be taken as $0.25\,mm$. Therefore, the maximum carburizing depth is:

$$h_{e\,max} = h_{e\,min} + 0.250 \tag{3.3}$$

The relation between the top land thickness and the maximum effective case depth is given as:

$$h_{e\,max} = 0.56 s_{na} \tag{3.4}$$

By equating the (3.3) and (*3.4*),

$$s_{na\,min} = \frac{\left(0.264693\left(\frac{25.4}{m_n}\right)^{-1.12481} \cdot 25.4 + 0.250\right)}{0.56} \tag{3.5}$$

3.3. Contact Stress Criteria

Load cycle formula is given as: [14]

$$N = 60Lnq \tag{3.6}$$

Aerospace gears are considered as resisted to $5000\ hours$ life. After $5000\ hours$ the gears are inspected. If there exist no failure in gears, the gears are expected as having infinite life. Therefore, the life is taken as $5000\ hours$ in this study. Since the single gear pairs are considered in this study, q is taken as unity.Allowable contact stress number for steel gears is given in Table 3.2.

Table 3.2 *Allowable contact stress number, s_{ac} , for steel gears [14]*

Material designation	Heat treatment	Minimum surface hardness[1]	Allowable contact stress number[2], s_{ac} lb/in^2		
			Grade 1	Grade 2	Grade 3
Steel[3]	Through hardened[4]	see figure 8	see figure 8	see figure 8	--
	Flame[5] or induction hardened[5]	50 HRC	170 000	190 000	--
		54 HRC	175 000	195 000	--
	Carburized and hardened[5]	see table 9	180 000	225 000	275 000
	Nitrided[5] (through hardened steels)	83.5 HR15N	150 000	163 000	175 000
		84.5 HR15N	155 000	168 000	180 000
2.5% Chrome (no aluminum)	Nitrided[5]	87.5 HR15N	155 000	172 000	189 000
Nitralloy 135M	Nitrided[5]	90.0 HR15N	170 000	183 000	195 000
Nitralloy N	Nitrided[5]	90.0 HR15N	172 000	188 000	205 000
2.5% Chrome (no aluminum)	Nitrided[5]	90.0 HR15N	176 000	196 000	216 000

NOTES
1) Hardness to be equivalent to that at the start of active profile in the center of the face width.
2) See tables 7 through 10 for major metallurgical factors for each stress grade of steel gears.
3) The steel selected must be compatible with the heat treatment process selected and hardness required.
4) These materials must be annealed or normalized as a minimum.
5) The allowable stress numbers indicated may be used with the case depths prescribed in 16.1.

Grade 3 carburized and hardened steel is considered in this study. Therefore, allowable contact stress number is:

$$s_{ac} = 275\ ksi \tag{3.7}$$

Contact strength stress cycle factor, Z_N , is associated with the lubrication regime in AGMA 925. If the specific film thickness is greater than or equal to 1.0 indicates the beginning of regime III and the end of regime II lubrication. Specific film thickness between 0.4 and 1.0 indicates operation within regime II and specific film thickness less than or equal to 0.4 indicates regime I.

Table 3.3 *Stress cycle factor equations for regimes I, II and III [14]*

Regime of lubrication	Stress cycle factor for surface durability	
Regime III	$Z_N = 1.47$	for $N < 10\ 000$ cycles
	$Z_N = 2.46604 \times N^{-0.056}$	for $N \geq 10\ 000$ cycles
Regime II	$Z_N = 3.83441 \times N^{-0.094}$	for $N \geq 100\ 000$ cycles
Regime I	$Z_N = 7.82078 \times N^{-0.156}$	for $N \geq 100\ 000$ cycles

Since the pinion has a higher rotational speed than the gear, number of load cycle of the pinion is higher than the number of load cycle of the gear. Because of that, pinion has a lower allowable contact stress number than the gear has. Therefore, considering only the contact stress of the pinion is enough to evaluate the contact stress elimination.

Permissible allowable contact stress number of the pinion is:

$$s_{acp} = s_{ac} \frac{Z_N}{K_T} \frac{C_H}{K_R} \tag{3.8}$$

The case hardened aerospace gears have minimum 60 HRC surface hardness values. Surface hardness values of the pinion and the gear are almost the same. In [2001-D04], hardness ratio factor for case hardened pinions (48 HRC or harder) are run with through hardened gears (180 to 400 HB) is given in Figure 3-2.

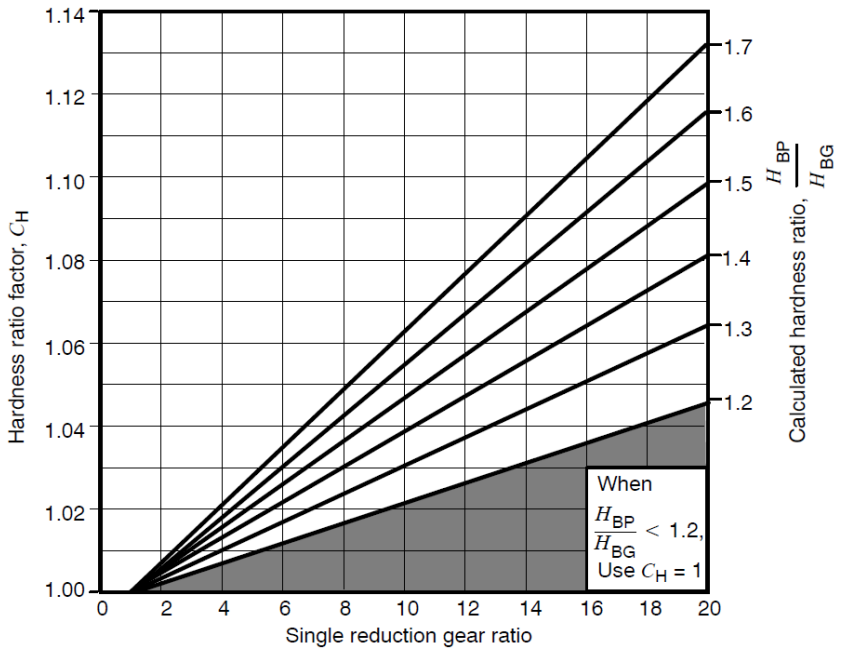

Figure 3-2 *Hardness ratio factor, C_H (through hardened) [14]*

As seen from Figure 3-2, if the ratio of the hardness value of the pinion to hardness ratio value of the gear is lower than 1.2, hardness ratio factor is taken as unity even for the gear pairs which have a minimum 5 HRC hardness value difference between the pinion and the gear. In this study, the gear pairs which have a small amount of difference between the hardness value of the pinion and the hardness ratio of the gear are considered. Therefore, it is suitable to consider the hardness ratio factor as unity.

The temperature factor, K_T, is generally taken as unity when gears operate with temperatures of oil or gear blank not exceeding $250^{\circ} F$. In normal operating conditions, temperature of oil or gear blank is not higher than $250^{\circ} F$. Therefore, the temperature factor is taken as unity.

The allowable stress numbers given in Table 3.2 and Table 3.5 are based upon a statistical probability of one failure in 100. Therefore, reliability factor, K_R, is taken as unity as given in Table 3.4.

Table 3.4 *Reliability factors, K_R [14]*

Requirements of application	K_R [1)]
Fewer than one failure in 10 000	1.50
Fewer than one failure in 1000	1.25
Fewer than one failure in 100	1.00
Fewer than one failure in 10	0.85 [2)]
Fewer than one failure in 2	0.70 [2) 3)]

NOTES
1) Tooth breakage is sometimes considered a greater hazard than pitting. In such cases a greater value of K_R is selected for bending.
2) At this value plastic flow might occur rather than pitting.
3) From test data extrapolation.

The contact stress reserve factor is:

$$R_c = \frac{s_{acp}}{s_c} \tag{3.9}$$

3.4. Bending Stress Criteria

Allowable bending stress number, s_{at} , for steel gears is given in Table 3.5.

Table 3.5 *Allowable bending stress number, s_{at} , for steel gears [14]*

Material designation	Heat treatment	Minimum surface hardness[1]	Allowable bending stress number[2], s_{at} lb/in^2		
			Grade 1	Grade 2	Grade 3
Steel[3]	Through hardened	see figure 9	see figure 9	see figure 9	--
	Flame[4] or induction hardened[4] with type A pattern[5]	see table 8	45 000	55 000	--
	Flame[4] or induction hardened[4] with type B pattern[5]	see table 8	22 000	22 000	--
	Carburized and hardened[4]	see table 9	55 000	65 000 or 70 000[6]	75 000
	Nitrided[4] [7] (through hardened steels)	83.5 HR15N	see figure 10	see figure 10	--
Nitralloy 135M, Nitralloy N, and 2.5% Chrome (no aluminum)	Nitrided[4] [7]	87.5 HR15N	see figure 11	see figure 11	see figure 11

NOTES
[1] Hardness to be equivalent to that at the root diameter in the center of the tooth space and face width.
[2] See tables 7 through 10 for major metallurgical factors for each stress grade of steel gears.
[3] The steel selected must be compatible with the heat treatment process selected and hardness required.
[4] The allowable stress numbers indicated may be used with the case depths prescribed in 16.1.
[5] See figure 12 for type A and type B hardness patterns.
[6] If bainite and microcracks are limited to grade 3 levels, 70,000 psi may be used.
[7] The overload capacity of nitrided gears is low. Since the shape of the effective S-N curve is flat, the sensitivity to shock should be investigated before proceeding with the design. [7]

Grade 3 carburized and hardened steel is considered in this study. Therefore, allowable bending stress number is:

$$s_{at} = 75\ ksi \tag{3.10}$$

Bending strength stress cycle factor is given in Figure 3-3 . Bending strength stress cycle factor is specified as:

$$Y_N = 1.6831 \cdot N^{-0.0323} \tag{3.11}$$

Permissible allowable bending stress number is: [14]

$$s_{atp} = \frac{s_{at} Y_N}{K_T K_R} \tag{3.12}$$

The bending stress reserve factor is:

$$R_t = \frac{S_{atp}}{S_t} \tag{3.13}$$

Bending strength stress cycle factor is given in Figure 3-3 .

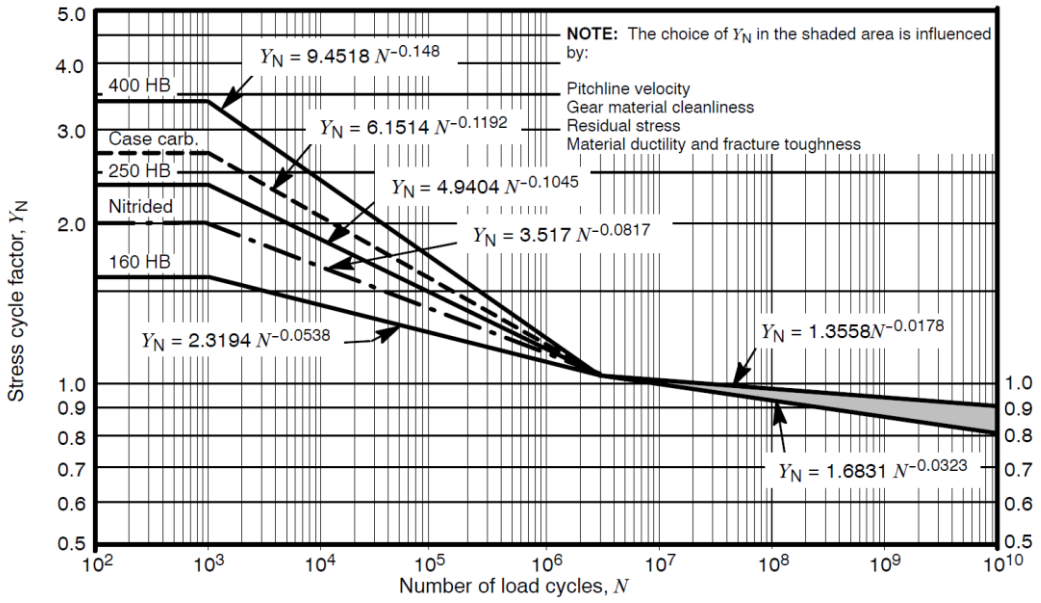

Figure 3-3 *Bending strength stress cycle factor, Y_N [14]*

Table 3.6 *Minimum and maximum values of the constraint functions used in optimization*

Constraint	***Minimum Value***	***Maximum Value***
c_1	$0.16 \cdot m_t$	$0.40 \cdot m_t$
c_2	$0.16 \cdot m_t$	$0.40 \cdot m_t$
s_{na}	$\dfrac{\left(0.264693\left(\dfrac{25.4}{m_n}\right)^{-1.12481} \cdot 25.4 + 0.250\right)}{0.56}$	
m_c	1	
Ic_1	$0.10 \cdot m_t$	
Ic_2	$0.10 \cdot m_t$	
$Tiff_1$	$0.20 \cdot m_t$	
$Tiff_2$	$0.20 \cdot m_t$	
R_c	1	
R_{t1}	1	
R_{t2}	1	
Q	10	

3.5. Optimization Steps

Optimization steps are given in this chapter.

3.5.1. Cross Combination of Normal Module, Helix Angle, Pinion Profile Shifting Coefficient, Pressure Angle and Pinion Number of Teeth

The initial assignments of the normal module, helix angle, pinion profile shift coefficient, pressure angle and pinion number of teeth are implemented.

Table 3.7 *Initial assignments of the design variables*

$$m_n = m_{n_{min}} : m_{n_{inc}} : m_{n_{max}}$$

$$\beta = \beta_{min} : \beta_{inc} : \beta_{max}$$

$$x_1 = x_{1_{min}} : x_{1_{inc}} : x_{1_{max}}$$

$$\alpha_n = \alpha_{n_{min}} : \alpha_{n_{inc}} : \alpha_{n_{max}}$$

$$z_1 = z_{1_{min}} : z_{1_{inc}} : z_{1_{max}}$$

$$z_2 = m_G z_1$$

Cross combination of the m_n , β , x_1 , α_n and z_1 is obtained. Cross combination matrix is named as $Combs1$.

Table 3.8 *First cross combination of the design variables*

$$m_n = Combs1(:,1)$$

$$\beta = Combs1(:,2)$$

$$x_1 = Combs1(:,3)$$

$$\alpha_n = Combs1(:,4)$$

$$z_1 = Combs1(:,5)$$

$$z_2 = Combs1(:,6) = m_G Combs1(:,5)$$

3.5.2. Evaluation of Pinion Addendum Radius and Gear Dedendum Radius

Addendum radius of the pinion is evaluated by using the following algorithm given in Table 3.9.

Table 3.9 *Evaluation of addendum radius of the pinion*

$$r_{a1_{pre}}(1,:) = \frac{m_n}{cos\beta}\frac{z_1}{2} + y_1\frac{m_n}{cos\beta}$$

$$for\ i = 2 : \frac{(y_2 - y_1)}{inc1} + 1$$

$$r_{a1_{pre}}(i,:) = \frac{m_n}{cos\beta}\frac{z_1}{2} + y_1\frac{m_n}{cos\beta} + \left(inc1\ \frac{m_n}{cos\beta}\right)(i-1)$$

$$end$$

$$num_1 = \frac{(y_2 - y_1)}{inc1} + 1 \qquad (3.14)$$

Therefore, num_1 times addendum radii for external and internal pinion (for each row of $Combs1$) are obtained by applying increment of $inc1$.

Dedendum radii of the each gear set is evaluated by using the following algorithm given in Table 3.10.

Table 3.10 *Evaluation of dedendum radius of the gear*

$$r_{f2_{pre}}(1,:) = \frac{m_n}{cos\beta}\frac{z_2}{2} + y_7\frac{m_n}{cos\beta}$$

$$for\ i = 2 : \frac{(y_8 - y_7)}{inc4} + 1$$

$$r_{f2_{pre}}(i,:) = \frac{m_n}{cos\beta}\frac{z_2}{2} + y_7\frac{m_n}{cos\beta} + \left(inc4\ \frac{m_n}{cos\beta}\right)(i-1)$$

$$end$$

$$num_4 = \frac{(y_8 - y_7)}{inc4} + 1 \tag{3.15}$$

For example

$$Combs1 = \begin{bmatrix} (m_n)_1\ (\beta)_1\ (x_1)_1\ (\alpha_n)_1\ (z_1)_1\ (z_2)_1 \\ (m_n)_2\ (\beta)_2\ (x_1)_2\ (\alpha_n)_2\ (z_1)_2\ (z_2)_2 \end{bmatrix} \tag{3.16}$$

If $num1$ is taken as ‘’3’’.

$$\frac{(m_n)_1}{cos(\beta)_1}\frac{(z_1)_1}{2} + y_1\frac{(m_n)_1}{cos(\beta)_1} = r_{a1_{pre}}(1,1) \tag{3.17}$$

$$\frac{(m_n)_2}{cos(\beta)_2}\frac{(z_1)_2}{2} + y_1\frac{(m_n)_2}{cos(\beta)_2} = r_{a1_{pre}}(1,2) \tag{3.18}$$

$$r_{a1_{pre}} = \begin{bmatrix} r_{a1_{pre}}(1,1) & r_{a1_{pre}}(1,2) \\ r_{a1_{pre}}(1,1) + \left(inc1\ \frac{(m_n)_1}{cos(\beta)_1}\right)\cdot 1 & r_{a1_{pre}}(1,2) + \left(inc1\ \frac{(m_n)_2}{cos(\beta)_2}\right) \\ r_{a1_{pre}}(1,1) + \left(inc1\ \frac{(m_n)_1}{cos(\beta)_1}\right)\cdot 2 & r_{a1_{pre}}(1,2) + \left(inc1\ \frac{(m_n)_2}{cos(\beta)_2}\right) \end{bmatrix} \quad (3.19)$$

If $num4$ is taken as ‘’3’’.

$$\frac{(m_n)_1}{cos(\beta)_1}\frac{(z_1)_1}{2} + y_7\frac{(m_n)_1}{cos(\beta)_1} = r_{f2_{pre}}(1,1) \quad (3.20)$$

$$\frac{(m_n)_2}{cos(\beta)_2}\frac{(z_1)_2}{2} + y_7\frac{(m_n)_2}{cos(\beta)_2} = r_{f2_{pre}}(1,2) \quad (3.21)$$

$$r_{f2_{pre}} = \begin{bmatrix} r_{f2_{pre}}(1,1) & r_{f2_{pre}}(1,2) \\ r_{f2_{pre}}(1,1) + \left(inc4\ \frac{(m_n)_1}{cos(\beta)_1}\right)\cdot 1 & r_{f2_{pre}}(1,2) + \left(inc4\ \frac{(m_n)_2}{cos(\beta)_2}\right)\cdot 1 \\ r_{f2_{pre}}(1,1) + \left(inc4\ \frac{(m_n)_1}{cos(\beta)_1}\right)\cdot 2 & r_{f2_{pre}}(1,2) + \left(inc4\ \frac{(m_n)_2}{cos(\beta)_2}\right)\cdot 2 \end{bmatrix} \quad (3.22)$$

$$r_{f2_{pre}} = \begin{bmatrix} r_{f2_{pre}}(1,1) & r_{f2_{pre}}(1,2) \\ r_{f2_{pre}}(1,1) + \left(inc4\ \frac{(m_n)_1}{cos(\beta)_1}\right)\cdot 1 & r_{f2_{pre}}(1,2) + \left(inc4\ \frac{(m_n)_2}{cos(\beta)_2}\right)\cdot 1 \\ r_{f2_{pre}}(1,1) + \left(inc4\ \frac{(m_n)_1}{cos(\beta)_1}\right)\cdot 2 & r_{f2_{pre}}(1,2) + \left(inc4\ \frac{(m_n)_2}{cos(\beta)_2}\right)\cdot 2 \end{bmatrix} \quad (3.23)$$

Cross combination of the $r_{a1_{pre}}$ and $r_{f2_{pre}}$ is implemented to obtain r_{a1} and r_{f2}.

$$r_{a1} = \begin{bmatrix} r_{a1_{pre}}(1,1) \\ r_{a1_{pre}}(2,1) \\ r_{a1_{pre}}(3,1) \\ r_{a1_{pre}}(1,1) \\ r_{a1_{pre}}(2,1) \\ r_{a1_{pre}}(3,1) \\ r_{a1_{pre}}(1,1) \\ r_{a1_{pre}}(2,1) \\ r_{a1_{pre}}(3,1) \\ r_{a1_{pre}}(1,2) \\ r_{a1_{pre}}(2,2) \\ r_{a1_{pre}}(3,2) \\ r_{a1_{pre}}(1,2) \\ r_{a1_{pre}}(2,2) \\ r_{a1_{pre}}(3,2) \\ r_{a1_{pre}}(1,2) \\ r_{a1_{pre}}(2,2) \\ r_{a1_{pre}}(3,2) \end{bmatrix} \quad r_{f2} = \begin{bmatrix} r_{f2_{pre}}(1,1) \\ r_{f2_{pre}}(1,1) \\ r_{f2_{pre}}(1,1) \\ r_{f2_{pre}}(2,1) \\ r_{f2_{pre}}(2,1) \\ r_{f2_{pre}}(2,1) \\ r_{f2_{pre}}(3,1) \\ r_{f2_{pre}}(3,1) \\ r_{f2_{pre}}(3,1) \\ r_{f2_{pre}}(1,2) \\ r_{f2_{pre}}(1,2) \\ r_{f2_{pre}}(1,2) \\ r_{f2_{pre}}(2,2) \\ r_{f2_{pre}}(2,2) \\ r_{f2_{pre}}(2,2) \\ r_{f2_{pre}}(3,2) \\ r_{f2_{pre}}(3,2) \\ r_{f2_{pre}}(3,2) \end{bmatrix} \tag{3.24}$$

After obtaining the r_{a1} and r_{f2}, combination of the m_n , β , x_1 , α_n , z_1 , z_2 , r_{a1} and r_{f2} is evaluated by expanding the each row of the $Combs1$ $(num1 \cdot num4)$ times. Therefore second combination is expressed as:

$$Combs2 = \begin{bmatrix} (m_n)_1 & (\beta)_1 & (x_1)_1 & (\alpha_n)_1 & (z_1)_1 & (z_2)_1 & r_{a1}(1,1) & r_{f2}(1,1) \\ (m_n)_1 & (\beta)_1 & (x_1)_1 & (\alpha_n)_1 & (z_1)_1 & (z_2)_1 & r_{a1}(1,2) & r_{f2}(1,2) \\ (m_n)_1 & (\beta)_1 & (x_1)_1 & (\alpha_n)_1 & (z_1)_1 & (z_2)_1 & r_{a1}(1,3) & r_{f2}(1,3) \\ (m_n)_1 & (\beta)_1 & (x_1)_1 & (\alpha_n)_1 & (z_1)_1 & (z_2)_1 & r_{a1}(1,4) & r_{f2}(1,4) \\ (m_n)_1 & (\beta)_1 & (x_1)_1 & (\alpha_n)_1 & (z_1)_1 & (z_2)_1 & r_{a1}(1,5) & r_{f2}(1,5) \\ (m_n)_1 & (\beta)_1 & (x_1)_1 & (\alpha_n)_1 & (z_1)_1 & (z_2)_1 & r_{a1}(1,6) & r_{f2}(1,6) \\ (m_n)_1 & (\beta)_1 & (x_1)_1 & (\alpha_n)_1 & (z_1)_1 & (z_2)_1 & r_{a1}(1,7) & r_{f2}(1,7) \\ (m_n)_1 & (\beta)_1 & (x_1)_1 & (\alpha_n)_1 & (z_1)_1 & (z_2)_1 & r_{a1}(1,8) & r_{f2}(1,8) \\ (m_n)_1 & (\beta)_1 & (x_1)_1 & (\alpha_n)_1 & (z_1)_1 & (z_2)_1 & r_{a1}(1,9) & r_{f2}(1,9) \\ (m_n)_2 & (\beta)_2 & (x_1)_2 & (\alpha_n)_2 & (z_1)_2 & (z_2)_2 & r_{a1}(1,10) & r_{f2}(1,10) \\ (m_n)_2 & (\beta)_2 & (x_1)_2 & (\alpha_n)_2 & (z_1)_2 & (z_2)_2 & r_{a1}(1,11) & r_{f2}(1,11) \\ (m_n)_2 & (\beta)_2 & (x_1)_2 & (\alpha_n)_2 & (z_1)_2 & (z_2)_2 & r_{a1}(1,12) & r_{f2}(1,12) \\ (m_n)_2 & (\beta)_2 & (x_1)_2 & (\alpha_n)_2 & (z_1)_2 & (z_2)_2 & r_{a1}(1,13) & r_{f2}(1,13) \\ (m_n)_2 & (\beta)_2 & (x_1)_2 & (\alpha_n)_2 & (z_1)_2 & (z_2)_2 & r_{a1}(1,14) & r_{f2}(1,14) \\ (m_n)_2 & (\beta)_2 & (x_1)_2 & (\alpha_n)_2 & (z_1)_2 & (z_2)_2 & r_{a1}(1,15) & r_{f2}(1,15) \\ (m_n)_2 & (\beta)_2 & (x_1)_2 & (\alpha_n)_2 & (z_1)_2 & (z_2)_2 & r_{a1}(1,16) & r_{f2}(1,16) \\ (m_n)_2 & (\beta)_2 & (x_1)_2 & (\alpha_n)_2 & (z_1)_2 & (z_2)_2 & r_{a1}(1,17) & r_{f2}(1,17) \\ (m_n)_2 & (\beta)_2 & (x_1)_2 & (\alpha_n)_2 & (z_1)_2 & (z_2)_2 & r_{a1}(1,18) & r_{f2}(1,18) \end{bmatrix} \quad (3.25)$$

Operating center distance for external gear pair is:

$$a_w = \frac{m_n}{cos\beta}\frac{(z_1 + z_2)}{2} \quad (3.26)$$

Operating center distance for internal gear pair is:

$$a_w = \frac{m_n}{cos\beta}\frac{(z_2 - z_1)}{2} \quad (3.27)$$

3.5.3. Gear Root Clearance Elimination

The gear root clearance elimination is implemented by applying the following algorithm given in Table 3.11.

Table 3.11 *Gear root clearance elimination algorithm*

$for\ i = 1{:}\ size(c_2)$ $if\ c_2(i) < 0.17m_t\ \|\|\ c_2(i) > 0.35m_t$ $Combs2(i,:) = [\,]$ end end

3.5.4. Pinion Top Land Thickness Elimination

Pinion top land thickness elimination is implemented by applying the following algorithm given in Table 3.12.

Table 3.12 *Pinion top land thickness elimination algorithm*

$$for\ i = 1{:}\ size(s_{nan1})$$
$$if\ s_{nan1}(i) < s_{nan1\ min}$$
$$Combs2(i,:) = [\,]$$
$$end$$
$$end$$

Therefore, the gear pair sets which do not satisfy the pinion top land criteria is eliminated.

3.5.5. Evaluation of Gear Addendum Radius and Pinion Dedendum Radius

After pinion top land thickness elimination is completed, evaluation of r_{a2} and r_{f1} is done. Addendum radius of the gear is evaluated by using the following algorithm given in Table 3.13 .

Table 3.13 *Evaluation of addendum radius of the gear*

$$r_{a2_{pre}}(1,:) = \frac{m_n}{cos\beta}\frac{z_2}{2} + y_3\frac{m_n}{cos\beta}$$
$$for\ i = 2:\ \frac{(y_4 - y_3)}{inc2} + 1$$
$$r_{a1_{pre}}(i,:) = \frac{m_n}{cos\beta}\frac{z_2}{2} + y_3\frac{m_n}{cos\beta} + \left(inc2\ \frac{m_n}{cos\beta}\right)(i-1)$$
$$end$$

$$num_2 = \frac{(y_4 - y_3)}{inc2} + 1 \tag{3.28}$$

Therefore, num_2 times addendum radii for external and internal gear (for each row of $Combs1$) are obtained by applying increment of $inc2$.

Pinion dedendum radii of the each gear set is evaluated by using the following algorithm given in Table 3.14.

Table 3.14 *Evaluation of dedendum radius of the pinion*

$$r_{f1_{pre}}(1,:) = \frac{m_n}{cos\beta}\frac{z_1}{2} + y_6\frac{m_n}{cos\beta}$$

$$for\ i = 2 : \frac{(y_6 - y_5)}{inc3} + 1$$

$$r_{f1_{pre}}(i,:) = \frac{m_n}{cos\beta}\frac{z_1}{2} + y_6\frac{m_n}{cos\beta} + \left(inc3\ \frac{m_n}{cos\beta}\right)(i-1)$$

$$end$$

$$num_3 = \frac{(y_6 - y_5)}{inc3} + 1 \tag{3.29}$$

Let's assume after the gear root clearance elimination and pinion top land thickness elimination is completed, $Combs2$ becomes:

$$Combs2 = \begin{bmatrix} (m_n)_1 & (\beta)_1 & (x_1)_1 & (\alpha_n)_1 & (z_1)_1 & (z_2)_1 & r_{a1}(1,9) & r_{f2}(1,9) \\ (m_n)_2 & (\beta)_2 & (x_1)_2 & (\alpha_n)_2 & (z_1)_2 & (z_2)_2 & r_{a1}(1,6) & r_{f2}(1,6) \end{bmatrix} \tag{3.30}$$

If $num2$ is taken as ''3''.

$$\frac{(m_n)_1}{cos(\beta)_1}\frac{(z_2)_1}{2} + y_3\frac{(m_n)_1}{cos(\beta)_1} = r_{a2_{pre}}(1,1) \tag{3.31}$$

$$\frac{(m_n)_2}{cos(\beta)_2}\frac{(z_2)_2}{2} + y_3\frac{(m_n)_2}{cos(\beta)_2} = r_{a2_{pre}}(1,2) \tag{3.32}$$

$$r_{a2_{pre}} = \begin{bmatrix} r_{a2_{pre}}(1,1) & r_{a2_{pre}}(1,2) \\ r_{a2_{pre}}(1,1) + \left(inc2\ \frac{(m_n)_1}{cos(\beta)_1}\right)\cdot 1 & r_{a2_{pre}}(1,2) + \left(inc2\frac{(m_n)_2}{cos(\beta)_2}\right)\cdot 1 \\ r_{a2_{pre}}(1,1) + \left(inc2\ \frac{(m_n)_1}{cos(\beta)_1}\right)\cdot 2 & r_{a2_{pre}}(1,2) + \left(inc2\frac{(m_n)_2}{cos(\beta)_2}\right)\cdot 2 \end{bmatrix} \tag{3.33}$$

If $num3$ is taken as ‘’3’’.

$$\frac{(m_n)_1}{cos(\beta)_1}\frac{(z_1)_1}{2} + y_5\frac{(m_n)_1}{cos(\beta)_1} = r_{f1_{pre}}(1,1) \tag{3.34}$$

$$\frac{(m_n)_2}{cos(\beta)_2}\frac{(z_1)_2}{2} + y_5\frac{(m_n)_2}{cos(\beta)_2} = r_{f1_{pre}}(1,2) \tag{3.35}$$

$$r_{f1_{pre}} = \begin{bmatrix} r_{f1_{pre}}(1,1) & r_{f1_{pre}}(1,2) \\ r_{f1_{pre}}(1,1) + \left(inc3\ \frac{(m_n)_1}{cos(\beta)_1}\right)\cdot 1 & r_{f1_{pre}}(1,2) + \left(inc3\ \frac{(m_n)_2}{cos(\beta)_2}\right)\cdot 1 \\ r_{f1_{pre}}(1,1) + \left(inc3\ \frac{(m_n)_1}{cos(\beta)_1}\right)\cdot 2 & r_{f1_{pre}}(1,2) + \left(inc3\ \frac{(m_n)_2}{cos(\beta)_2}\right)\cdot 2 \end{bmatrix} \tag{3.36}$$

Cross combination of the $r_{a2_{pre}}$ and $r_{f1_{pre}}$ is implemented to obtain r_{a2} and r_{f1}.

$$r_{a2} = \begin{bmatrix} r_{a2_{pre}}(1,1) \\ r_{a2_{pre}}(2,1) \\ r_{a2_{pre}}(3,1) \\ r_{a2_{pre}}(1,1) \\ r_{a2_{pre}}(2,1) \\ r_{a2_{pre}}(3,1) \\ r_{a2_{pre}}(1,1) \\ r_{a2_{pre}}(2,1) \\ r_{a2_{pre}}(3,1) \\ r_{a2_{pre}}(1,2) \\ r_{a2_{pre}}(2,2) \\ r_{a2_{pre}}(3,2) \\ r_{a2_{pre}}(1,2) \\ r_{a2_{pre}}(2,2) \\ r_{a2_{pre}}(3,2) \\ r_{a2_{pre}}(1,2) \\ r_{a2_{pre}}(2,2) \\ r_{a2_{pre}}(3,2) \end{bmatrix} \quad r_{f1} = \begin{bmatrix} r_{f1_{pre}}(1,1) \\ r_{f1_{pre}}(1,1) \\ r_{f1_{pre}}(1,1) \\ r_{f1_{pre}}(2,1) \\ r_{f1_{pre}}(2,1) \\ r_{f1_{pre}}(2,1) \\ r_{f1_{pre}}(3,1) \\ r_{f1_{pre}}(3,1) \\ r_{f1_{pre}}(3,1) \\ r_{f1_{pre}}(1,2) \\ r_{f1_{pre}}(1,2) \\ r_{f1_{pre}}(1,2) \\ r_{f1_{pre}}(2,2) \\ r_{f1_{pre}}(2,2) \\ r_{f1_{pre}}(2,2) \\ r_{f1_{pre}}(3,2) \\ r_{f1_{pre}}(3,2) \\ r_{f1_{pre}}(3,2) \end{bmatrix} \tag{3.37}$$

After obtaining the r_{a2} and r_{f1}, combination of the m_n , β , x_1 , α_n , z_1 , z_2 , r_{a1} , r_{f2} , r_{a2} and r_{f1} is evaluated by expanding the each row of the $Combs2$ $(num2 \cdot num3)$ times. Therefore third combination is expressed as:

$$Combs3 = \begin{bmatrix}
(m_n)_1 & (\beta)_1 & (x_1)_1 & (\alpha_n)_1 & (z_1)_1 & (z_2)_1 & r_{a1}(1,6) & r_{f2}(1,6) & r_{a2}(1,1) & r_{f1}(1,1) \\
(m_n)_1 & (\beta)_1 & (x_1)_1 & (\alpha_n)_1 & (z_1)_1 & (z_2)_1 & r_{a1}(1,6) & r_{f2}(1,6) & r_{a2}(1,2) & r_{f1}(1,2) \\
(m_n)_1 & (\beta)_1 & (x_1)_1 & (\alpha_n)_1 & (z_1)_1 & (z_2)_1 & r_{a1}(1,6) & r_{f2}(1,6) & r_{a2}(1,3) & r_{f1}(1,3) \\
(m_n)_1 & (\beta)_1 & (x_1)_1 & (\alpha_n)_1 & (z_1)_1 & (z_2)_1 & r_{a1}(1,6) & r_{f2}(1,6) & r_{a2}(1,4) & r_{f1}(1,4) \\
(m_n)_1 & (\beta)_1 & (x_1)_1 & (\alpha_n)_1 & (z_1)_1 & (z_2)_1 & r_{a1}(1,6) & r_{f2}(1,6) & r_{a2}(1,5) & r_{f1}(1,5) \\
(m_n)_1 & (\beta)_1 & (x_1)_1 & (\alpha_n)_1 & (z_1)_1 & (z_2)_1 & r_{a1}(1,6) & r_{f2}(1,6) & r_{a2}(1,6) & r_{f1}(1,6) \\
(m_n)_1 & (\beta)_1 & (x_1)_1 & (\alpha_n)_1 & (z_1)_1 & (z_2)_1 & r_{a1}(1,6) & r_{f2}(1,6) & r_{a2}(1,7) & r_{f1}(1,7) \\
(m_n)_1 & (\beta)_1 & (x_1)_1 & (\alpha_n)_1 & (z_1)_1 & (z_2)_1 & r_{a1}(1,6) & r_{f2}(1,6) & r_{a2}(1,8) & r_{f1}(1,8) \\
(m_n)_1 & (\beta)_1 & (x_1)_1 & (\alpha_n)_1 & (z_1)_1 & (z_2)_1 & r_{a1}(1,6) & r_{f2}(1,6) & r_{a2}(1,9) & r_{f1}(1,9) \\
(m_n)_2 & (\beta)_2 & (x_1)_2 & (\alpha_n)_2 & (z_1)_2 & (z_2)_2 & r_{a1}(1,9) & r_{f2}(1,6) & r_{a2}(1,10) & r_{f1}(1,10) \\
(m_n)_2 & (\beta)_2 & (x_1)_2 & (\alpha_n)_2 & (z_1)_2 & (z_2)_2 & r_{a1}(1,9) & r_{f2}(1,6) & r_{a2}(1,11) & r_{f1}(1,11) \\
(m_n)_2 & (\beta)_2 & (x_1)_2 & (\alpha_n)_2 & (z_1)_2 & (z_2)_2 & r_{a1}(1,9) & r_{f2}(1,6) & r_{a2}(1,12) & r_{f1}(1,12) \\
(m_n)_2 & (\beta)_2 & (x_1)_2 & (\alpha_n)_2 & (z_1)_2 & (z_2)_2 & r_{a1}(1,9) & r_{f2}(1,6) & r_{a2}(1,13) & r_{f1}(1,13) \\
(m_n)_2 & (\beta)_2 & (x_1)_2 & (\alpha_n)_2 & (z_1)_2 & (z_2)_2 & r_{a1}(1,9) & r_{f2}(1,6) & r_{a2}(1,14) & r_{f1}(1,14) \\
(m_n)_2 & (\beta)_2 & (x_1)_2 & (\alpha_n)_2 & (z_1)_2 & (z_2)_2 & r_{a1}(1,9) & r_{f2}(1,6) & r_{a2}(1,15) & r_{f1}(1,15) \\
(m_n)_2 & (\beta)_2 & (x_1)_2 & (\alpha_n)_2 & (z_1)_2 & (z_2)_2 & r_{a1}(1,9) & r_{f2}(1,6) & r_{a2}(1,16) & r_{f1}(1,16) \\
(m_n)_2 & (\beta)_2 & (x_1)_2 & (\alpha_n)_2 & (z_1)_2 & (z_2)_2 & r_{a1}(1,9) & r_{f2}(1,6) & r_{a2}(1,17) & r_{f1}(1,17) \\
(m_n)_2 & (\beta)_2 & (x_1)_2 & (\alpha_n)_2 & (z_1)_2 & (z_2)_2 & r_{a1}(1,9) & r_{f2}(1,6) & r_{a2}(1,18) & r_{f1}(1,18)
\end{bmatrix} \quad (3.38)$$

3.5.6. Pinion Root Clearance Elimination

The gear root clearance elimination is implemented by applying the following algorithm given in Table 3.15.

Table 3.15 *Pinion root clearance elimination algorithm*

$for\ i = 1{:}\ size(c_1)$
$if\ c_1(i) < 0.17m_t\ \ ||\ c_1(i) > 0.35m_t$
$Combs3(i,:) = [\,]$
end
end

3.5.7. Gear Top Land Thickness Elimination

Gear top land thickness elimination is implemented by applying the following algorithm given in Table 3.16.

Table 3.16 *Gear top land thickness elimination algorithm*

$for\ i = 1{:}\ size(s_{nan2})$
$if\ s_{nan2}(i) < s_{nan2\ min}$
$Combs3(i,:) = [\,]$
end
end

3.5.8. Contact Ratio Elimination

The contact ratio is implemented by applying the following algorithm given in Table 3.17.

Table 3.17 *Contact ratio elimination algorithm*

$for\ i = 1{:}\ size(m_c)$
$if\ m_c(i) < 1$
$Combs3(i,:) = [\,]$
end
end

3.5.9. Involute Clearance Elimination

Pinion involute clearance elimination is implemented by applying the following algorithm given in Table 3.18.

Table 3.18 *Pinion involute clearance elimination algorithm*

$for\ i = 1{:}\ size(Ic_1)$
$if\ \ Ic_1(i) > 0.1m_t$
$Combs3(i,:) = [\,]$
end
end

Gear involute clearance elimination is implemented by applying the following algorithm given in Table 3.19.

Table 3.19 *Gear involute clearance elimination algorithm*

$$for\ i = 1{:}\ size(Ic_2)$$
$$if\ \ Ic_2(i) > 0.1m_t$$
$$Combs3(i,:) = [\,]$$
$$end$$
$$end$$

3.5.10. Tiff Clearance Elimination

Pinion tiff clearance elimination is implemented by applying the following algorithm given in Table 3.20.

Table 3.20 *Pinion tiff clearance elimination algorithm*

$$for\ i = 1{:}\ size(Tiff_1)$$
$$if\ \ Tiff_1(i) < 0.2m_t$$
$$Combs3(i,:) = [\,]$$
$$end$$
$$end$$

Gear tiff clearance elimination is implemented by applying the following algorithm given in Table 3.21.

Table 3.21 *Gear tiff clearance elimination algorithm*

$$for\ i = 1{:}\ size(Tiff_2)$$
$$if\ \ Tiff_2(i) < 0.2m_t$$
$$Combs3(i,:) = [\,]$$
$$end$$
$$end$$

3.5.11. Contact Stress Elimination

Contact stress elimination is implemented by applying the following algorithm given in Table 3.22.

Table 3.22 *Contact stress elimination algorithm*

$for\ i = 1{:}\ size(R_c)$ $if\ R_c(i) < 1$ $Combs3(i,:) = [\,]$ end end

3.5.12. Bending Stress Elimination

Bending stress elimination is implemented by applying the following algorithm given in Table 3.23 and Table 3.24.

Table 3.23 *Pinion bending stress elimination algorithm*

$for\ i = 1{:}\ size(R_{t1})$ $if\ R_{t1}(i) < 1$ $Combs3(i,:) = [\,]$ end end

Table 3.24 *Gear bending stress elimination algorithm*

$for\ i = 1{:}\ size(R_{t2})$ $if\ R_{t2}(i) < 1$ $Combs3(i,:) = [\,]$ end end

3.5.13. Scuffing Elimination

Scuffing elimination is implemented by applying the following algorithm given in Table 3.25.

Table 3.25 *Scuffing elimination algorithm*

$for\ i = 1{:}\ size(Q)$
$if\ Q(i) < 1$
$Combs3(i,:) = [\,]$
end
end

After all the eliminations are implemented, the gear pair which has the lowest operating center distance is specified as the optimum gear pair among the remaining gear pairs.

CHAPTER 4

SENSITIVITY ANALYSIS AND CASE STUDIES

4.1. Sensitivity Analysis and Case Studies of External Gear Pair and Internal Gear Pair

Sensitivity analysis of external and internal gear pairs are implemented in this section. Relatively high and low speed analyses are conducted to observe the speed effect on the sensitivities of the design variables. The main aim in this section is to observe the effect of the change of the increment of design variables on objective function. The required increment values for each design variable are determined in this section.

4.1.1. Sensitivity Analysis of External Gear Pair

The external gear pairs are examined in the case studies from 1 to 10. The rotational speed of the pinion is taken as $4000\ rpm$ in the cases from 1 to 5. The pinion rotational speed is taken as $1500\ rpm$ in the cases from 6 to 10. Difference between the pinion rotational speed is applied to observe the relatively high and low speeds on the sensitivity of the design variables.

Table 4.1 gives the pinion and gear rotational speeds and the power input in the cases from 1 to 5. Table 4.2 gives the upper and lower bounds and the increment values of the pinion and gear addendum and dedendum radii.

Table 4.1 *Speed and power values for the analysis from Case 1 to Case 5*

Parameter	***Value***
n_1	$4000\ rpm$
n_2	$1017.81\ rpm$
$Power$	$1700\ kW$

Table 4.2 *Lower and upper bounds and increment values for addendum and dedendum radii for the analysis from Case 1 to Case 5*

r_{a1}	y_1	$inc1$	y_2
	0.8	0.1	1.20
r_{a2}	y_3	$inc2$	y_4
	0.8	0.1	1.20
r_{f1}	y_5	$inc3$	y_6
	-1.5	0.1	-1.10
r_{f2}	y_8	$inc4$	y_7
	-1.5	0.1	-1.10

Initial assignments of the design variables are given in Table 4.3. In the first case, pinion number of teeth is started from 10 and it is ended at 50 by increasing its value 1. The module is started from 2 mm and it is ended at 7.7 mm by increasing its value 0.3 mm. The pressure angle is started from 15° and it is ended at 35° by increasing its value 1°. The pinion profile shifting coefficient is started from -0.6 and it is ended at 0.6 by increasing its value 0.2. The helix angle is started from 5° and it is ended at 21° by increasing its value 2°. In the second cases, all the design parameters are kept as the same as they are in the first case except the parameter of the module. The module values are taken as constant values to observe the effect of the increment value of the module on objective function. In the third cases, all the design parameters are kept as the same as they are in the first case except the parameter of the helix angle. The helix angle values are taken as constant values to observe the effect of the increment value of the helix angle on objective function. In the fourth cases, all the design parameters are kept as the same as they are in the first case except the parameter of the pinion profile shifting coefficient. The pinion profile shifting coefficient values are taken as constant values to observe the effect of the increment value of the pinion profile shifting coefficient on objective function. In the fifth cases, all the design parameters are kept as the same as they are in the first case except the parameter of the pressure angle. The pressure angle values are taken as constant values to observe the effect of the increment value of the pressure angle on objective function.

Table 4.3 *Input parameters of the studies from Case1 to Case 5*

Case	z_1	$m_n\ (mm)$	$\alpha_n(deg)$	$\beta(deg)$	x_1
1	10 : 1 : 50	2 : 0.3 : 7.7	15 : 1 : 35	5 : 2 : 21	−0.6 : 0.2 : 0.6
2 A	10 : 1 : 50	2.9	15 : 1 : 35	5 : 2 : 21	−0.6 : 0.2 : 0.6
2 B	10 : 1 : 50	3.0	15 : 1 : 35	5 : 2 : 21	−0.6 : 0.2 : 0.6
2 C	10 : 1 : 50	3.1	15 : 1 : 35	5 : 2 : 21	−0.6 : 0.2 : 0.6
2 D	10 : 1 : 50	3.2	15 : 1 : 35	5 : 2 : 21	−0.6 : 0.2 : 0.6
2 E	10 : 1 : 50	3.3	15 : 1 : 35	5 : 2 : 21	−0.6 : 0.2 : 0.6
2 F	10 : 1 : 50	3.4	15 : 1 : 35	5 : 2 : 21	−0.6 : 0.2 : 0.6
2 G	10 : 1 : 50	3.5	15 : 1 : 35	5 : 2 : 21	−0.6 : 0.2 : 0.6
2 H	10 : 1 : 50	3.6	15 : 1 : 35	5 : 2 : 21	−0.6 : 0.2 : 0.6
3 A	10 : 1 : 50	2 : 0.3 : 7.7	15 : 1 : 35	10	−0.6 : 0.2 : 0.6
3 B	10 : 1 : 50	2 : 0.3 : 7.7	15 : 1 : 35	11	−0.6 : 0.2 : 0.6
3 C	10 : 1 : 50	2 : 0.3 : 7.7	15 : 1 : 35	12	−0.6 : 0.2 : 0.6
3 D	10 : 1 : 50	2 : 0.3 : 7.7	15 : 1 : 35	13	−0.6 : 0.2 : 0.6
3 E	10 : 1 : 50	2 : 0.3 : 7.7	15 : 1 : 35	14	−0.6 : 0.2 : 0.6
3 F	10 : 1 : 50	2 : 0.3 : 7.7	15 : 1 : 35	15	−0.6 : 0.2 : 0.6
3 G	10 : 1 : 50	2 : 0.3 : 7.7	15 : 1 : 35	16	−0.6 : 0.2 : 0.6
3 H	10 : 1 : 50	2 : 0.3 : 7.7	15 : 1 : 35	17	−0.6 : 0.2 : 0.6
4 A	10 : 1 : 50	2 : 0.3 : 7.7	15 : 1 : 35	5 : 2 : 21	−0.2
4 B	10 : 1 : 50	2 : 0.3 : 7.7	15 : 1 : 35	5 : 2 : 21	−0.1
4 C	10 : 1 : 50	2 : 0.3 : 7.7	15 : 1 : 35	5 : 2 : 21	0
4 D	10 : 1 : 50	2 : 0.3 : 7.7	15 : 1 : 35	5 : 2 : 21	0.1
4 E	10 : 1 : 50	2 : 0.3 : 7.7	15 : 1 : 35	5 : 2 : 21	0.2
4 F	10 : 1 : 50	2 : 0.3 : 7.7	15 : 1 : 35	5 : 2 : 21	0.3
5 A	10 : 1 : 50	2 : 0.3 : 7.7	21	5 : 2 : 21	−0.6 : 0.2 : 0.6
5 B	10 : 1 : 50	2 : 0.3 : 7.7	21.5	5 : 2 : 21	−0.6 : 0.2 : 0.6
5 C	10 : 1 : 50	2 : 0.3 : 7.7	22	5 : 2 : 21	−0.6 : 0.2 : 0.6
5 D	10 : 1 : 50	2 : 0.3 : 7.7	22.5	5 : 2 : 21	−0.6 : 0.2 : 0.6
5 E	10 : 1 : 50	2 : 0.3 : 7.7	23	5 : 2 : 21	−0.6 : 0.2 : 0.6
5 F	10 : 1 : 50	2 : 0.3 : 7.7	23.5	5 : 2 : 21	−0.6 : 0.2 : 0.6
5 G	10 : 1 : 50	2 : 0.3 : 7.7	24	5 : 2 : 21	−0.6 : 0.2 : 0.6
5 H	10 : 1 : 50	2 : 0.3 : 7.7	24.5	5 : 2 : 21	−0.6 : 0.2 : 0.6

Table 4.4 *Optimized design variables (Case1 – Case 5)*

	z_1	z_2	m_n	α_n	β	x_1	r_{a1}	r_{a2}	r_{f1}	r_{f2}	a_w
Case	-	-	*mm*	*deg*	*deg*	-	*mm*	*mm*	*mm*	*mm*	*mm*
1	37	145	3.2	23	13	0.2	64.698	241.058	56.816	233.176	298.860
2 A	41	161	2.9	24	19	0.2	66.249	249.355	59.502	242.608	309.777
2 B	40	157	3.0	26	15	0.2	65.533	246.292	58.390	239.149	305.924
2 C	37	145	3.1	22	21	0.2	65.415	243.728	57.446	235.759	302.170
2 D	37	145	3.2	23	13	0.2	64.698	241.058	56.816	233.176	298.860
2 E	37	145	3.3	23	7	0.2	65.498	244.039	57.519	236.060	302.555
2 F	35	138	3.4	23	15	0.2	65.823	246.044	57.023	237.560	304.475
2 G	35	138	3.5	23	13	0.2	67.172	251.085	58.551	242.464	310.714
2 H	35	138	3.6	24	9	0.2	68.159	254.777	59.047	246.029	315.282
3 A	44	173	2.9	22	10	0.2	68.318	257.665	60.956	250.303	319.504
3 B	38	149	3.2	24	11	0.2	65.850	245.796	58.026	237.972	304.800
3 C	38	149	3.2	23	12	0.2	66.084	246.670	57.905	238.819	305.884
3 D	37	145	3.2	23	13	0.2	64.698	241.058	56.816	233.176	298.860
3 E	37	145	3.2	23	14	0.2	64.970	242.071	57.055	234.155	300.115
3 F	37	145	3.2	23	15	0.2	65.264	243.166	57.313	235.215	301.472
3 G	37	145	3.2	23	16	0.2	65.580	244.346	57.591	236.356	302.935
3 H	37	145	3.2	22	17	0.2	65.920	245.612	57.890	237.581	304.505
4 A	50	197	2.6	24	21	-0.2	71.852	277.384	65.725	270.978	343.945
4 B	40	157	3.2	25	7	-0.1	67.382	256.633	59.967	249.218	317.567
4 C	38	149	3.2	24	13	0	65.683	247.955	57.801	240.073	307.070
4 D	35	138	3.2	24	21	0.1	63.412	239.594	55.871	231.710	296.493
4 E	37	145	3.2	23	13	0.2	64.698	241.058	56.816	233.176	298.860
4 F	37	145	3.2	24	15	0.3	65.264	242.834	57.644	235.215	301.472
5 A	41	161	2.9	21	21	0.2	67.407	253.165	59.641	245.399	313.738
5 B	37	145	3.2	21.5	21	0.2	67.525	251.591	58.956	243.364	311.917
5 C	37	145	3.2	22	17	0.2	65.920	245.612	57.890	237.581	304.505
5 D	37	145	3.2	22.5	15	0.2	65.264	243.166	57.313	235.215	301.472
5 E	37	145	3.2	23	13	0.2	64.698	241.058	56.816	233.176	298.860
5 F	37	145	3.2	23.5	13	0.2	64.698	241.058	56.488	233.176	298.860
5 G	38	149	3.2	24	11	0.2	65.850	245.796	58.026	237.972	304.800
5 H	38	149	3.2	24.5	13	0	65.683	247.955	57.801	240.073	307.070

Table 4.4 and Table 4.5 gives the pinion and gear rotational speeds and the power input in the cases from 1 to 6. Table 4.6 gives the upper and lower bounds and the increment values of the pinion and gear addendum and dedendum radii.

Table 4.5 *Speed and power values for the analysis from Case 6 to Case 10*

Parameter	***Value***
n_1	$1500\ rpm$
n_2	$381.679\ rpm$
$Power$	$1700\ kW$

Table 4.6 *Lower and upper bounds and increment values for addendum and dedendum radii for the analysis form Case 6 to Case 10*

$\boldsymbol{r_{a1}}$	$\boldsymbol{y_1}$	$\boldsymbol{inc1}$	$\boldsymbol{y_2}$
	0.8	0.1	1.20
$\boldsymbol{r_{a2}}$	$\boldsymbol{y_3}$	$\boldsymbol{inc2}$	$\boldsymbol{y_4}$
	0.8	0.1	1.20
$\boldsymbol{r_{f1}}$	$\boldsymbol{y_5}$	$\boldsymbol{inc3}$	$\boldsymbol{y_6}$
	-1.5	0.1	-1.10
$\boldsymbol{r_{f2}}$	$\boldsymbol{y_8}$	$\boldsymbol{inc4}$	$\boldsymbol{y_7}$
	-1.5	0.1	-1.10

Initial assignments of the design variables are given in Table 4.7. In the sixth case, pinion number of teeth is started from 1 and it is ended at 50 by increasing its value 1. The module is started from $2\ mm$ and it is ended at $7.7\ mm$ by increasing its value $0.3\ mm$. The pressure angle is started from 15° and it is ended at 35° by increasing its value 2°. The pinion profile shifting coefficient is started from -0.6 and it is ended at 0.6 by increasing its value 0.2. The helix angle is started from 5° and it is ended at 21° by increasing its number at 2°.

In the seventh cases, all the design parameters are kept as the same as they are in the sixth case except the parameter of the module. The module values are taken as constant values to observe the effect of the increment value of the module on objective function.

In the eight cases, all the design parameters are kept as the same as they are in the sixth case except the parameter of the helix angle. The helix angle values are taken as constant values to observe the effect of the increment value of the helix angle on objective function. In the ninth cases, all the design parameters are kept as the same as they are in the sixth case except the parameter of the pinion profile shifting coefficient. The pinion profile shifting coefficient values are taken as constant values to observe the effect of the increment value of the pinion profile shifting coefficient on objective function. In the tenth cases, all the design parameters are kept as the same as they are in the sixth case except the parameter of the pressure angle. The pressure angle values are taken as constant values to observe the effect of the increment value of the pressure angle on objective function.

Table 4.7 *Input parameters of the studies from Case 6 to Case 10*

Case	z_1	$m_n\ (mm)$	$\alpha_n(deg)$	$\beta(deg)$	x_1
6	10 : 1 : 50	2 : 0.3 : 7.7	15 : 1 : 35	5 : 2 : 21	−0.6 : 0.2 : 0.6
7 A	10 : 1 : 50	4.1	15 : 1 : 35	5 : 2 : 21	−0.6 : 0.2 : 0.6
7 B	10 : 1 : 50	4.2	15 : 1 : 35	5 : 2 : 21	−0.6 : 0.2 : 0.6
7 C	10 : 1 : 50	4.3	15 : 1 : 35	5 : 2 : 21	−0.6 : 0.2 : 0.6
7 D	10 : 1 : 50	4.4	15 : 1 : 35	5 : 2 : 21	−0.6 : 0.2 : 0.6
7 E	10 : 1 : 50	4.5	15 : 1 : 35	5 : 2 : 21	−0.6 : 0.2 : 0.6
7 F	10 : 1 : 50	4.6	15 : 1 : 35	5 : 2 : 21	−0.6 : 0.2 : 0.6
7 G	10 : 1 : 50	4.7	15 : 1 : 35	5 : 2 : 21	−0.6 : 0.2 : 0.6
7 H	10 : 1 : 50	4.8	15 : 1 : 35	5 : 2 : 21	−0.6 : 0.2 : 0.6
8 A	10 : 1 : 50	2 : 0.3 : 7.7	15 : 1 : 35	18	−0.6 : 0.2 : 0.6
8 B	10 : 1 : 50	2 : 0.3 : 7.7	15 : 1 : 35	19	−0.6 : 0.2 : 0.6
8 C	10 : 1 : 50	2 : 0.3 : 7.7	15 : 1 : 35	20	−0.6 : 0.2 : 0.6
8 D	10 : 1 : 50	2 : 0.3 : 7.7	15 : 1 : 35	21	−0.6 : 0.2 : 0.6
8 E	10 : 1 : 50	2 : 0.3 : 7.7	15 : 1 : 35	22	−0.6 : 0.2 : 0.6
8 F	10 : 1 : 50	2 : 0.3 : 7.7	15 : 1 : 35	23	−0.6 : 0.2 : 0.6
8 G	10 : 1 : 50	2 : 0.3 : 7.7	15 : 1 : 35	24	−0.6 : 0.2 : 0.6
8 H	10 : 1 : 50	2 : 0.3 : 7.7	15 : 1 : 35	25	−0.6 : 0.2 : 0.6
9 A	10 : 1 : 50	2 : 0.3 : 7.7	15 : 1 : 35	5 : 2 : 21	−0.1
9 B	10 : 1 : 50	2 : 0.3 : 7.7	15 : 1 : 35	5 : 2 : 21	0
9 C	10 : 1 : 50	2 : 0.3 : 7.7	15 : 1 : 35	5 : 2 : 21	0.1
9 D	10 : 1 : 50	2 : 0.3 : 7.7	15 : 1 : 35	5 : 2 : 21	0.2
9 E	10 : 1 : 50	2 : 0.3 : 7.7	15 : 1 : 35	5 : 2 : 21	0.3
10 A	10 : 1 : 50	2 : 0.3 : 7.7	22	5 : 2 : 21	−0.6 : 0.2 : 0.6
10 B	10 : 1 : 50	2 : 0.3 : 7.7	22.5	5 : 2 : 21	−0.6 : 0.2 : 0.6
10 C	10 : 1 : 50	2 : 0.3 : 7.7	23	5 : 2 : 21	−0.6 : 0.2 : 0.6
10 D	10 : 1 : 50	2 : 0.3 : 7.7	23.5	5 : 2 : 21	−0.6 : 0.2 : 0.6
10 E	10 : 1 : 50	2 : 0.3 : 7.7	24	5 : 2 : 21	−0.6 : 0.2 : 0.6
10 F	10 : 1 : 50	2 : 0.3 : 7.7	24.5	5 : 2 : 21	−0.6 : 0.2 : 0.6
10 G	10 : 1 : 50	2 : 0.3 : 7.7	25	5 : 2 : 21	−0.6 : 0.2 : 0.6
10 H	10 : 1 : 50	2 : 0.3 : 7.7	25.5	5 : 2 : 21	−0.6 : 0.2 : 0.6

Table 4.8 *Optimized design variables (Case6 – Case10)*

	z_1	z_2	m_n	α_n	β	x_1	r_{a1}	r_{a2}	r_{f1}	r_{f2}	a_w
Case	-	-	*mm*	*deg*	*deg*	-	*mm*	*mm*	*mm*	*mm*	*mm*
6	35	138	4.4	22	21	0.2	88.134	329.913	75.880	318.130	407.678
7 A	40	157	4.1	23	17	0.2	90.892	340.414	80.602	330.125	422.303
7 B	38	149	4.2	22	19	0.2	89.729	335.372	78.179	324.267	415.328
7 C	38	149	4.3	24	13	0.2	89.145	332.748	78.553	322.157	412.626
7 D	35	138	4.4	22	21	0.2	88.134	329.913	75.880	318.130	407.678
7 E	35	138	4.5	23	19	0.2	88.999	332.675	77.576	321.252	411.679
7 F	35	138	4.6	24	15	0.2	89.054	332.883	77.149	321.453	411.936
7 G	33	130	4.7	23	21	0.2	89.109	331.766	76.523	319.683	410.302
7 H	33	130	4.8	23	21	0.2	91.004	338.825	78.151	326.485	419.032
8 A	37	145	4.4	24	18	0	90.215	340.506	79.112	328.939	421.005
8 B	37	145	4.4	23	19	0.2	91.675	341.569	80.041	330.401	423.471
8 C	37	145	4.4	22	10	0.2	92.243	344.155	80.537	332.449	426.097
8 D	35	138	4.4	22	21	0.2	88.134	329.913	75.880	318.130	407.678
8 E	35	138	4.4	22	22	0.2	88.742	332.189	76.403	320.325	410.490
8 F	37	145	4.4	23	23	0	93.210	351.807	81.738	339.857	434.979
8 G	38	149	4.1	25	24	0.2	90.209	337.947	79.887	327.625	419.629
8 H	35	138	4.4	21	25	0.2	90.786	339.840	78.649	327.703	419.946
9 A	38	149	4.4	26	13	-0.1	89.863	341.390	79.477	331.004	422.222
9 B	37	145	4.4	24	17	0	89.720	338.637	78.678	327.594	418.695
9 C	35	138	4.4	23	21	0.1	87.663	329.913	76.351	318.130	407.678
9 D	35	138	4.4	22	21	0.2	88.134	329.913	75.880	318.130	407.678
9 E	43	169	3.8	24	21	0.3	92.397	347.201	82.628	337.839	431.457
10 A	35	138	4.4	22	21	0.2	88.134	329.913	75.880	318.130	407.678
10 B	37	145	4.4	22.5	17	0.2	90.641	338.177	79.138	326.674	418.695
10 C	35	138	4.4	23	21	0.2	88.134	329.441	76.351	318.130	407.678
10 D	37	145	4.4	23.5	13	0.2	88.960	331.455	77.671	320.617	410.932
10 E	37	145	4.4	24	13	0.2	88.960	331.455	77.671	320.617	410.932
10 F	37	145	4.4	24.5	13	0.2	88.960	331.455	77.671	320.617	410.932
10 G	38	149	4.4	25	7	0.2	89.547	334.251	78.465	323.612	414.490
10 H	35	138	4.7	25.5	15	0	90.017	340.606	78.826	329.415	420.892

The optimized results of the cases from 1 to 5 are given in Table 4.8. It is concluded that the optimized center distance is 298.860 mm in the first case with the module of 3.2 mm. When the Case 2A is considered it is seen that the optimized center distance is 309.777 mm with the module of 2.9 mm. Sensitivity of the Case 2A is considered as follow:

$$Sensitivity = \frac{(309.777\ mm - 298.860\ mm)}{(298.860\ mm)} * 100$$

The sensitivity calculation is conducted as given above for all other points in each case study. The module sensitivity and the center distance relation at 4000 rpm and 1500 rpm are given in Figure 4-1 and Figure 4-2, respectively. The optimum center distance and the optimum module value are obtained as 298.86 mm and 3.2 mm respectively in the first case. It is seen that the optimum center distances are 302.17 mm and 302.555 mm when the module values are adjusted to 3.1 mm and 3.2 mm, respectively. Therefore, changing the module value 0.1 mm around the actual optimum module deviates the center distance value 3.70 mm at most. The sensitivity of the module parameter is 1.23 % at most 0.1 mm around the actual optimum module value. When the 0.1 mm increment of the module is considered sensitivity of the module is always in a decreasing manner if the module values are moved away from the optimum module point. The optimum center distance and the optimum module value are obtained as 407.678 mm and 4.4 mm respectively in the sixth case. It is seen that the optimum center distances are 412.626 mm and 411.679 mm when the module values are adjusted to 4.3 mm and 4.5 mm, respectively. Therefore, changing the module value 0.1 mm around the actual optimum module deviates the center distance value 4.948 mm at most. The sensitivity of the module parameter is 1.21 % at most 0.1 mm around the actual optimum module value. When the 0.1 mm increment of the module is considered sensitivity of the module is always in a decreasing manner if the module values are moved away from the optimum module

point. The increment of the module value is specified as $0.1\,mm$ which gives a sensitivity value of $1.23\,\%$ at most.

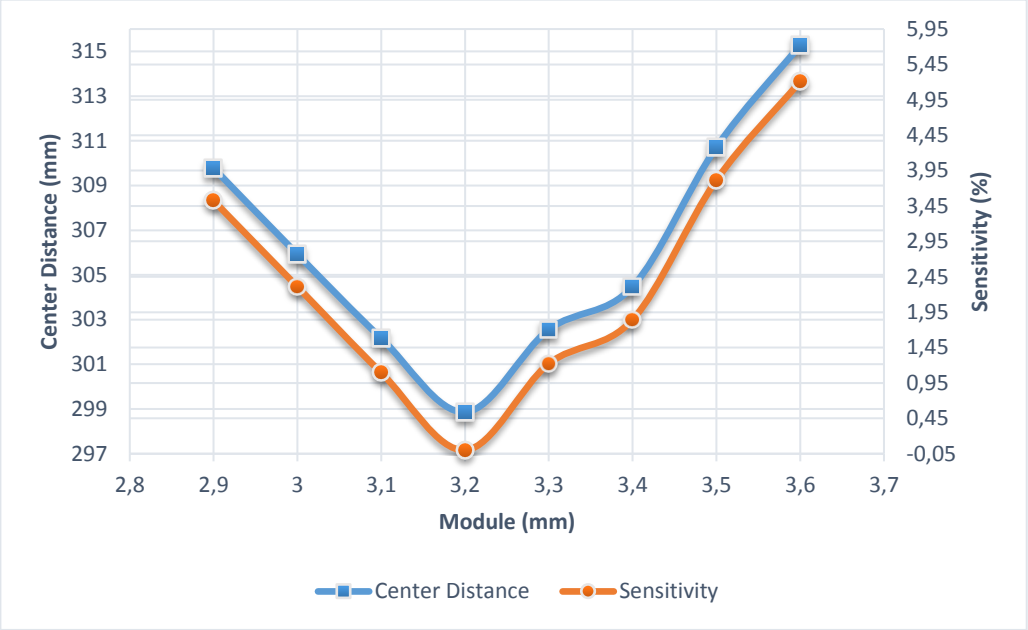

Figure 4-1 *Module sensitivity and center distance relation of external gear pair at relatively higher pinion rotational speed (4000 rpm)*

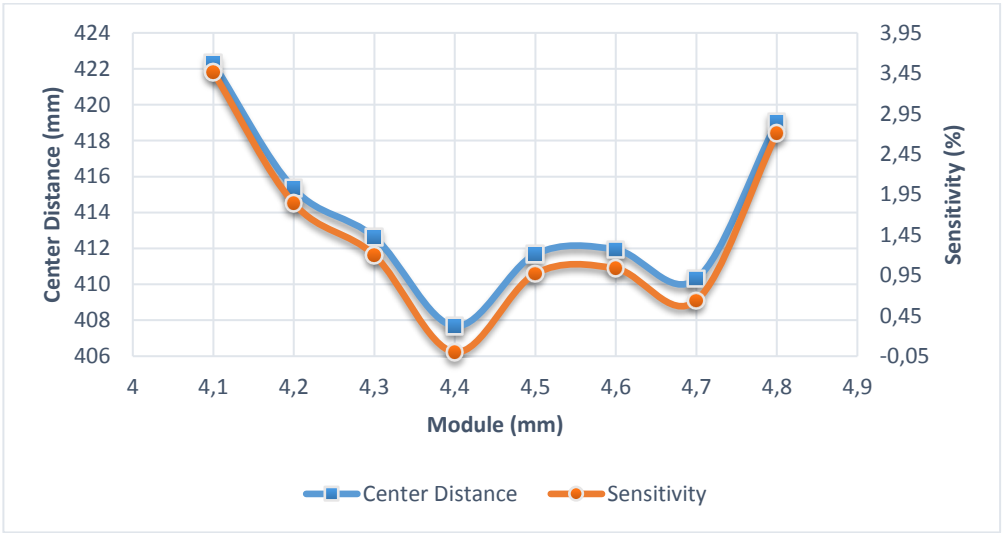

Figure 4-2 *Module sensitivity and center distance relation of external gear pair at relatively lower pinion rotational speed (1500 rpm)*

The helix angle sensitivity and the center distance relation at 4000 rpm and 1500 rpm are given in Figure 4-3 and Figure 4-4, respectively. The optimum center distance and the optimum helix angle value are obtained as $298.86\ mm$ and 13° respectively in the first case. It is seen that the optimum center distances are $305.884\ mm$ and $300.115\ mm$ when the helix angle values are adjusted to 12° and 14°, respectively. Therefore, changing the helix angle value 1° around the actual optimum helix angle deviates the center distance value $7.02\ mm$ at most. The sensitivity of the helix angle parameter is $2.35\ \%$ at most 1° around the actual optimum helix angle value. When the 1° increment of the helix angle is considered sensitivity of the helix angle in a decreasing manner if the helix angle values are moved away from the optimum helix angle point.

The optimum center distance and the optimum helix angle value are obtained as $407.678\ mm$ and 21° respectively in the sixth case. It is seen that the optimum center distances are $426.097\ mm$ and $410.49\ mm$ when the helix angle values are adjusted to 20° and 22°, respectively. Therefore, changing the helix angle value 1° around the actual optimum helix angle deviates the center distance value $18.419\ mm$ at most. The sensitivity of the helix angle parameter is $4.52\ \%$ at most 1°around the actual optimum helix angle value. When the 1° increment of the helix angle is considered sensitivity of the module is not always in a decreasing manner if the helix angle values are moved away from the optimum helix angle point. The sensitivity value does not show a consistent behavior as opposite to obtained in $4000\ rpm$. Therefore, when the rotational speed of the pinion is decreased the helix angle does not keep its consistent behavior any more. Although this inconsistency, the sensitivity of the helix angle is still below the $5\ \%$ 1°around the actual optimum helix angle value. The increment of the helix angle value is specified as 1° which gives a sensitivity value of $4.52\ \%$ at most.

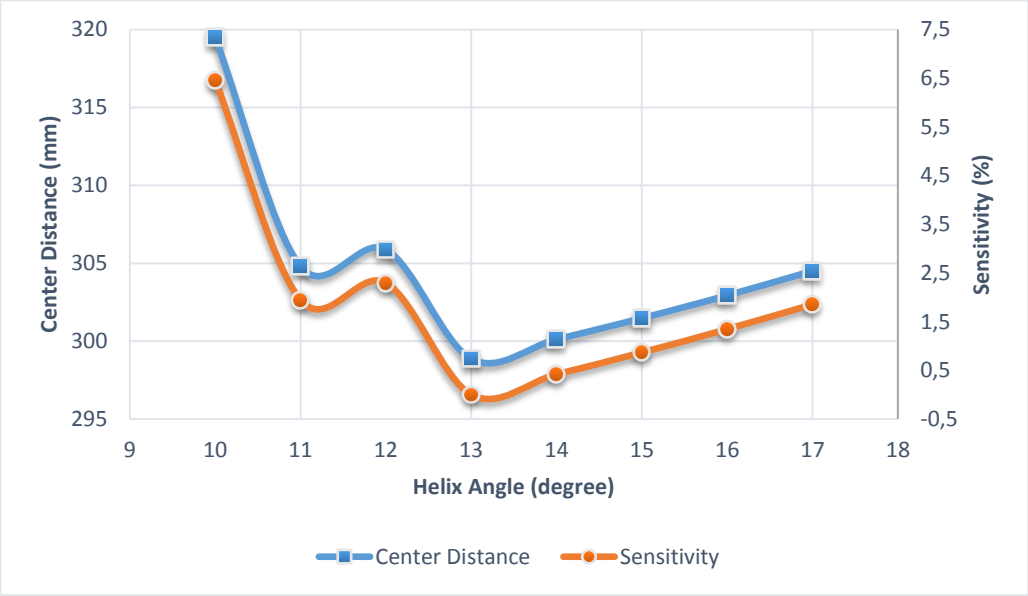

Figure 4-3 *Helix angle sensitivity and center distance relation of external gear pair at relatively higher pinion rotational speed (4000 rpm)*

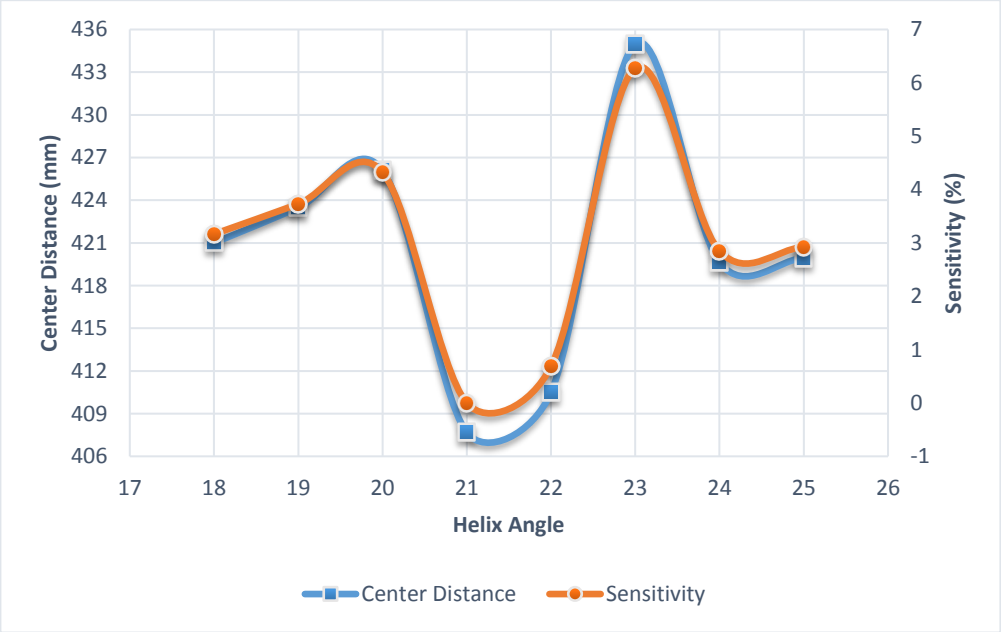

Figure 4-4 *Helix angle sensitivity and center distance relation of external gear pair at relatively lower pinion rotational speed (1500 rpm)*

The pinion profile shifting coefficient sensitivity and the center distance relation at 4000 rpm and 1500 rpm are given in Figure 4-5 and Figure 4-6, respectively. The optimum center distance and the optimum profile shifting coefficient are obtained as $298.86\ mm$ and 0.2 respectively in the first case. It is seen that the optimum center distances are $296.493\ mm$ and $301.472\ mm$ when the pinion profile shifting coefficient values are adjusted to 0.1 and 0.3, respectively. Therefore, changing the pinion profile shifting coefficient value 0.1 around the actual optimum profile shifting coefficient deviates the center distance value $2.61\ mm$ at most. The sensitivity of the pinion profile shifting coefficient parameter is $0.87\ \%$ at most 0.1 around the actual optimum pinion profile shifting coefficient value. When the 0.1 increment of the pinion profile shifting coefficient is considered sensitivity of the pinion profile shifting coefficient in a decreasing manner if the pinion profile shifting coefficient values are moved away from the optimum pinion profile shifting coefficient point.

The optimum center distance and the optimum pinion profile shifting coefficient value are obtained as $407.678\ mm$ and 0.2 respectively in the sixth case. It is seen that the optimum center distances are $407.678\ mm$ and $431.457\ mm$ when the pinion profile shifting coefficient values are adjusted to 0.1 and 0.3, respectively. Therefore, changing the pinion profile shifting coefficient value 0.1 around the actual optimum pinion profile shifting coefficient deviates the center distance value $23.78\ mm$ at most. The sensitivity of the pinion profile shifting coefficient parameter is $5.83\ \%$ at most 0.1 around the actual optimum pinion profile shifting coefficient value. When the 0.1 increment of the pinion profile shifting coefficient is considered sensitivity of the pinion profile shifting coefficient is in a decreasing manner if the pinion profile shifting coefficient values are moved away from the optimum pinion profile shifting coefficient point.

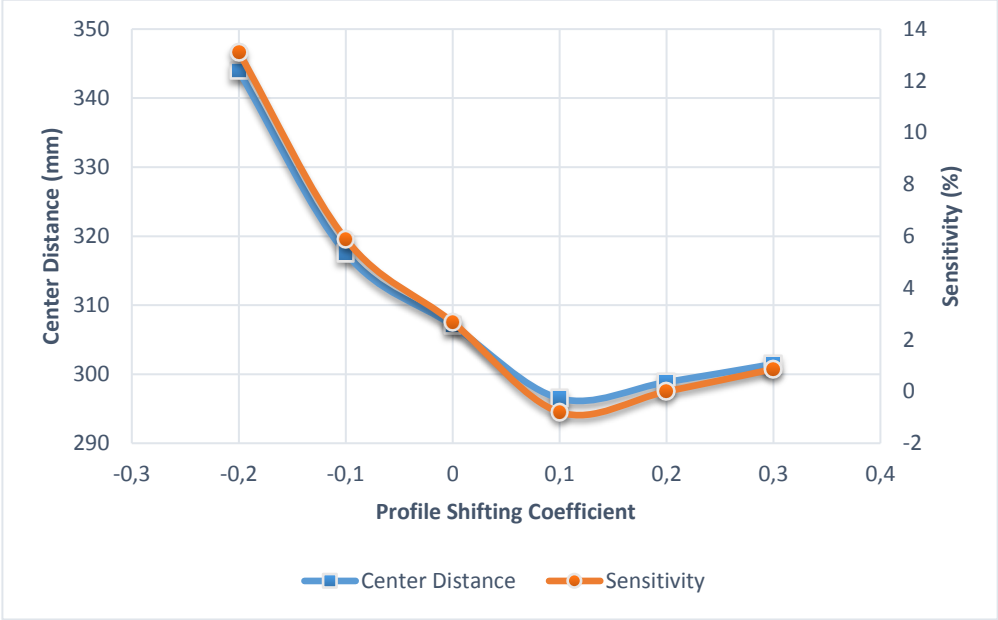

Figure 4-5 *Pinion profile shifting coefficient sensitivity and center distance relation of external gear pair at relatively higher pinion rotational speed (4000 rpm)*

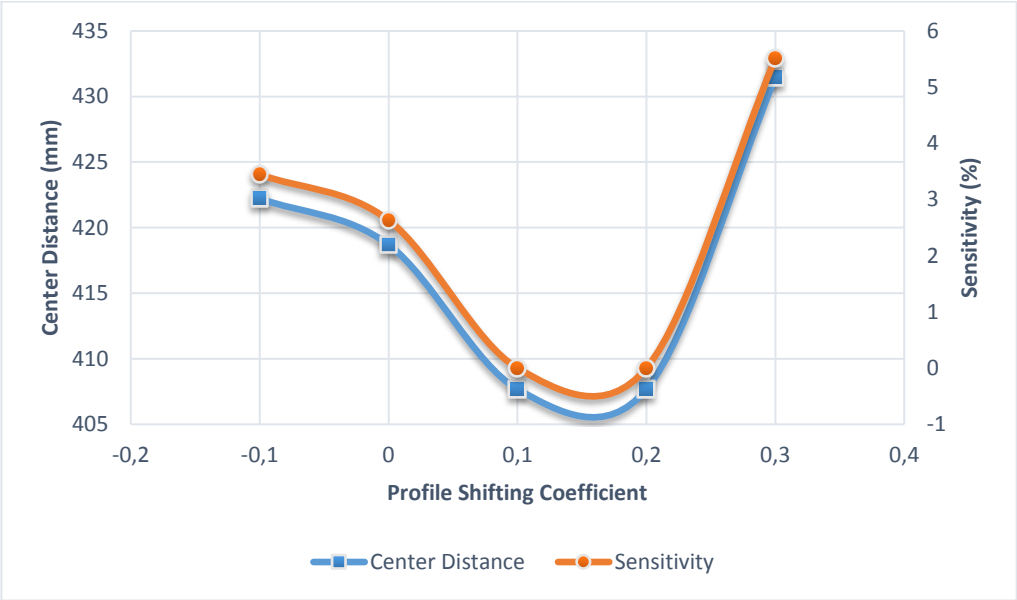

Figure 4-6 *Pinion profile shifting coefficient sensitivity and center distance relation of external gear pair at relatively higher pinion rotational speed (1500 rpm)*

The pressure angle sensitivity and the center distance relation at 4000 rpm and 1500 rpm are given in Figure 4-7 and Figure 4-8, respectively. The optimum center distance and the optimum pressure angle value are obtained as $298.86\,mm$ and 23° respectively in the first case. It is seen that the optimum center distances are $301.472\,mm$ and $298.86\,mm$ when the pressure angle values are adjusted to 22.5° and 23.5°, respectively. Therefore, changing the pressure angle value 0.5° around the actual optimum pressure angle deviates the center distance value $2.61\,mm$ at most. The sensitivity of the pressure angle parameter is $0.87\,\%$ at most 0.5° around the actual optimum pressure angle value. When the 0.5° increment of the pressure angle is considered sensitivity of the pressure angle in a decreasing manner if the pressure angle values are moved away from the optimum pressure angle point.

The optimum center distance and the optimum pressure angle value are obtained as $407.678\,mm$ and 23° respectively in the sixth case. It is seen that the optimum center distances are $418.695\,mm$ and $410.932\,mm$ when the pressure angle values are adjusted to 22.5° and 23.5°, respectively. Therefore, changing the pressure angle value 0.5° around the actual optimum pressure angle deviates the center distance value $11.017\,mm$ at most. The sensitivity of the pressure angle parameter is $2.7\,\%$ at most 0.5°around the actual optimum pressure angle value. When the 0.5° increment of the pressure angle is considered sensitivity of the pressure angle is not always in a decreasing manner if the pressure angle values are moved away from the optimum pressure angle point. The sensitivity value does not show a consistent behavior as opposite to obtained in $4000\,rpm$. Therefore, when the rotational speed of the pinion is decreased the pressure angle does not keep its consistent behavior any more. Although this inconsistency, the sensitivity of the pressure angle is still below the $5\,\%$ 0.5°around the actual optimum pressure angle value. The increment of the pressure angle value is specified as 0.5° which gives a sensitivity value of $2.7\,\%$ at most.

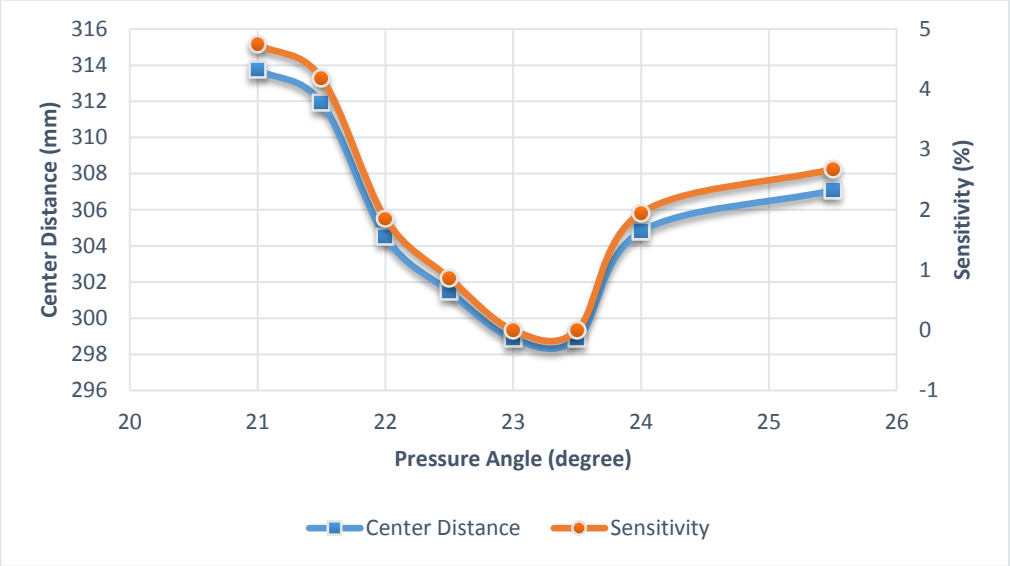

Figure 4-7 *Pressure angle sensitivity and center distance relation of external gear pair at relatively higher pinion rotational speed (4000 rpm)*

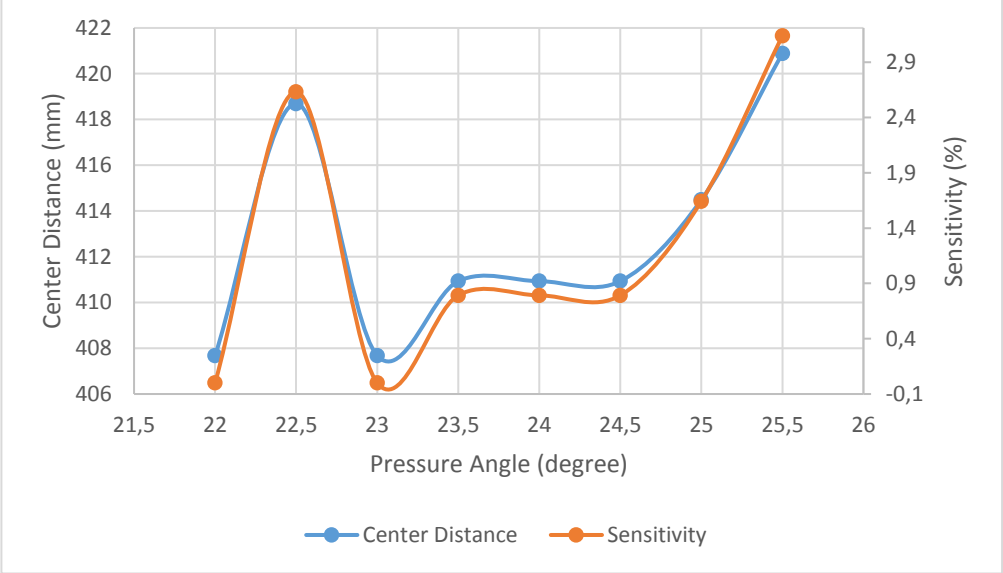

Figure 4-8 *Pressure angle sensitivity and center distance relation of external gear pair at relatively lower pinion rotational speed (1500 rpm)*

4.1.2. Addendum and Dedendum Radii Sensitivity of External Gear Pairs

Sensitivity analysis of the addendum and dedendum radii is evaluated in this section. Initial assignments of the design variables and pinion and gear rotational speeds and input power are given in Table 4.9. In the EX2 case, all the design parameters are almost kept as the same as they are in the EX1 case except the increment of the addendum and dedendum radii. In EX3 case, all the design parameters are kept as the same as they are in the EX1 case except the increment of the addendum and dedendum radii.

Table 4.9 *Input parameters and initial assignment of the design variables of Case EX1, EX2 and EX3*

PARAMATERS	***EX 1***	***EX 2***	***EX 3***
N_1	$10:1:50$	$13:1:47$	$10:1:50$
m_n (mm)	$2:0.3:7.7$	$3.2:0.3:7.7$	$2.0:0.3:7.7$
α_n (degree)	$15:1:35$	$15:1:35$	$15:1:35$
β (degree)	$5:2:21$	$5:2:21$	$5:2:21$
x_1	$-0.6:0.2:0.6$	$-0.6:0.2:0.6$	$-0.6:0.2:0.6$
y_1	0.80	0.80	0.80
y_2	1.20	1.20	1.20
y_3	0.80	0.80	0.80
y_4	1.20	1.20	1.20
y_5	-1.50	-1.50	-1.50
y_6	-1.10	-1.10	-1.10
y_7	-1.50	-1.50	-1.50
y_8	-1.10	-1.10	-1.10
$\boldsymbol{inc1}$	0.2	0.1	0.05
$\boldsymbol{inc2}$	0.2	0.1	0.05
$\boldsymbol{inc3}$	0.2	0.1	0.05
$\boldsymbol{inc4}$	0.2	0.1	0.05
$\boldsymbol{n_1}$	$4000\ rpm$	$4000\ rpm$	$4000\ rpm$
$\boldsymbol{n_2}$	$1017.81\ rpm$	$1017.81\ rpm$	$1017.81\ rpm$
$Power$	$1700\ kW$	$1700\ kW$	$1700\ kW$

When the optimized results of the Case EX1, Case EX2 and Case EX3 are considered It is seen that the optimum center distances are $307.07\ mm$, $298.860\ mm$ and $296.493\ mm$, respectively. The optimum center is obtained as $298.860\ mm$ in the first case. Therefore, changing the increment value of the addendum and dedendum radii $0.05\ mm$ around the actual optimum increment of the addendum and dedendum radii the center distance value $8.21\ mm$ at most. The sensitivity of the increment of the addendum and dedendum radii is $2.75\ \%$ at most $0.05\ mm$ around the actual optimum increment of the addendum and dedendum radii.

Table 4.10 *Optimized design variables (Case EX1 – Case Ex3)*

Case Study	**EX 1**	**EX 2**	**EX 3**
$\boldsymbol{m_n}$	$3.2\ mm$	$3.2\ mm$	$3.2\ mm$
$\boldsymbol{\beta}$	13°	13°	21°
$\boldsymbol{x_1}$	0	0.2	0.2
$\boldsymbol{r_{a1}}$	$65.683\ mm$	$64.698\ mm$	$63.926\ mm$
$\boldsymbol{r_{a2}}$	$247.955\ mm$	$241.058\ mm$	$239.594\ mm$
$\boldsymbol{r_{f1}}$	$58.130\ mm$	$56.816\ mm$	$55.528\ mm$
$\boldsymbol{r_{f2}}$	$240.401\ mm$	$233.176\ mm$	$231.367\ mm$
$\boldsymbol{N_1}$	38	37	35
$\boldsymbol{N_2}$	149	145	138
$\boldsymbol{\alpha_n}$	24°	23°	23°
$\boldsymbol{a_w}$	$307.070\ mm$	$298.860\ mm$	$296.493\ mm$

Initial assignments of the design variables and pinion and gear rotational speeds and input power are given in Table 4.11. In the EX4 case, pinion number of teeth is started from 1 and it is ended at 50 by increasing its value 1. The module is started from $2\ mm$ and it is ended at $7.7\ mm$ by increasing its value $0.3\ mm$. The pressure angle is started from 15° and it is ended at 35° by increasing its value 1°. The pinion profile shifting coefficient is started from -0.6 and it is ended at 0.6 by increasing its value 0.2. The helix angle is started from 5° and it is ended at 21° by increasing its value 2°.

In the EX5 case, all the design parameters are kept as the same as they are in the EX1 case except the increment of the addendum and dedendum radii. In EX6 case, all the design parameters are kept as the same as they are in the EX1 case except the increment of the addendum and dedendum radii.

Table 4.11 *Input parameters and initial assignment of the design variables of Case EX4, EX5 and EX6*

PARAMATERS	***EX 4***	***EX 5***	***EX 6***
N_1	$10:1:50$	$10:1:50$	$10:1:50$
m_n (mm)	$2:0.3:7.7$	$2:0.3:7.7$	$2.0:0.3:7.7$
α_n (degree)	$15:1:35$	$15:1:35$	$15:1:35$
β (degree)	$5:2:21$	$5:2:21$	$5:2:21$
x_1	$-0.6:0.2:0.6$	$-0.6:0.2:0.6$	$-0.6:0.2:0.6$
y_1	0.80	0.80	0.80
y_2	1.20	1.20	1.20
y_3	0.80	0.80	0.80
y_4	1.20	1.20	1.20
y_5	-1.50	-1.50	-1.50
y_6	-1.10	-1.10	-1.10
y_7	-1.50	-1.50	-1.50
y_8	-1.10	-1.10	-1.10
$\boldsymbol{inc1}$	0.2	0.1	0.05
$\boldsymbol{inc2}$	0.2	0.1	0.05
$\boldsymbol{inc3}$	0.2	0.1	0.05
$\boldsymbol{inc4}$	0.2	0.1	0.05
$\boldsymbol{n_1}$	$1500\ rpm$	$1500\ rpm$	$1500\ rpm$
$\boldsymbol{n_2}$	$381.679\ rpm$	$381.679\ rpm$	$381.679\ rpm$
$Power$	$1700\ kW$	$1700\ kW$	$1700\ kW$

The optimized results of the Case EX4, Case EX5 and Case EX6 are given in Table 4.12. It is seen that when the increments of the addendum and dedendum radii are taken as $0.2\ mm, 0.1\ mm\ and\ 0.05\ mm$ the optimum center distances are same. Changing the increment of the addendum and dedendum radii has not an effect on the center distance when the rotational speed of the pinion is decreased.

Table 4.12 *Optimized design variables (Case EX4 – Case Ex6)*

Case Study	Inc 0.2	Inc 0.1	Inc 0.05
m_n	4.4 mm	4.4 mm	4.4 mm
β	21°	21°	21°
x_1	0.2	0.2	0.2
r_{a1}	88.134 mm	88.134 mm	88.134 mm
r_{a2}	329.913 mm	329.913 mm	329.913 mm
r_{f1}	76.351 mm	75.880 mm	75.880 mm
r_{f2}	318.130 mm	318.130 mm	318.130 mm
N_1	35	35	35
N_2	138	138	138
α_n	22°	22°	22°
a_w	407.678 mm	407.678 mm	407.678 mm

4.1.3. Detailed Optimization of Case 1

As discussed in the previous sections, the increment of the all design parameters are specified according to sensitivity analyses. In this section, the specified increments for each design parameter are used to obtain more optimum results. Initial assignments of the design variables, rotational speed of the pinion and the gear and the input power is given in Table 4.13. Optimization result of the first case study is given in

Table 4.4. The first case study is evaluated again by changing the increments of each design variables. In Case 1 Detailed A, increment of the module, pressure angle, helix angle and pinion profile shifting coefficient are changed from 0.3 mm , 1°, 2° and 0.2 to 0.1 mm , 0.5°, 1° and 0.1 respectively to observe the more optimal results. In Case 1 Detailed B, the increment of the design variables are kept constant as in Case 1 Detailed A. However, increment of the addendum and dedendum radii is changed from 0.1 mm to 0.05 mm.

Table 4.13 *Input parameters and initial assignment of the design variables of Case 1 Detailed A and Case 1 Detailed B*

PARAMATERS	***Case 1***	***Case 1 Detailed A***	***Case 1 Detailed B***
N_1	$10:1:50$	$35:1:41$	$33:1:38$
m_n (mm)	$2:0.3:7.7$	$2.9:0.1:3.4$	$3.1:0.1:3.3$
α_n (degree)	$15:1:35$	$21:0.5:28$	$22.5:0.5:26$
β (degree)	$5:2:21$	$10:1:20$	$13:1:20$
x_1	$-0.6:0.2:0.6$	$-0.1:0.1:0.3$	$0.1:0.1:0.2$
y_1	0.80	0.80	0.80
y_2	1.20	1.20	1.20
y_3	0.80	0.80	0.80
y_4	1.20	1.20	1.20
y_5	-1.50	-1.50	-1.50
y_6	-1.10	-1.10	-1.10
y_7	-1.50	-1.50	-1.50
y_8	-1.10	-1.10	-1.10
$\boldsymbol{inc1}$	0.1	0.1	0.05
$\boldsymbol{inc2}$	0.1	0.1	0.05
$\boldsymbol{inc3}$	0.1	0.1	0.05
$\boldsymbol{inc4}$	0.1	0.1	0.05
$\boldsymbol{n_1}$	$4000\ rpm$	$4000\ rpm$	$4000\ rpm$
$\boldsymbol{n_2}$	$1017.81\ rpm$	$1017.81\ rpm$	$1017.81\ rpm$
$Power$	$1700\ kW$	$1700\ kW$	$1700\ kW$

The optimized results of the Case 1, Case 1 Detailed A and Case 1 Detailed B are given in Table 4.14. As seen from Table 4.14, the more optimal results are obtained when the increment of the design variable and the increment of the addendum and dedendum radii are deceased to values which are obtained as results of sensitivity analyses.

Table 4.14 *Optimized design variables (Case 1 Detailed A – Case 1 Detailed B)*

Case Study	Case 1	Case 1 Detailed A	Case 1 Detailed B
m_n	3.2 mm	3.3 mm	3.3 mm
β	13°	15°	14°
x_1	0.2	0.1	0.1
r_{a1}	64.698 mm	63.204 mm	63.089 mm
r_{a2}	241.058 mm	238.807 mm	237.732 mm
r_{f1}	56.816 mm	55.346 mm	55.437 mm
r_{f2}	233.176 mm	230.949 mm	229.739 mm
N_1	37	35	35
N_2	145	138	138
α_n	23°	25.5°	25°
a_w	298.860 mm	295.520 mm	294.189 mm

4.1.4. Detailed Optimization of Case 6

Initial assignments of the design variables, rotational speed of the pinion and the gear and the input power is given in Table 4.15. Optimization result of the sixth case study is given in Table 4.8. The sixth case study is evaluated again by changing the increments of each design variables. In Case 6 Detailed A, increment of the module, pressure angle, helix angle and pinion profile shifting coefficient are changed from $0.3\ mm$, 1°, 2° and 0.2 to $0.1\ mm$, 0.5°, 1° and 0.1 respectively to observe the more optimal results. In Case 6 Detailed B, the increment of the design variables are kept constant. However, increment of the addendum and dedendum radii are changed from $0.1\ mm$ to $0.05\ mm$.

Table 4.15 *Input parameters and initial assignment of the design variables of Case 6 Detailed A and Case 6 Detailed B*

PARAMATERS	***Case 6***	***Case 6 Detailed A***	***Case 6 Detailed B***
N_1	$10:1:50$	$27:1:41$	$33:1:38$
m_n (mm)	$2:0.3:7.7$	$4.0:0.1:5.6$	$3.1:0.1:3.3$
α_n (degree)	$15:1:35$	$20:0.5:28$	$22.5:0.5:26$
β (degree)	$5:2:21$	$7:1:21$	$13:1:20$
x_1	$-0.6:0.2:0.6$	$-0.1:0.1:0.3$	$0.1:0.1:0.2$
y_1	0.80	0.80	0.80
y_2	1.20	1.20	1.20
y_3	0.80	0.80	0.80
y_4	1.20	1.20	1.20
y_5	-1.50	-1.50	-1.50
y_6	-1.10	-1.10	-1.10
y_7	-1.50	-1.50	-1.50
y_8	-1.10	-1.10	-1.10
$\boldsymbol{inc1}$	0.1	0.1	0.05
$\boldsymbol{inc2}$	0.1	0.1	0.05
$\boldsymbol{inc3}$	0.1	0.1	0.05
$\boldsymbol{inc4}$	0.1	0.1	0.05
$\boldsymbol{n_1}$	$1500\ rpm$	$1500\ rpm$	$1500\ rpm$
$\boldsymbol{n_2}$	$381.679\ rpm$	$381.679\ rpm$	$381.679\ rpm$
$Power$	$1700\ kW$	$1700\ kW$	$1700\ kW$

The optimized results of the Case 1, Case 1 Detailed A and Case 1 Detailed B are given in Table 4.16. As seen from Table 4.16, the more optimal results are obtained when the increment of the design variable and the increment of the addendum and dedendum radii are deceased to values which are obtained as results of sensitivity analyses.

Table 4.16 *Optimized design variables (Case 6 Detailed A – Case 6 Detailed B)*

Case Study	**Case 6**	**Actual Case 6 A Detailed**	**Actual Case 6 B Detailed**
$\boldsymbol{m_n}$	4.4 mm	4.2 mm	4.4 mm
$\boldsymbol{\beta}$	21°	20°	20°
$\boldsymbol{x_1}$	0.2	0.2	0.2
$\boldsymbol{r_{a1}}$	88.134 mm	88.050 mm	87.561 mm
$\boldsymbol{r_{a2}}$	329.913 mm	328.512 mm	327.533 mm
$\boldsymbol{r_{f1}}$	75.880 mm	76.876 mm	75.620 mm
$\boldsymbol{r_{f2}}$	318.130 mm	317.338 mm	316.061 mm
$\boldsymbol{N_1}$	35	37	35
$\boldsymbol{N_2}$	138	145	138
$\boldsymbol{\alpha_n}$	22°	22°	23°
$\boldsymbol{a_w}$	407.678 mm	406.729 mm	405.026 mm

4.2. Sensitivity Analysis and Case Studies of Internal Gear Pair

The internal gear pairs are examined in the case studies from 11 to 20. The rotational speed of the pinion is taken as $900\ rpm$ in the cases from 11 to 15. The pinion rotational speed is taken as $3000\ rpm$ in the cases from 16 to 20. Difference between the pinion rotational speed is applied to observe the relatively high and low speeds on the sensitivity of the design variables. Table 4.17 gives the pinion and gear rotational speeds and the power input in the cases from 11 to 15. Table 4.18 gives the upper and lower bounds and the increment values of the pinion and gear addendum and dedendum radii.

Table 4.17 *Speed and power values for the analysis from Case 11 to Case 15*

Parameter	***Value***
n_1	$900\ rpm$
n_2	$329\ rpm$
$Power$	$1700\ kW$

Table 4.18 *Lower and upper bounds and increment values for addendum and dedendum radii for the analysis from Case 11 to Case 15*

r_{a1}	y_1	$inc1$	y_2
	0.80	0.1	1.20
r_{a2}	y_3	$inc2$	y_4
	-1.20	0.1	-0.80
r_{f1}	y_5	$inc3$	y_6
	-1.40	0.1	-1.00
r_{f2}	y_8	$inc4$	y_7
	1.00	0.1	1.40

Initial assignments of the design variables are given in Table 4.19. In the 11th case, pinion number of teeth is started from 10 and it is ended at 50 by increasing its value 1. The module is started from 2 mm and it is ended at 7.7 mm by increasing its value 0.3 mm. The pressure angle is started from 15° and it is ended at 35° by increasing its value 1°. The pinion profile shifting coefficient is started from -0.6 and it is ended at 0.6 by increasing its value 0.2. The helix angle is started from 5° and it is ended at 21° by increasing its value 2°. In the 12th cases, all the design parameters are kept as the same as they are in the 11th case except the parameter of the module. The module values are taken as constant values to observe the effect of the increment value of the module on objective function. In the 13th cases, all the design parameters are kept as the same as they are in the 11th case except the parameter of the helix angle. The helix angle values are taken as constant values to observe the effect of the increment value of the helix angle on objective function. In the 14th cases, all the design parameters are kept as the same as they are in the 11th case except the parameter of the pinion profile shifting coefficient. The pinion profile shifting coefficient values are taken as constant values to observe the effect of the increment value of the pinion profile shifting coefficient on objective function. In the 15th cases, all the design parameters are kept as the same as they are in the 11th case except the parameter of the pressure angle. The pressure angle values are taken as constant values to observe the effect of the increment value of the pressure angle on objective function.

Table 4.19 *Input parameters of the studies from Case 11 to Case 15*

Case	N_1	m_n (mm)	$\alpha_n(deg)$	$\beta(deg)$	x_1
11	10 : 1 : 50	2 : 0.3 : 7.7	15 : 1 : 35	5 : 2 : 21	−0.6 : 0.2 : 0.6
12 A	10 : 1 : 50	6.8	15 : 1 : 35	5 : 2 : 21	−0.6 : 0.2 : 0.6
12 B	10 : 1 : 50	6.9	15 : 1 : 35	5 : 2 : 21	−0.6 : 0.2 : 0.6
12 C	10 : 1 : 50	7.0	15 : 1 : 35	5 : 2 : 21	−0.6 : 0.2 : 0.6
12 D	10 : 1 : 50	7.1	15 : 1 : 35	5 : 2 : 21	−0.6 : 0.2 : 0.6
12 E	10 : 1 : 50	7.2	15 : 1 : 35	5 : 2 : 21	−0.6 : 0.2 : 0.6
12 F	10 : 1 : 50	7.3	15 : 1 : 35	5 : 2 : 21	−0.6 : 0.2 : 0.6
12 G	10 : 1 : 50	7.4	15 : 1 : 35	5 : 2 : 21	−0.6 : 0.2 : 0.6
12 H	10 : 1 : 50	7.5	15 : 1 : 35	5 : 2 : 21	−0.6 : 0.2 : 0.6
13 A	10 : 1 : 50	2 : 0.3 : 7.7	15 : 1 : 35	6	−0.6 : 0.2 : 0.6
13 B	10 : 1 : 50	2 : 0.3 : 7.7	15 : 1 : 35	7	−0.6 : 0.2 : 0.6
13 C	10 : 1 : 50	2 : 0.3 : 7.7	15 : 1 : 35	8	−0.6 : 0.2 : 0.6
13 D	10 : 1 : 50	2 : 0.3 : 7.7	15 : 1 : 35	9	−0.6 : 0.2 : 0.6
13 E	10 : 1 : 50	2 : 0.3 : 7.7	15 : 1 : 35	10	−0.6 : 0.2 : 0.6
13 F	10 : 1 : 50	2 : 0.3 : 7.7	15 : 1 : 35	11	−0.6 : 0.2 : 0.6
13 G	10 : 1 : 50	2 : 0.3 : 7.7	15 : 1 : 35	12	−0.6 : 0.2 : 0.6
13 H	10 : 1 : 50	2 : 0.3 : 7.7	15 : 1 : 35	13	−0.6 : 0.2 : 0.6
13 I	10 : 1 : 50	2 : 0.3 : 7.7	15 : 1 : 35	14	−0.6 : 0.2 : 0.6
13 J	10 : 1 : 50	2 : 0.3 : 7.7	15 : 1 : 35	15	−0.6 : 0.2 : 0.6
13 K	10 : 1 : 50	2 : 0.3 : 7.7	15 : 1 : 35	16	−0.6 : 0.2 : 0.6
13 L	10 : 1 : 50	2 : 0.3 : 7.7	15 : 1 : 35	17	−0.6 : 0.2 : 0.6
14 A	10 : 1 : 50	2 : 0.3 : 7.7	15 : 1 : 35	5 : 2 : 21	−0.1
14 B	10 : 1 : 50	2 : 0.3 : 7.7	15 : 1 : 35	5 : 2 : 21	0
14 C	10 : 1 : 50	2 : 0.3 : 7.7	15 : 1 : 35	5 : 2 : 21	0.1
14 D	10 : 1 : 50	2 : 0.3 : 7.7	15 : 1 : 35	5 : 2 : 21	0.2
15 A	10 : 1 : 50	2 : 0.3 : 7.7	27.5	5 : 2 : 21	−0.6 : 0.2 : 0.6
15 B	10 : 1 : 50	2 : 0.3 : 7.7	28	5 : 2 : 21	−0.6 : 0.2 : 0.6
15 C	10 : 1 : 50	2 : 0.3 : 7.7	28.5	5 : 2 : 21	−0.6 : 0.2 : 0.6
15 D	10 : 1 : 50	2 : 0.3 : 7.7	29	5 : 2 : 21	−0.6 : 0.2 : 0.6
15 E	10 : 1 : 50	2 : 0.3 : 7.7	29.5	5 : 2 : 21	−0.6 : 0.2 : 0.6
15 F	10 : 1 : 50	2 : 0.3 : 7.7	30	5 : 2 : 21	−0.6 : 0.2 : 0.6
15 G	10 : 1 : 50	2 : 0.3 : 7.7	30.5	5 : 2 : 21	−0.6 : 0.2 : 0.6
15 H	10 : 1 : 50	2 : 0.3 : 7.7	31	5 : 2 : 21	−0.6 : 0.2 : 0.6
15 I	10 : 1 : 50	2 : 0.3 : 7.7	31.5	5 : 2 : 21	−0.6 : 0.2 : 0.6
15 J	10 : 1 : 50	2 : 0.3 : 7.7	32	5 : 2 : 21	−0.6 : 0.2 : 0.6
15 K	10 : 1 : 50	2 : 0.3 : 7.7	32.5	5 : 2 : 21	−0.6 : 0.2 : 0.6
15 L	10 : 1 : 50	2 : 0.3 : 7.7	33	5 : 2 : 21	−0.6 : 0.2 : 0.6

Table 4.20 *Optimized design variables (Case 11- Case15)*

	z_1	z_2	m_n	α_n	β	x_1	r_{a1}	r_{a2}	r_{f1}	r_{f2}	a_w
Case	-	-	*mm*	*deg*	*deg*	-	*mm*	*mm*	*mm*	*mm*	*mm*
11	25	68	7.1	29	7	0	95.855	236.060	80.117	251.797	153.796
12 A	26	71	6.8	28	7	0.2	96.600	237.732	81.528	252.804	154.149
12 B	25	68	6.9	28	15	0	95.722	235.732	80.006	251.448	153.583
12 C	25	68	7.0	28	13	0	96.267	237.076	80.462	252.881	154.459
12 D	25	68	7.1	29	7	0	95.855	236.060	80.117	251.797	153.796
12 E	25	68	7.2	29	5	0	96.849	238.508	80.948	254.408	155.391
12 F	25	68	7.3	29	5	0	98.194	241.820	82.072	257.942	157.550
12 G	23	63	7.4	26	19	0.2	98.613	239.488	80.612	257.488	156.528
12 H	23	63	7.5	28	15	0	96.281	236.820	79.199	253.902	155.291
13 A	25	68	7.1	29	6	0	95.664	235.591	79.958	251.297	153.491
13 B	25	68	7.1	29	7	0	95.855	236.060	80.117	251.797	153.796
13 C	25	68	7.1	28	8	0.2	97.509	238.037	81.018	253.810	154.150
13 D	25	68	7.1	29	9	0	96.326	237.221	80.511	253.035	154.553
13 E	25	68	7.1	29	10	0	96.608	237.915	80.747	253.775	155.005
13 F	35	96	5.0	27	11	0.2	94.741	240.417	83.025	251.623	155.354
13 G	35	96	5.0	27	12	0.2	95.078	241.272	83.321	252.518	155.907
13 H	31	85	5.6	28	13	0	94.256	238.513	81.612	251.157	155.177
13 I	31	85	5.6	28	14	0	94.652	239.515	81.954	252.212	155.829
13 J	37	101	4.7	27	15	0.2	95.370	241.830	84.178	252.535	155.706
13 K	37	101	4.7	27	16	0	94.855	242.026	84.098	252.782	156.461
13 L	29	79	5.9	27	17	0.2	96.245	238.763	82.672	252.336	154.240
14 A	37	101	4.7	29	15	-0.1	93.910	240.857	83.692	251.075	155.706
14 B	25	68	7.1	29	7	0	95.854	236.060	80.117	251.797	153.796
14 C	29	79	5.9	27	17	0.1	95.629	80.117	82.055	251.719	154.240
14 D	26	71	6.8	28	7	0.2	96.600	251.797	81.528	252.804	154.149
15 A	29	79	5.9	27.5	17	0	95.012	237.529	81.438	251.102	154.240
15 B	26	71	6.8	28	7	0.2	96.600	237.732	81.528	252.804	154.149
15 C	25	68	7.1	28.5	7	0	95.854	236.060	80.117	251.797	153.796
15 D	25	68	7.1	29	7	0	95.854	236.060	80.117	251.797	153.796
15 E	50	137	4.4	29.5	5	0	114.395	298.576	105.120	307.852	192.131
15 F	50	137	3.8	30	21	0	105.015	275.563	96.874	283.296	177.060
15 G	40	109	4.4	30.5	21	0	98.031	253.090	88.605	262.045	162.600
15 H	34	93	5	31	21	0	95.332	244.757	84.620	254.933	157.994
15 I	37	101	4.7	31.5	17	0	94.855	244.263	85.025	253.601	157.272
15 J	35	96	5	32	13	0	93.907	242.208	84.157	251.958	156.511
15 K	34	93	5.3	32.5	9	0	95.516	245.229	84.784	255.425	158.300
15 L	34	93	5.9	33	5	0	105.421	270.660	94.168	281.913	174.715

The optimized results of the cases from 11 to 15 are given in Table 4.20. Table 4.21 gives the pinion and gear rotational speeds and the power input in the cases from 16 to 20. Table 4.22 gives the upper and lower bounds and the increment values of the pinion and gear addendum and dedendum radii.

Table 4.21 *Speed and power values for the analysis from Case 16 to Case 20*

Parameter	***Value***
n_1	$3000\ rpm$
n_2	$1096.67\ rpm$
$Power$	$1700\ kW$

Table 4.22 *Lower and upper bounds and increment values for addendum and dedendum radii for the analysis from Case 16 to Case 20*

$\boldsymbol{r_{a1}}$	$\boldsymbol{y_1}$	$\boldsymbol{inc1}$	$\boldsymbol{y_2}$
	0.80	0.1	1.20
$\boldsymbol{r_{a2}}$	$\boldsymbol{y_3}$	$\boldsymbol{inc2}$	$\boldsymbol{y_4}$
	-1.20	0.1	-0.80
$\boldsymbol{r_{f1}}$	$\boldsymbol{y_5}$	$\boldsymbol{inc3}$	$\boldsymbol{y_6}$
	-1.40	0.1	-1.00
$\boldsymbol{r_{f2}}$	$\boldsymbol{y_8}$	$\boldsymbol{inc4}$	$\boldsymbol{y_7}$
	1.00	0.1	1.40

Initial assignments of the design variables are given in Table 4.23. In the 16th case, pinion number of teeth is started from 10 and it is ended at 50 by increasing its value 1. The module is started from 2 mm and it is ended at 7.7 mm by increasing its value 0.3 mm. The pressure angle is started from 15° and it is ended at 35° by increasing its value 1°. The pinion profile shifting coefficient is started from -0.6 and it is ended at 0.6 by increasing its value 0.2. The helix angle is started from 5° and it is ended at $21^\circ$by increasing its value 2°. In the 17th cases, all the design parameters are kept as the same as they are in the 16th case except the parameter of the module. The module values are taken as constant values to observe the effect of the increment value of the module on objective function. In the 18th, all the design parameters are kept as the same as they are in the 16th case except the parameter of the helix angle. The helix

angle values are taken as constant values to observe the effect of the increment value of the helix angle on objective function. In the 19th cases, all the design parameters are kept as the same as they are in the 16th case except the parameter of the pinion profile shifting coefficient. The pinion profile shifting coefficient values are taken as constant values to observe the effect of the increment value of the pinion profile shifting coefficient on objective function. In the 20th cases, all the design parameters are kept as the same as they are in the 16th case except the parameter of the pressure angle. The pressure angle values are taken as constant values to observe the effect of the increment value of the pressure angle on objective function.

Table 4.23 *Input parameters of the studies from (Case 16 – Case 20)*

Case	N_1	$m_n\ (mm)$	$\alpha_n(deg)$	$\beta(deg)$	x_1
16	10 : 1 : 50	2 : 0.3 : 7.7	15 : 1 : 35	5 : 2 : 21	−0.6 : 0.2 : 0.6
17 A	10 : 1 : 50	4.3	15 : 1 : 35	5 : 2 : 21	−0.6 : 0.2 : 0.6
17 B	10 : 1 : 50	4.4	15 : 1 : 35	5 : 2 : 21	−0.6 : 0.2 : 0.6
17 C	10 : 1 : 50	4.5	15 : 1 : 35	5 : 2 : 21	−0.6 : 0.2 : 0.6
17 D	10 : 1 : 50	4.6	15 : 1 : 35	5 : 2 : 21	−0.6 : 0.2 : 0.6
17 E	10 : 1 : 50	4.7	15 : 1 : 35	5 : 2 : 21	−0.6 : 0.2 : 0.6
17 F	10 : 1 : 50	4.8	15 : 1 : 35	5 : 2 : 21	−0.6 : 0.2 : 0.6
17 G	10 : 1 : 50	4.9	15 : 1 : 35	5 : 2 : 21	−0.6 : 0.2 : 0.6
17 H	10 : 1 : 50	5.0	15 : 1 : 35	5 : 2 : 21	−0.6 : 0.2 : 0.6
18 A	10 : 1 : 50	2 : 0.3 : 7.7	15 : 1 : 35	8	−0.6 : 0.2 : 0.6
18 B	10 : 1 : 50	2 : 0.3 : 7.7	15 : 1 : 35	9	−0.6 : 0.2 : 0.6
18 C	10 : 1 : 50	2 : 0.3 : 7.7	15 : 1 : 35	10	−0.6 : 0.2 : 0.6
18 D	10 : 1 : 50	2 : 0.3 : 7.7	15 : 1 : 35	11	−0.6 : 0.2 : 0.6
18 E	10 : 1 : 50	2 : 0.3 : 7.7	15 : 1 : 35	12	−0.6 : 0.2 : 0.6
18 F	10 : 1 : 50	2 : 0.3 : 7.7	15 : 1 : 35	13	−0.6 : 0.2 : 0.6
18 G	10 : 1 : 50	2 : 0.3 : 7.7	15 : 1 : 35	14	−0.6 : 0.2 : 0.6
18 H	10 : 1 : 50	2 : 0.3 : 7.7	15 : 1 : 35	15	−0.6 : 0.2 : 0.6
19 A	10 : 1 : 50	2 : 0.3 : 7.7	15 : 1 : 35	5 : 2 : 21	−0.1
19 B	10 : 1 : 50	2 : 0.3 : 7.7	15 : 1 : 35	5 : 2 : 21	0
19 C	10 : 1 : 50	2 : 0.3 : 7.7	15 : 1 : 35	5 : 2 : 21	0.1
19 D	10 : 1 : 50	2 : 0.3 : 7.7	15 : 1 : 35	5 : 2 : 21	0.2
20 A	10 : 1 : 50	2 : 0.3 : 7.7	24.5	5 : 2 : 21	−0.6 : 0.2 : 0.6
20 B	10 : 1 : 50	2 : 0.3 : 7.7	25	5 : 2 : 21	−0.6 : 0.2 : 0.6
20 C	10 : 1 : 50	2 : 0.3 : 7.7	25.5	5 : 2 : 21	−0.6 : 0.2 : 0.6
20 D	10 : 1 : 50	2 : 0.3 : 7.7	26	5 : 2 : 21	−0.6 : 0.2 : 0.6
20 E	10 : 1 : 50	2 : 0.3 : 7.7	26.5	5 : 2 : 21	−0.6 : 0.2 : 0.6
20 F	10 : 1 : 50	2 : 0.3 : 7.7	27	5 : 2 : 21	−0.6 : 0.2 : 0.6
20 G	10 : 1 : 50	2 : 0.3 : 7.7	27.5	5 : 2 : 21	−0.6 : 0.2 : 0.6
20 H	10 : 1 : 50	2 : 0.3 : 7.7	28	5 : 2 : 21	−0.6 : 0.2 : 0.6

Table 4.24 *Optimized design variables (Case 16 – Case 20)*

	z_1	z_2	m_n	α_n	β	x_1	r_{a1}	r_{a2}	r_{f1}	r_{f2}	a_w
Case	-	-	*mm*	*deg*	*deg*	-	*mm*	*mm*	*mm*	*mm*	*mm*
16	25	68	4.7	26	11	0.2	65.116	158.482	53.625	169.494	102.941
17 A	26	71	4.3	24	21	0.2	64.944	159.365	54.350	169.959	103.633
17 B	26	71	4.4	25	17	0.2	64.875	159.196	53.832	169.779	103.524
17 C	26	71	4.5	26	11	0.2	64.638	158.614	53.635	169.158	103.145
17 D	25	68	4.6	25	17	0.2	65.418	159.217	54.355	170.280	103.419
17 E	25	68	4.7	26	11	0.2	65.116	158.482	54.104	169.494	102.941
17 F	25	68	4.8	26	7	0.2	65.770	160.073	54.647	171.196	103.975
17 G	23	63	4.9	25	19	0.2	65.298	158.580	52.860	170.499	103.647
17 H	23	63	5.0	25	17	0.2	65.879	159.991	53.330	172.016	104.569
18 A	37	101	3.2	25	8	0	63.013	159.634	55.258	167.389	103.406
18 B	37	101	3.2	25	9	0	63.178	160.051	55.402	167.826	103.676
18 C	25	68	4.7	26	10	0.2	64.906	157.970	53.452	168.947	102.609
18 D	25	68	4.7	26	11	0.2	65.116	158.482	53.625	169.494	102.941
18 E	25	68	4.7	26	12	0.2	65.348	159.050	53.816	170.097	103.308
18 F	25	68	4.7	26	13	0.2	65.601	159.662	54.507	170.757	103.708
18 G	25	68	4.7	26	14	0.2	65.877	160.333	54.252	171.474	104.144
18 H	25	68	4.7	26	15	0.2	66.175	161.058	54.497	172.249	104.615
19 A	25	68	4.7	25	11	-0.1	63.680	157.524	53.146	168.058	102.941
19 B	25	68	4.7	25	11	0	64.159	158.003	53.146	168.537	102.941
19 C	25	68	4.7	25	11	0.1	64.159	158.961	54.583	168.537	102.941
19 D	25	68	4.7	25	11	0.2	65.116	158.482	53.625	169.494	102.941
20 A	37	101	3.2	24.5	9	0	63.178	160.051	55.402	167.826	103.676
20 B	26	71	4.4	25	17	0.2	64.875	159.196	53.832	169.779	103.524
20 C	25	68	4.7	25.5	11	0.2	65.116	158.482	53.625	169.494	102.941
20 D	25	68	4.7	26	11	0.2	65.116	158.482	53.625	169.494	102.941
20 E	26	71	4.4	26.5	11	0	63.955	158.736	53.372	168.858	103.524
20 F	25	68	4.7	27	11	0.2	65.116	158.961	54.583	169.494	102.941
20 G	25	68	4.7	27.5	11	0	64.159	158.003	53.146	168.537	102.941
20 H	25	68	4.7	28	11	0	64.159	158.003	53.146	168.537	102.941

The optimized results of the cases from 16 to 20 are given in Table 4.24. The module sensitivity and the center distance relation at 900 rpm and 3000 rpm are given in Figure 4-9 and Figure 4-10, respectively. The optimum center distance and the optimum module value are obtained as $153.796\ mm$ and 7.1 mm respectively in the 11^{th} case. It is seen that the optimum center distances are $154.459\ mm$ and $155.391\ mm$ when the module values are adjusted to $7.0\ mm$ and $7.2\ mm$, respectively. Therefore, changing the module value $0.1\ mm$ around the actual optimum module deviates the center distance value $1.59\ mm$ at most. The sensitivity of the module parameter is $1.04\ \%$ at most $0.1\ mm$ around the actual optimum module value. When the $0.1\ mm$ increment of the module is considered sensitivity of the module is not always in a decreasing manner if the module values are moved away from the optimum module point. When the module is moved away from the actual optimum point there can be local optimum points as observed at $7.50\ mm$ module.

The optimum center distance and the optimum module value are obtained as $102.941\ mm$ and 4.7 mm respectively in the 16^{th} case. It is seen that the optimum center distances are $103.419\ mm$ and $103.975\ mm$ when the module values are adjusted to $4.6\ mm$ and $4.7\ mm$, respectively. Therefore, changing the module value $0.1\ mm$ around the actual optimum module deviates the center distance value $1.034\ mm$ at most. The sensitivity of the module parameter is $1.00\ \%$ at most $0.1\ mm$ around the actual optimum module value. When the $0.1\ mm$ increment of the module is considered sensitivity of the module is in a decreasing manner if the module values are moved away from the optimum module point. The increment of the module value is specified as $0.1\ mm$ which gives a sensitivity value of $1.00\ \%$ at most.

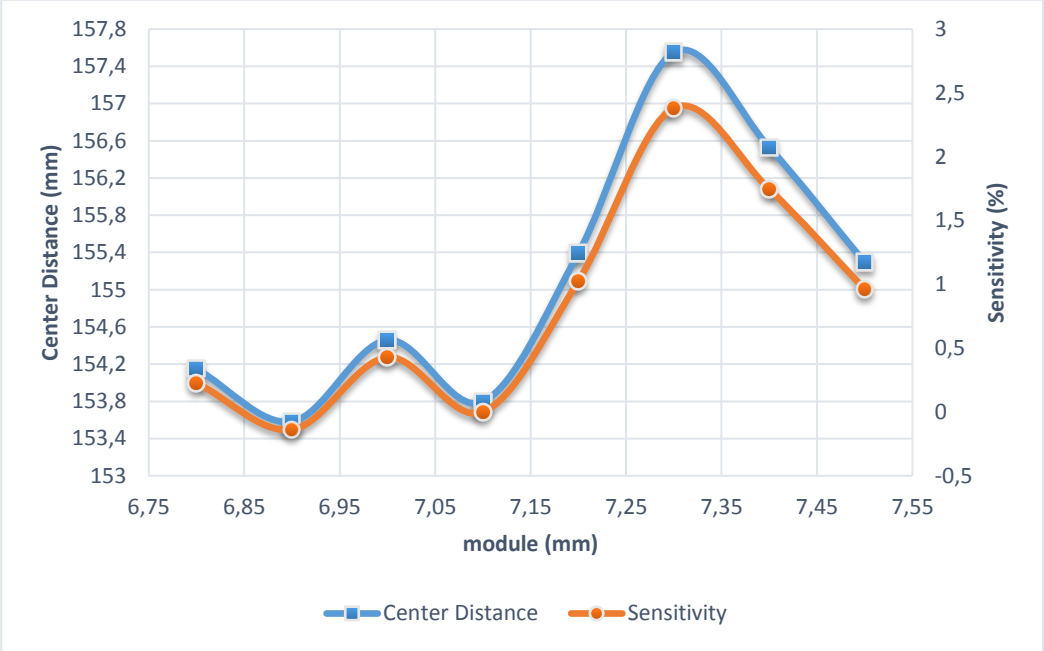

Figure 4-9 *Module sensitivity and center distance relation of internal gear pair at relatively lower pinion rotational speed (900 rpm)*

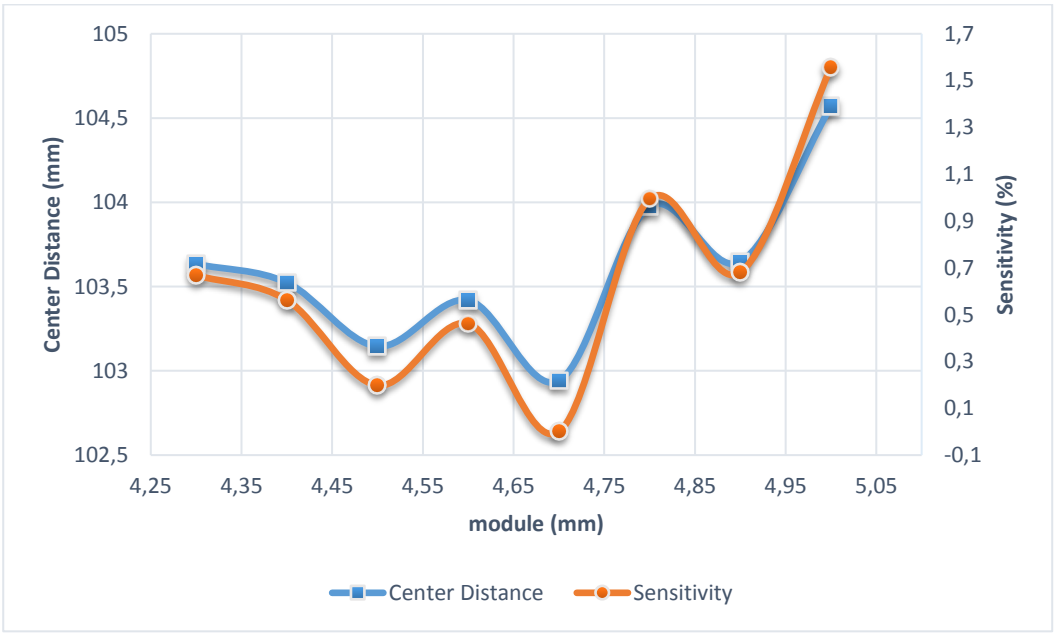

Figure 4-10 *Module sensitivity and center distance relation of internal gear pair at relatively higher pinion rotational speed (3000 rpm)*

The helix angle sensitivity and the center distance relation at 900 rpm and 3000 rpm are given in Figure 4-11 and Figure 4-12 respectively. The optimum center distance and the optimum helix angle value are obtained as $153.796\ mm$ and 7° respectively in the first case. It is seen that the optimum center distances are $153.491\ mm$ and $154.15\ mm$ when the helix angle values are adjusted to 6° and 8°, respectively. Therefore, changing the helix angle value 1° around the actual optimum helix angle deviates the center distance value $0.36\ mm$ at most. The sensitivity of the helix angle parameter is $0.23\ \%$ at most 1° around the actual optimum helix angle value. When the 1° increment of the helix angle is considered sensitivity of the helix angle is not in a decreasing manner if the helix angle values are moved away from the optimum helix angle point. The sensitivity of the helix angle has an inconsistent behavior at relatively lower speed like it is also observed in external gear pairs as seen in Figure 4-4.

The optimum center distance and the optimum helix angle value are obtained as $102.941\ mm$ and 11° respectively in the sixth case. It is seen that the optimum center distances are $102.609\ mm$ and $103.308\ mm$ when the helix angle values are adjusted to 10° and 12°, respectively. Therefore, changing the helix angle value 1° around the actual optimum helix angle deviates the center distance value $0.37\ mm$ at most. The sensitivity of the helix angle parameter is $0.35\ \%$ at most 1°around the actual optimum helix angle value. When the 1° increment of the helix angle is considered sensitivity of the module is not always in a decreasing manner if the helix angle values are moved away from the optimum helix angle point. When the 1° increment of the helix angle is considered sensitivity of the helix angle is in a decreasing manner if the pinion helix angle values are moved away from the optimum pinion profile helix angle point. The increment of the helix angle value is specified as 1° which gives a sensitivity value of $0.35\ \%$ at most.

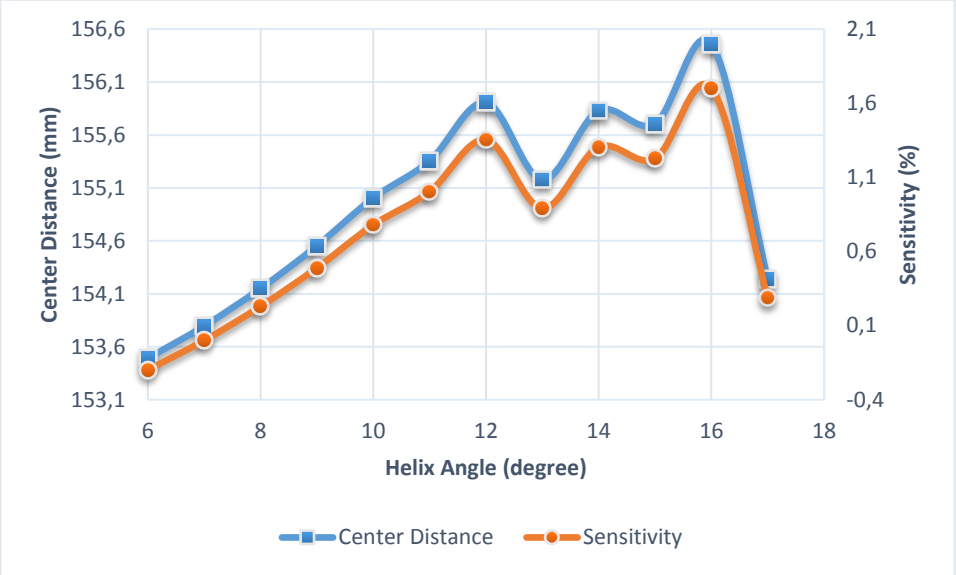

Figure 4-11 *Helix angle sensitivity and center distance relation of internal gear pair at relatively lower pinion rotational speed (900 rpm)*

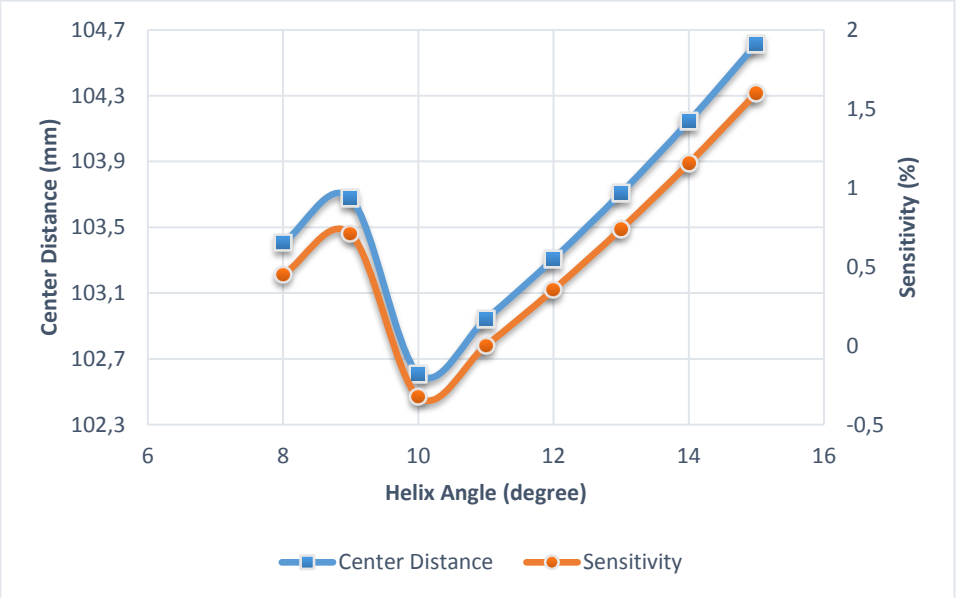

Figure 4-12 *Helix angle sensitivity and center distance relation of internal gear pair at relatively higher pinion rotational speed (3000 rpm)*

The pinion profile shifting coefficient sensitivity and the center distance relation at 900 is given in Figure 4-13. The optimum center distance and the optimum profile shifting coefficient are obtained as 153.796 mm and 0 respectively in the 11^{th} case. It is seen that the optimum center distances are 155.706 mm and 154.24 mm when the pinion profile shifting coefficient values are adjusted to -0.1 and 0.1, respectively. Therefore, changing the pinion profile shifting coefficient value 0.1 around the actual optimum profile shifting coefficient deviates the center distance value 1.91 mm at most. The sensitivity of the pinion profile shifting coefficient parameter is 1.24 % at most 0.1 around the actual optimum pinion profile shifting coefficient value. When the 0.1 increment of the pinion profile shifting coefficient is considered sensitivity of the pinion profile shifting coefficient in a decreasing manner if the pinion profile shifting coefficient values are moved away from the optimum pinion profile shifting coefficient point. When Table 4.24 is considered, it is seen that changing of the pinion profile shifting coefficient does not effect the value of the optimum center distance in internal gear pairs at relatively high speed. The increment of the pinion profile shifting coefficient value is specified as 0.1 which gives a sensitivity value of 1.24 % at most.

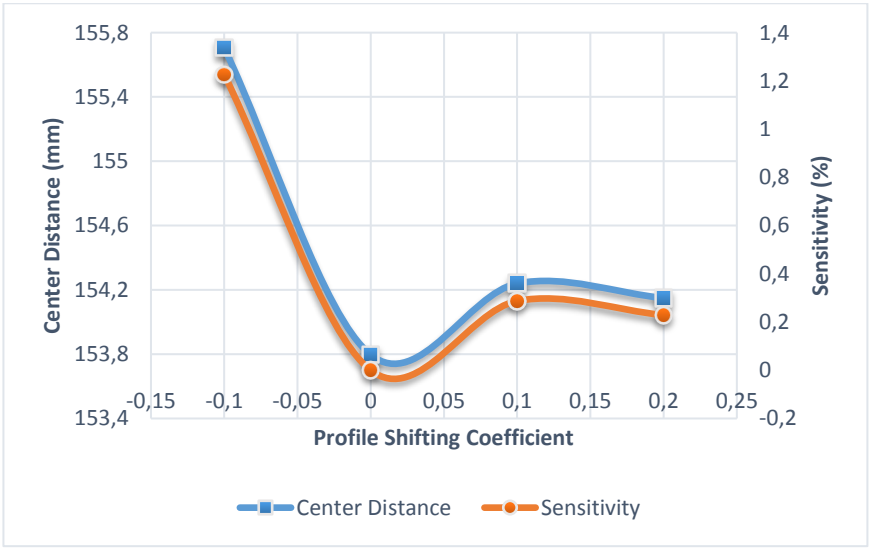

Figure 4-13 *Pinion profile shifting coefficient sensitivity and center distance relation of internal gear pair at relatively lower pinion rotational speed (900 rpm)*

The pressure angle sensitivity and the center distance relation at 900 rpm and 3000 rpm are given in Figure 4-14 and Figure 4-15, respectively. The optimum center distance and the optimum pressure angle value are obtained as $153.796\ mm$ and 29° respectively in the 11^{th} case. It is seen that the optimum center distances are $153.796\ mm$ and $192.131\ mm$ when the pressure angle values are adjusted to 28.5° and 29.5°, respectively. Therefore, changing the pressure angle value 0.5° around the actual optimum pressure angle deviates the center distance value $38.33\ mm$ at most. The sensitivity of the pressure angle parameter is $24.93\ \%$ at most 0.5° around the actual optimum pressure angle value. When the 0.5° increment of the pressure angle is considered sensitivity of the pressure angle is not in a decreasing manner if the pressure angle values are moved away from the optimum pressure angle point. It is seen that the sensitivity has sudden jumps in some points. However, when the 28.50° is considered, the sensitivity of the pressure angle becomes very high. The 0.5° increment of the pressure angle is enough to obtain the optimum point if the initially assigned interval is wide enough. The optimum center distance and the optimum pressure angle value are obtained as $102.941\ mm$ and 26° respectively in the 16^{th} case. It is seen that the optimum center distances are $102.941\ mm$ and $103.524\ mm$ when the pressure angle values are adjusted to 25.5° and 24.5°, respectively. Therefore, changing the pressure angle value 0.5° around the actual optimum pressure angle deviates the center distance value $0.583\ mm$ at most. The sensitivity of the pressure angle parameter is $0.57\ \%$ at most 0.5°around the actual optimum pressure angle value. When the 0.5° increment of the pressure angle is considered sensitivity of the pressure angle is always in a decreasing manner if the pressure angle values are moved away from the optimum pressure angle point. However, the sensitivity value does not show a consistent behavior as it is observed in 900 rpm. Therefore, when the rotational speed of the pinion is decreased the pressure angle does not keep its consistent behavior any more. Although this inconsistency, the sensitivity of the pressure angle is still below the $5\ \%$ 0.5°around the actual optimum pressure angle value. The increment of the pressure angle value is specified as 0.5°.

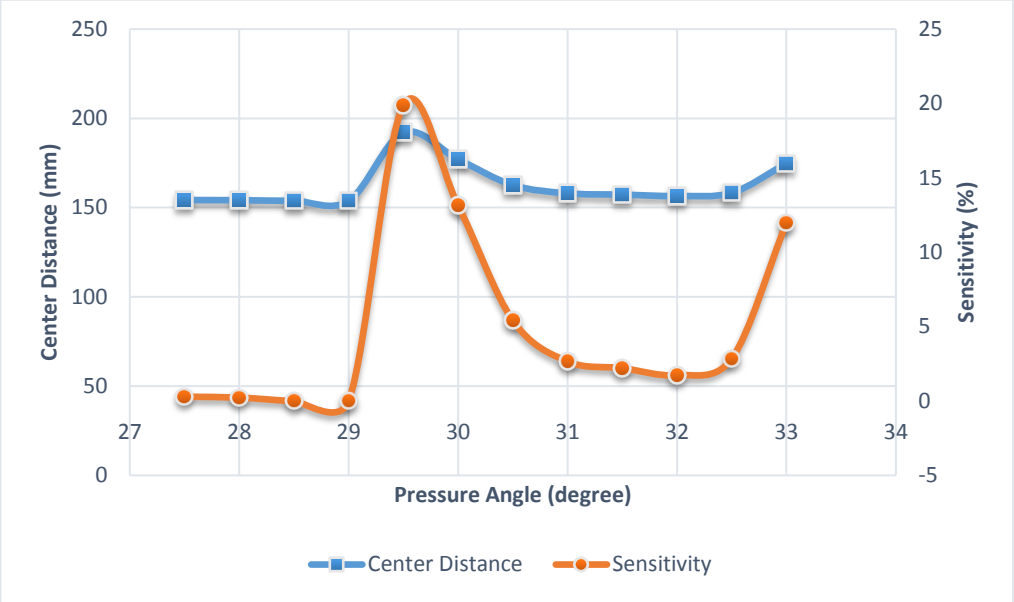

Figure 4-14 *Pressure angle sensitivity and center distance relation of internal gear pair at relatively lower pinion rotational speed (900 rpm)*

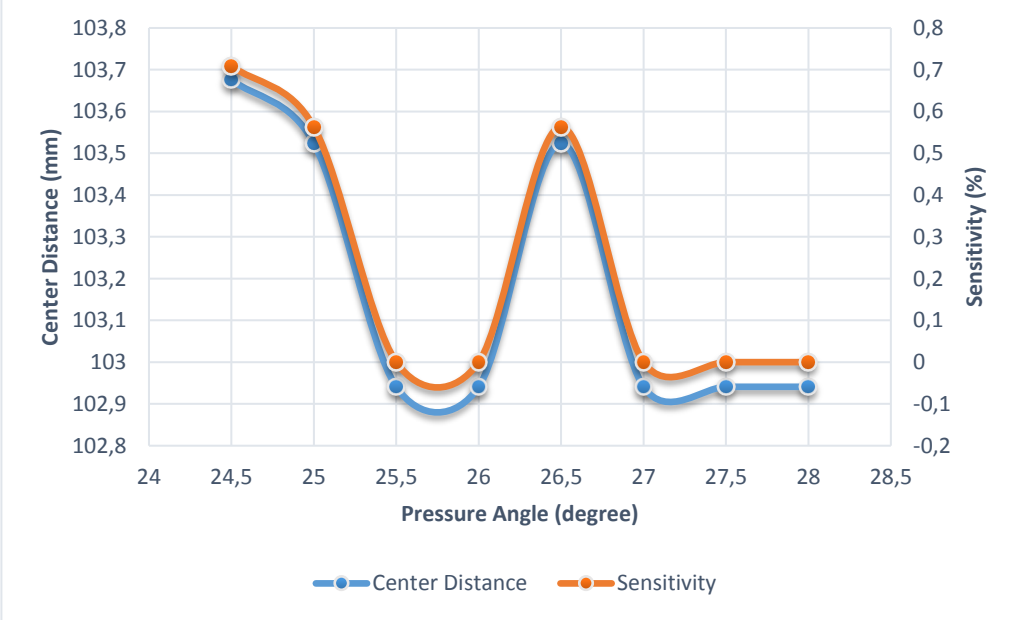

Figure 4-15 *Pressure angle sensitivity and center distance relation of internal gear pair at relatively higher pinion rotational speed (3000 rpm)*

4.2.1. Addendum and Dedendum Radii Sensitivity of Internal Gear Pairs

Sensitivity analysis of the addendum and dedendum radii is evaluated in this section. Initial assignments of the design variables and pinion and gear rotational speeds and input power are given in Table 4.25. In the INT1 case, pinion number of teeth is started from 1 and it is ended at 50 by increasing its value 1. The module is started from 2 mm and it is ended at 7.7 mm by increasing its value 0.3 mm. The pressure angle is started from 15° and it is ended at 35° by increasing its value 1°. The pinion profile shifting coefficient is started from -0.6 and it is ended at 0.6 by increasing its value 0.2. The helix angle is started from 5° and it is ended at 21° by increasing its value 2°. In the INT2 case, all the design parameters are kept as the same as they are in the INT1 case except the increment of the addendum and dedendum radii. In INT3 case, all the design parameters are kept as the same as they are in the INT1 case except the increment of the addendum and dedendum radii.

Table 4.25 *Input parameters and initial assignment of the design variables of Case INT1, INT2 and INT3*

PARAMATERS	***INT 1***	***INT 2***	***INT 3***
N_1	$10:1:50$	$10:1:50$	$20:1:40$
m_n (mm)	$2:0.3:7.7$	$2:0.3:7.7$	$4.4:0.3:7.7$
α_n (degree)	$15:1:35$	$15:1:35$	$25:1:35$
β (degree)	$5:2:21$	$5:2:21$	$5:2:21$
x_1	$-0.6:0.2:0.6$	$-0.6:0.2:0.6$	$-0.4:0.2:0.4$
y_1	0.80	0.80	0.80
y_2	1.20	1.20	1.20
y_3	-1.20	-1.20	-1.20
y_4	-0.80	-0.80	-0.80
y_5	-1.40	-1.40	-1.40
y_6	-1.00	-1.00	-1.00
y_7	1.00	1.00	1.00
y_8	1.40	1.40	1.40
$\boldsymbol{inc1}$	0.2	0.1	0.05
$\boldsymbol{inc2}$	0.2	0.1	0.05
$\boldsymbol{inc3}$	0.2	0.1	0.05
$\boldsymbol{inc4}$	0.2	0.1	0.05
$\boldsymbol{n_1}$	900 rpm	900 rpm	900 rpm
$\boldsymbol{n_2}$	329 rpm	329 rpm	329 rpm
$Power$	1700 kW	1700 kW	1700 kW

The optimized results of the Case INT1, Case INT2 and Case INT3 are given in Table 4.26. It is seen that when the increments of the addendum and dedendum radii are taken as $0.2\ mm, 0.1\ mm\ and\ 0.05\ mm$ the optimum center distances are $157.880\ mm, 153.796\ mm$ and $153.233\ mm$, respectively. The optimum center is obtained as $153.796\ mm$ in the 11^{th} case. Therefore, changing the increment value of the addendum and dedendum radii $0.05\ mm$ around the actual optimum increment of the addendum and dedendum radii the center distance value deviates $4.084\ mm$ at most. The sensitivity of the increment of the addendum and dedendum radii is 2.66 % at most $0.05\ mm$ around the actual optimum increment of the addendum and dedendum radii.

Table 4.26 *Optimized design variables (Case INT1 – CASE INT3)*

Case Study	**INT 1**	**INT 2**	**INT 3**
$\boldsymbol{m_n}$	$5\ mm$	$7.1\ mm$	$7.1\ mm$
$\boldsymbol{\beta}$	15°	7°	5°
$\boldsymbol{x_1}$	0	0	0.2
$\boldsymbol{r_{a1}}$	$94.728\ mm$	$95.854\ mm$	$97.285\ mm$
$\boldsymbol{r_{a2}}$	$244.325\ mm$	$236.060\ mm$	$235.551\ mm$
$\boldsymbol{r_{f1}}$	$84.375\ mm$	$80.117\ mm$	$80.180\ mm$
$\boldsymbol{r_{f2}}$	$254.678\ mm$	$251.797\ mm$	$252.300\ mm$
$\boldsymbol{N_1}$	35	25	25
$\boldsymbol{N_2}$	96	68	68
$\boldsymbol{\alpha_n}$	32°	29°	26°
$\boldsymbol{a_w}$	$157.880\ mm$	$153.796\ mm$	$153.233\ mm$

Initial assignments of the design variables and pinion and gear rotational speeds and input power are given in Table 4.27. In the INT4 case, pinion number of teeth is started from 1 and it is ended at 50 by increasing its value 1. The module is started from $2\ mm$ and it is ended at $7.7\ mm$ by increasing its value $0.3\ mm$. The pressure angle is started from 15° and it is ended at 35° by increasing its value 1°. The pinion profile shifting

coefficient is started from -0.6 and it is ended at 0.6 by increasing its value 0.2. The helix angle is started from 5° and it is ended at 21° by increasing its value 2°.

In the INT5 case, all the design parameters are kept as the same as they are in the INT4 case except the increment of the addendum and dedendum radii. In INT6 case, all the design parameters are kept as the same as they are in the INT4 case except the increment of the addendum and dedendum radii.

Table 4.27 *Input parameters and initial assignment of the design variables of Case INT4, INT5 and INT6*

PARAMATERS	***INT 4***	***INT 5***	***INT 6***
N_1	$10:1:50$	$10:1:50$	$20:1:40$
m_n (mm)	$2:0.3:7.7$	$2:0.3:7.7$	$4.1:0.3:7.7$
α_n (degree)	$15:1:35$	$15:1:35$	$25:1:35$
β (degree)	$5:2:21$	$5:2:21$	$5:2:21$
x_1	$-0.6:0.2:0.6$	$-0.6:0.2:0.6$	$-0.4:0.2:0.4$
y_1	0.80	0.80	0.80
y_2	1.20	1.20	1.20
y_3	-1.20	-1.20	-1.20
y_4	-0.80	-0.80	-0.80
y_5	-1.40	-1.40	-1.40
y_6	-1.00	-1.00	-1.00
y_7	1.00	1.00	1.00
y_8	1.40	1.40	1.40
$\boldsymbol{inc1}$	0.2	0.1	0.05
$\boldsymbol{inc2}$	0.2	0.1	0.05
$\boldsymbol{inc3}$	0.2	0.1	0.05
$\boldsymbol{inc4}$	0.2	0.1	0.05
$\boldsymbol{n_1}$	$3000\ rpm$	$3000\ rpm$	$3000\ rpm$
$\boldsymbol{n_2}$	$1096.67\ rpm$	$1096.67\ rpm$	$1096.67\ rpm$
$Power$	$1700\ kW$	$1700\ kW$	$1700\ kW$

The optimized results of the Case INT4, Case INT5 and Case INT6 are given in Table 4.28. It is seen that when the increments of the addendum and dedendum radii are taken as $0.2\ mm, 0.1\ mm\ and\ 0.05\ mm$ the optimum center distances are

105.299 mm, 104.569 mm and 102.941 mm respectively. The optimum center is obtained as 102.941 mm in the 16th case. Therefore, changing the increment value of the addendum and dedendum radii 0.05 mm around the actual optimum increment of the addendum and dedendum radii the center distance value deviates 1.628 mm at most. The sensitivity of the increment of the addendum and dedendum radii is 1.60 % at most 0.05 mm around the actual optimum increment of the addendum and dedendum radii.

Table 4.28 *Optimized design variables (Case INT4 – CASE INT6)*

Case Study	INT 4	INT 5	INT 6
m_n	3.8 mm	5.0 mm	4.7 mm
β	13°	17°	11°
x_1	0	0.2	0.2
r_{a1}	63.569 mm	65.879 mm	65.356 mm
r_{a2}	162.628 mm	159.991 mm	158.242 mm
r_{f1}	55.769 mm	53.330 mm	53.386 mm
r_{f2}	170.428 mm	172.016 mm	169.494 mm
N_1	31	23	25
N_2	85	63	68
α_n	31°	25°	25°
a_w	105.299 mm	104.569 mm	102.941 mm

4.2.2. Detailed optimization of Case 11

As discussed in the previous sections, the increment of the all design parameters are specified according to sensitivity analyses. In this section, the specified increments for each design parameter are used to obtain more optimum results.

Initial assignments of the design variables, rotational speed of the pinion and the gear and the input power is given in Table 4.29. Optimization result of the first case study is given in Table 4.20. The first case study is evaluated again by changing the increments of each design variables. In Case 11 Detailed A, increment of the module,

pressure angle, helix angle and pinion profile shifting coefficient are changed from $0.3\ mm$, $1^{\circ}, 2^{\circ}$ and 0.2 to $0.1\ mm$, $0.5^{\circ}, 1^{\circ}$ and 0.1 respectively to observe the more optimal results. In Case 11 Detailed B, the increment of the design variables are kept constant as in Case 11 Detailed A. However, increment of the addendum and dedendum radii is changed from $0.1\ mm$ to $0.05\ mm$.

Table 4.29 *Input parameters and initial assignment of the design variables of Case 11 Detailed A and Case 11 Detailed B*

PARAMATERS	***Case 11***	***Case 11 Detailed A***	***Case 11 Detailed B***
N_1	$10:1:50$	$20:1:40$	$23:1:27$
m_n (mm)	$2:0.3:7.7$	$4.0:0.1:8.0$	$6.5:0.1:7.5$
α_n (degree)	$15:1:35$	$25:0.5:33$	$25:0.5:32$
β (degree)	$5:2:21$	$5:1:21$	$5:1:21$
x_1	$-0.6:0.2:0.6$	$-0.2:0.1:0.4$	$-0.2:0.1:0.3$
y_1	0.80	0.80	0.80
y_2	1.20	1.20	1.20
y_3	-1.20	-1.20	-1.20
y_4	0.8	0.8	0.8
y_5	-1.40	-1.40	-1.40
y_6	-1.00	-1.00	-1.00
y_7	1	1	1
y_8	1.4	1.4	1.4
$\boldsymbol{inc1}$	0.1	0.1	0.05
$\boldsymbol{inc2}$	0.1	0.1	0.05
$\boldsymbol{inc3}$	0.1	0.1	0.05
$\boldsymbol{inc4}$	0.1	0.1	0.05
$\boldsymbol{n_1}$	$900\ rpm$	$900\ rpm$	$900\ rpm$
$\boldsymbol{n_2}$	$329\ rpm$	$329\ rpm$	$329\ rpm$
$Power$	$1700\ kW$	$1700\ kW$	$1700\ kW$

Table 4.30 *Optimized design variables (Case 11 Detailed A – Case 11 Detailed B)*

Case Study	**Case 11**	**Case 11 Detailed A**	**Case 11 Detailed B**
$\boldsymbol{m_n}$	7.1 mm	7.1 mm	7.1 mm
$\boldsymbol{\beta}$	7°	28.5°	5°
$\boldsymbol{x_1}$	0	0.1	0.2
$\boldsymbol{r_{a1}}$	95.855 mm	96.216 mm	97.285 mm
$\boldsymbol{r_{a2}}$	236.060 mm	235.908 mm	235.551 mm
$\boldsymbol{r_{f1}}$	80.117 mm	80.536 mm	80.180 mm
$\boldsymbol{r_{f2}}$	251.797 mm	251.587 mm	252.300 mm
$\boldsymbol{N_1}$	25	25	25
$\boldsymbol{N_2}$	68	68	68
$\boldsymbol{\alpha_n}$	29°	28.5°	26°
$\boldsymbol{a_w}$	153.796 mm	153.233 mm	153.233 mm

CHAPTER 5

VERIFICATION AND DISCUSSION OF THE RESULTS

For the verification of the results, the geometrical and material based constraints are evaluated for external and internal gear pairs. Evaluations of root clearance, top land thickness, contact ratio, involute clearance, tiff clearance, contact stress, bending stress and tooth temperature are verified in this section by comparing the results with Kissoft commercial gear design and analysis tool.

5.1. Verification of External and Internal Gear Pairs by Using Kissoft

The optimized gear pair which is obtained by Case 6 given in Table 4.8 and the optimized gear pair which is obtained by Case 11 given in Table 4.20 are verified in this section for the verification of the external and internal gear pairs, respectively.

The geometrical parameters and material based parameters are evaluated for the optimized gear pairs. Results are compared with the results of Kissoft commercial gear design and analysis tool. Results of Case 6 and Kissoft commercial tool are given in Table 5.1. Tooth contact temperature of the optimized gear pair in Case 6 is obtained by Kissoft and given in Figure 5-1. Results of the Case 11 and Kissoft commercial tool are given in Table 5.2. Tooth contact temperature of the optimized gear pair in Case 11 is obtained by Kissoft and given in Figure 5-2.

Table 5.1 *Results of the verification case study for external gear pairs*

Parameter	***Current Study***	***Kıssoft***
r_1	82.478 mm	82.478 mm
r_2	325.2 mm	325.2 mm
r_{b1}	75.694 mm	75.694 mm
r_{b2}	298.45 mm	298.45 mm
α_{wt}	23.402°	23.402°
r_{tf1}	87.909 mm	87.909 mm
r_{tf2}	329.688 mm	329.688 mm
R_{f1}	76.995 mm	77.028 mm
R_{f2}	319.171 mm	319.235 mm
P_{bt}	13.589 mm	13.589 mm
S_{n1b}	7.498 mm	7.498 mm
S_{n2b}	6.076 mm	6.076 mm
s_{nan1}	2.346 mm	2.346 mm
s_{nan2}	2.152 mm	2.152 mm
Z	23.391 mm	23.392 mm
m_p	1.721	1.721
m_F	2.994	2.994
P_x	38.572 mm	38.572 mm
c_1	1.414 mm	1.414 mm
c_2	1.885 mm	1.885 mm
$Tiff_1$	1.642 mm	1.609 mm
$Tiff_2$	1.472 mm	1.408 mm
Ic_1	1.301 mm	1.334 mm
Ic_2	20.721 mm	20.785 mm
J_1	0.6728	0.661
J_2	0.6827	0.661
s_{t1}	441.836 MPa	459.76 MPa
s_{t2}	435.451 MPa	459.69 MPa
I	0.272	0.272
s_c	1072 MPa	1072 MPa
θ_M	141.08 ℃	153.53 ℃

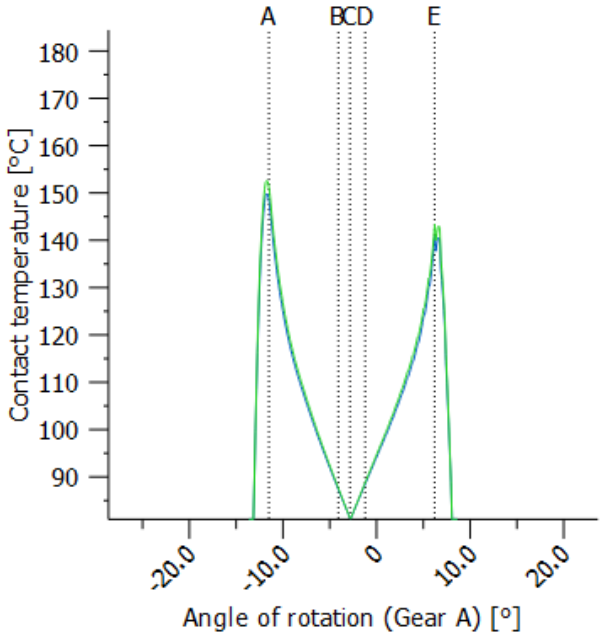

Figure 5-1 *Tooth contact temperature variation of the optimized gear pair in Case 6 with angle of rotation*

Table 5.2 *Results of the verification case study for internal gear pairs*

Parameter	Current Study	Kıssoft
r_1	89.417 mm	89.417 mm
r_2	243.213 mm	243.213 mm
r_{b1}	78.067 mm	78.067 mm
r_{b2}	212.343 mm	212.343 mm
α_{wt}	29.182°	29.182°
r_{tf1}	95.630 mm	95.630 mm
r_{tf2}	236.285 mm	236.285 mm
R_{f1}	81.481 mm	83.159 mm
R_{f2}	251.251 mm	249.092 mm
$\boldsymbol{P_{bt}}$	19.620 mm	19.620 mm
S_{n1b}	11.0277 mm	11.0277 mm
S_{n2b}	11.0281 mm	11.0281 mm
s_{nan1}	3.393 mm	3.393 mm
s_{nan2}	3.396 mm	3.396 mm
Z	26.581 mm	26.581 mm
m_p	1.355	1.355
m_F	0.684	0.684
P_x	183.026 mm	183.026 mm
c_1	2.147 mm	2.147 mm
c_2	2.146 mm	2.146 mm
Ic_1	3.414 mm	5.092 mm
Ic_2	23.717 mm	23.717 mm
J_1	0.6396	0.681
J_2	0.8032	0.853
s_{t1}	352.1888 MPa	332.11 MPa
s_{t2}	280.4582 MPa	265.09 MPa
I	0.3875	0.387
s_c	915 MPa	915 MPa
θ_M	135.6 ℃	125.0 ℃

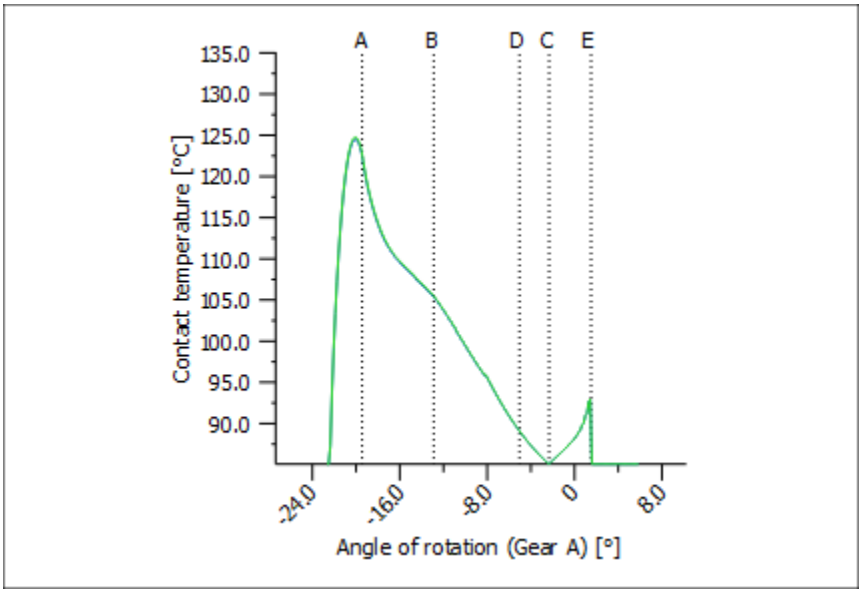

Figure 5-2 *Tooth contact temperature variation of the optimized gear pair in Case 11 with angle of rotation*

5.2. Discussion of the Sudden Changes in the Value of the Objective Function

When Figure 4-4, Figure 4-8, Figure 4-11, Figure 4-14 and Figure 4-15 are considered, it is seen that changes in the optimum center distance values are respectable. The reason of the sudden changes in the optimum center distance is discussed in this section. The optimized gear pair obtained by Case 8F given in Table 4.8 is considered to discuss the sudden changes in the value of the objective function.

When Figure 4-4 is considered, it is seen that the optimum center distance is about $435\ mm$. However, when the helix angle is 22° and 24° the optimum center distance is obtained as about $411\ mm$ and $420\ mm$ respectively.

It is stated in Table 4.8 that the optimum values of the pinion number of teeth, the gear number of teeth, the normal module, the pressure angle, the helix angle and the shifting coefficient are obtained as $37, 145, 4.4\ mm, 23^{\circ}, 23^{\circ}$ and 0, respectively. The optimum center distance is obtained as $434.979\ mm$.

Analysis of Case 21 is conducted around the optimum point of 8F which is given in Table 4.8 by applying the initial assignments of the design variables given in Table 5.3. However, the optimization eliminations are not implemented in this analysis to obtain the all possibilities and to observe the reasons of not converging to a more optimum point.

Table 5.3 *Initial assignments of case 21*

Case	z_1	$m_n\ (mm)$	$\alpha_n(deg)$	$\beta(deg)$	x_1
21	$35:1:40$	$4.1:0.3:4.7$	$20:1:26$	23	$-0.2:0.2:0.2$
n_1			$1500\ rpm$		
n_2			$381.679\ rpm$		
$Power$			$1700\ kW$		
r_{a1}			y_1	$inc1$	y_2
			0.8	0.1	1.20
r_{a2}			y_3	$inc2$	y_4
			0.8	0.1	1.20
r_{f1}			y_5	$inc3$	y_6
			-1.5	0.1	-1.10
r_{f2}			y_8	$inc4$	y_7
			-1.5	0.1	-1.10

As seen from Table 5.3, the given initial assignments of the design variables in Case 21 covers the values of the optimized design variables obtained in Case 8F given in Table 4.8. 157500 results are obtained without optimization eliminations. The different center distances among the obtained results are given in Table 5.4.

Table 5.4 *Center distance variation with normal module, pinion number of teeth and gear number of teeth in Case 21*

m_n	β	z_1	z_2	a_w
4.1 mm	23°	35	138	385.278 mm
4.1 mm	23°	37	145	405.321 mm
4.1 mm	23°	38	149	416.456 mm
4.1 mm	23°	40	157	438.727 mm
4.4 mm	23°	35	138	413.469 mm
4.4 mm	23°	37	145	434.979 mm
4.4 mm	23°	38	149	446.929 mm
4.4 mm	23°	40	157	470.829 mm
4.7 mm	23°	35	138	441.660 mm
4.7 mm	23°	37	145	464.636 mm
4.7 mm	23°	38	149	477.401 mm
4.7 mm	23°	40	157	502.931 mm

As given in Table 4.8, the optimized center distance value is 434.979 mm in Case 8F. As seen from Table 5.4, the center distance values which is lower than 434.979 mm are 385.278 mm, 405.321 mm, 413.469 mm and 416.456 mm. However, the iteration does not converge to a center distance value which is lower than 434.979 mm in Case 8F.

Addendum and dedendum radii for each gear pair set are evaluated by using the algorithms given in Table 3.9, Table 3.10, Table 3.13 and Table 3.14. When Table 5.3 is considered it is seen that the maximum addendum and dedendum radii for each gear pair set are obtained by using y_2, y_4, y_6 and y_7. The maximum addendum radii are 1.20 m_t higher than the pitch radii of each gear pair set while the maximum dedendum radii are 1.10 m_t lower than the pitch radii of each gear pair set. The maximum possible addendum and dedendum radii are given in Table 5.5 and Table 5.6, respectively.

Table 5.5 *The maximum addendum radii of the pinion and the gear with normal module, pinion number of teeth and gear number of teeth in Case 21*

m_n	β	z_1	z_2	r_{a1}	r_{a2}
4.1 mm	23°	35	138	83.291 mm	312.676 mm
4.1 mm	23°	37	145	87.745 mm	328.266 mm
4.1 mm	23°	38	149	89.972 mm	337.174 mm
4.4 mm	23°	35	138	89.386 mm	335.555 mm

Table 5.6 *The maximum dedendum radii of the pinion and the gear with normal module, pinion number of teeth and gear number of teeth in Case 21*

m_n	β	z_1	z_2	r_{f1}	r_{f2}
4.1 mm	23°	35	138	73.047 mm	302.432 mm
4.1 mm	23°	37	145	77.501 mm	318.021 mm
4.1 mm	23°	38	149	79.728 mm	326.929 mm
4.4 mm	23°	35	138	78.392 mm	324.561 mm

The optimum center distance can be obtained as 385.278 mm. The normal module is directly 4.1 mm and the pinion number of teeth is 35 and the gear number of teeth is 138 with the 23° helix angle and with 385.278 mm center distance as seen from Table 5.4. The results of Case 21 are filtered by taking the normal module, the pinion number of teeth, the gear number of teeth as 4.1 mm , 35 and 138, respectively. The addendum radii of the pinion and the gear are taken as 83.291 mm and 312.676 mm, respectively. The dedendum radii of the pinion and the gear are taken as 73.047 mm and 302.432 mm, respectively. There are remaining seven gear pairs among the results of Case 21 when the design parameters are selected as mentioned above. The bending stress safety factor and the pinion top land thickness relation are given in Figure 5-3.

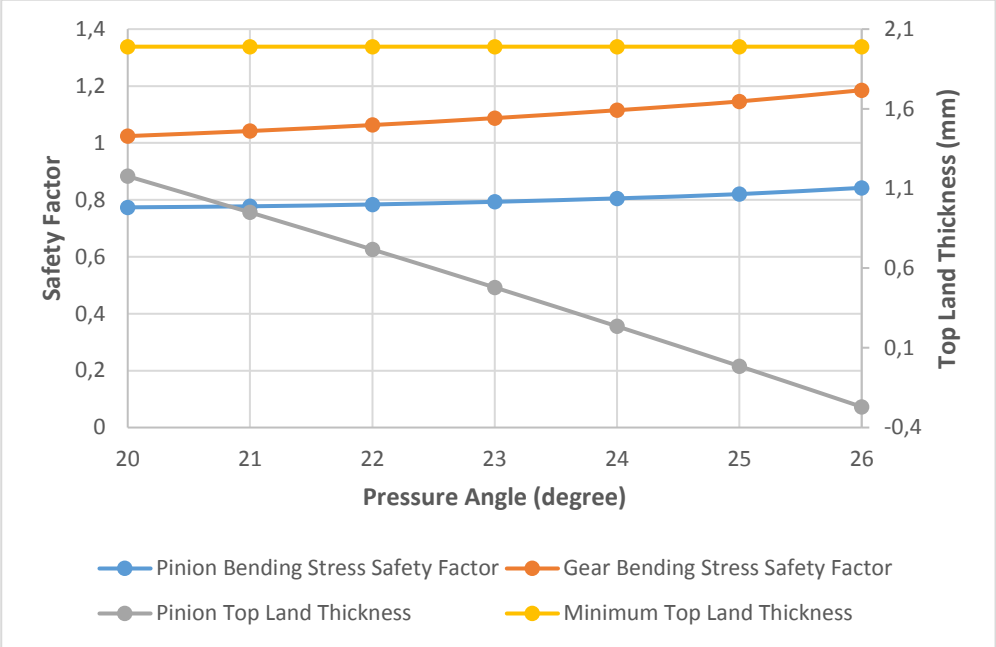

Figure 5-3 *Variation of safety factor and top land thickness vs pressure angle with -0.2 profile shifting coefficient* ($m_n = 4.1\ mm$, $z_1 = 35$, $z_2 = 138$, $\beta = 23^\circ$, $r_{a1} = 83.291\ mm$, $r_{a2} = 312.676\ mm$, $r_{f1} = 73.047\ mm$, $r_{f2} = 302.432\ mm$)

As seen from Figure 5-3, the pinion bending stress safety factor values are all below 1. The top land thickness values of the pinion are also below the minimum required top land thickness value. The pinion profile shifting coefficient can be increased to 0 by keeping the other parameters as the same to increase the pinion bending stress safety factor value. The following results given in Figure 5-4 are obtained with the 0 pinion profile shifting coefficient.

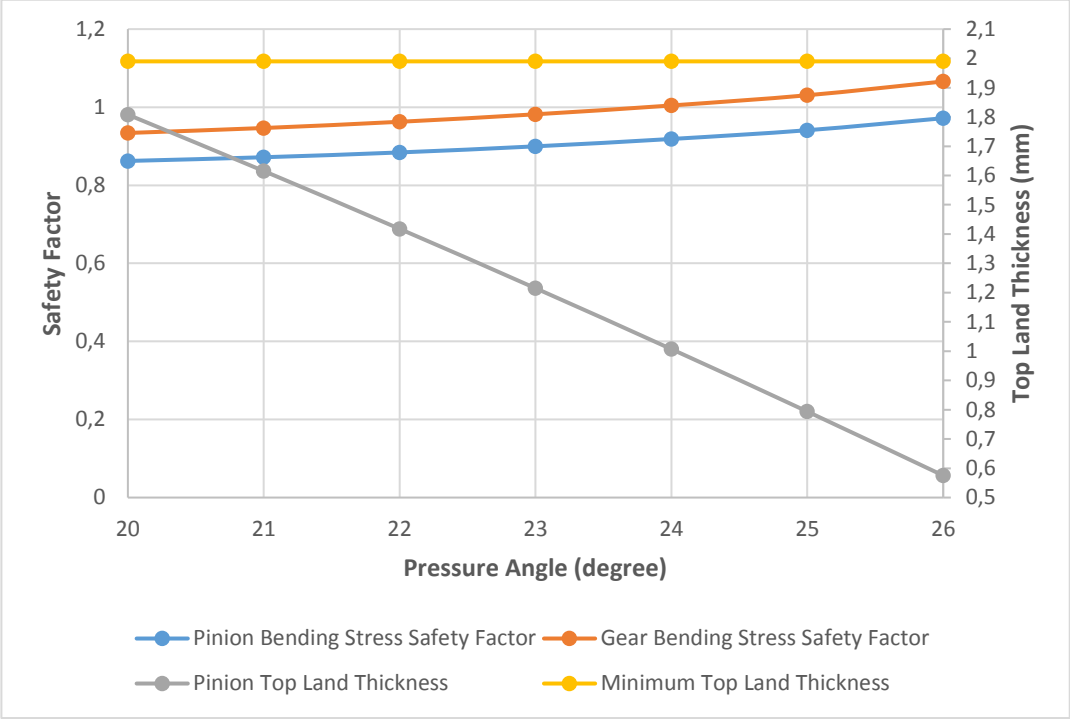

Figure 5-4 *Variation of safety factor and top land thickness vs pressure angle with 0 profile shifting coefficient* ($m_n = 4.1\ mm$, $z_1 = 35$, $z_2 = 138$, $\beta = 23^\circ$, $x_1 = 0$, $r_{a1} = 83.291\ mm$, $r_{a2} = 312.676\ mm$, $r_{f1} = 73.047\ mm$, $r_{f2} = 302.432\ mm$)

As seen from Figure 5-4, the pinion bending stress safety factor is increased and the gear bending stress safety factor is decreased. However, when the bending stress safety factor values are slightly higher than 1 the top land thickness values of the pinion are still below the minimum required top land thickness value. The gear bending stress safety factor values are all below the 1 when the profile shifting coefficient of the pinion is taken as 0.2. Therefore, the iteration can't converge to the optimum center distance of $385.278\ mm$. Because the bending stress safety factor values can be increased only by increasing the addendum radii. However, the maximum possible addendum radii are already implemented.

The optimum center distance can be obtained as $405.321\ mm$. The normal module is directly $4.1\ mm$ and the pinion number of teeth is 37 and the gear number of teeth is

145 with the 23° helix angle and with the 385.278 mm center distance as seen from Table 5.4. The results of Case 21 are filtered by taking the normal module, the pinion number of teeth, the gear number of teeth as 4.1 mm , 37 and 145, respectively. The addendum radii of the pinion and the gear are taken as 87.745 mm and 328.266 mm respectively. The dedendum radii of the pinion and the gear are taken as 77.501 mm and 318.021 mm, respectively. There are remaining seven gear pairs among the results of Case 21 when the design parameters are selected as mentioned above. The bending stress safety factor and the pinion top land thickness relation is given in Figure 5-5.

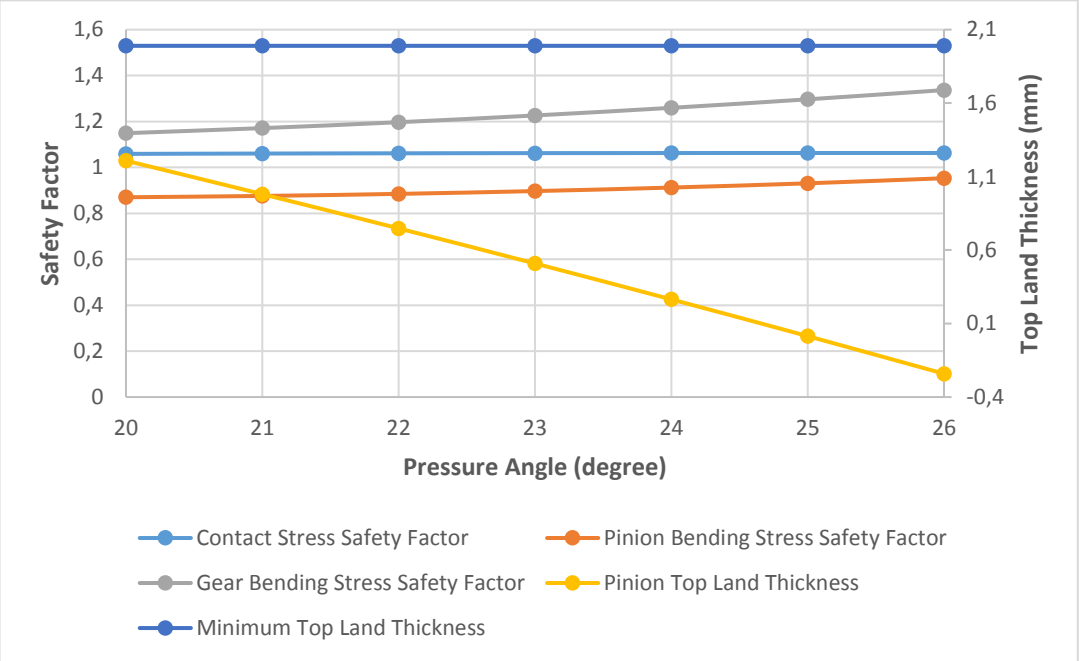

Figure 5-5 *Variation of safety factor and top land thickness vs pressure angle with -0.2 profile shifting coefficient* ($m_n = 4.1\ mm$, $z_1 = 37$, $z_2 = 145$, $\beta = 23^\circ$, $r_{a1} = 87.745\ mm$, $r_{a2} = 328.266\ mm$, $r_{f1} = 77.501\ mm$, $r_{f2} = 318.021\ mm$

As seen from Figure 5-5, the pinion bending stress safety factor values are below 1. The top land thickness values of the pinion are also below the minimum required top

land thickness values. The profile shifting coefficient can be increased to 0.2 to increase the pinion bending stress value and the pinion top land thickness. The obtained results with 0.2 pinion profile shifting coefficient are given in Figure 5-6.

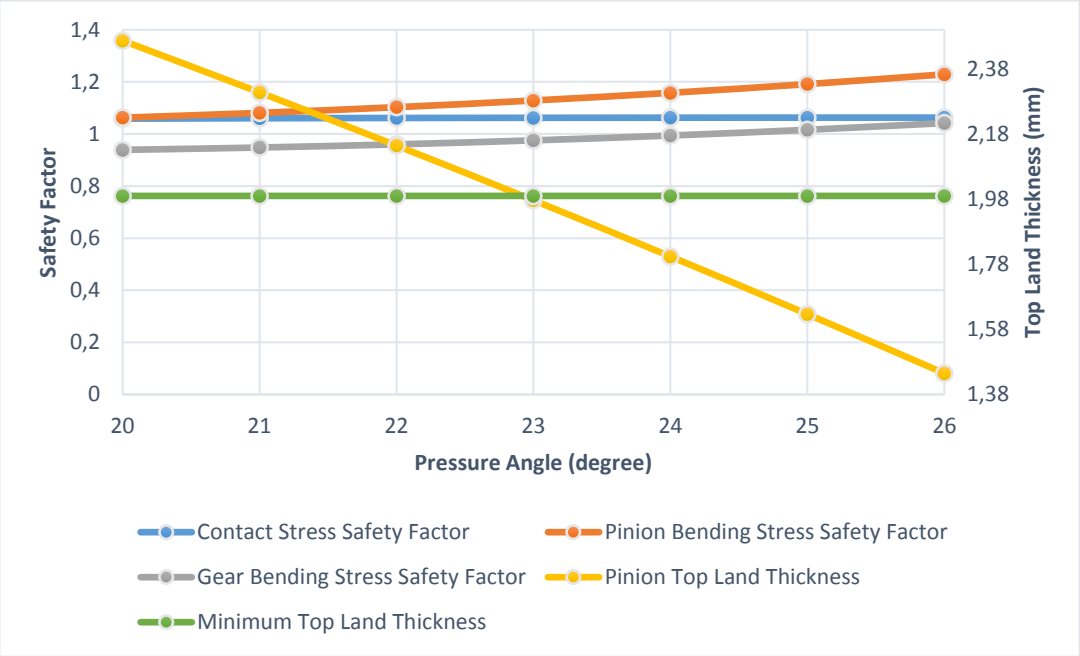

Figure 5-6 *Variation of safety factor and top land thickness vs pressure angle with 0.2 profile shifting coefficient* ($m_n = 4.1\ mm$, $z_1 = 37$, $z_2 = 145$, $\beta = 23^\circ$, $r_{a1} = 87.745\ mm$, $r_{a2} = 328.266\ mm$, $r_{f1} = 77.501\ mm$, $r_{f2} = 318.021\ mm$

It is seen from Figure 5-6 that the gear bending stress safety factor value is higher than 1 when the pressure angle is 25° and 26°. However, the pinion top land thickness is still below the minimum required top land thickness value. If the pressure angle is increased the top land thickness value becomes lower. If the pinion profile shifting coefficient value is increased the tooth thickness of the gear will be lower. Therefore, the gear bending stress safety factor values become lower than 1. As a result, the iteration can't converge to the optimum center distance of $405.321\ mm$.

The optimum center distance can be obtained as 413.469 mm. The normal module is directly 4.4 mm and the pinion number of teeth is 35 and the gear number of teeth is 138 with the 23° helix angle and with the 413.469 mm center distance as seen from Table 5.4. The results of Case 21 are filtered by taking the normal module, the pinion number of teeth, the gear number of teeth as 4.4 mm , 35 and 138, respectively. The addendum radii of the pinion and the gear are taken as 89.386 mm and 335.555 mm, respectively. The dedendum radii of the pinion and the gear are taken as 78.392 mm and 324.561 mm, respectively. There are remaining seven gear pairs among the results of Case 21 when the design parameters are selected as mentioned above. The bending stress safety factor and the pinion top land thickness relation is given in Figure 5-7.

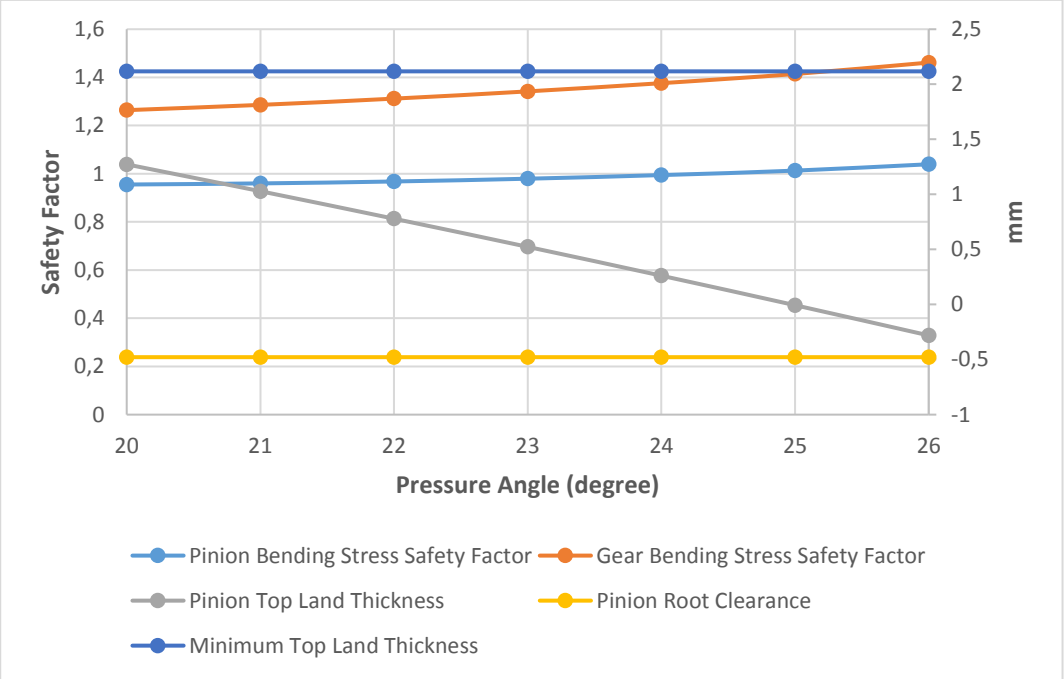

Figure 5-7 *Variation of safety factor, top land thickness and pinion root clearance vs pressure angle with -0.2 profile shifting coefficient* ($m_n = 4.4\ mm$, $z_1 = 35$, $z_2 = 138$, $\beta = 23^\circ$, $r_{a1} = 89.386\ mm$, $r_{a2} = 335.555\ mm$, $r_{f1} = 78.392\ mm$, $r_{f2} = 324.561\ mm$

It is seen from Figure 5-7 that all the pinion and all the gear bending stress safety factor values are almost higher than 1. However, the pinion root clearance is negative. The analysis results are filtered for 413.469 mm center distance. All the constraints are satisfied. However, it is observed that the gear top land thickness criteria is not satisfied while the other constraints are satisfied. There are remaining sixteen gear pairs when the all constraints are satisfied except the gear top land thickness constraint. The safety factor and the top land thickness relation for remaining gear pairs is given in Figure 5-8. All the addendum radii which are 0.8 m_t , 0.9 m_t , 1.0 m_t ,1.1 m_t and 1.2 m_t higher than the pitch radii of the gear pairs obtained in Case 21 are considered. All the dedendum radii which are 1.5 m_t , 1.4 m_t , 1.3 m_t ,1.2 m_t and 1.1 m_t lower than the pitch radii of the gear pairs obtained in Case 21.

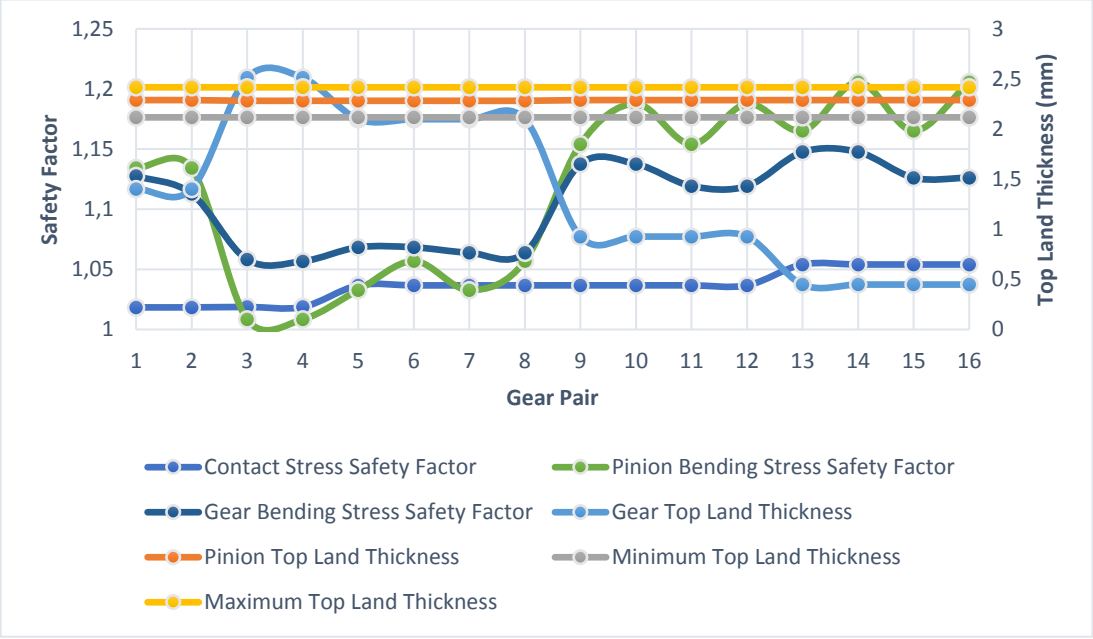

Figure 5-8 *Variation of safety factor and top land thickness* ($m_n = 4.4\,mm$, $z_1 = 35$, $z_2 = 138$, $\beta = 23^\circ$, $x_1 = 0$, 0.2 , $r_{a1} = all$, $r_{a2} = all$, $r_{f1} = all$, $r_{f2} = all$

As seen from Figure 5-8, the contact stress safety factor, the pinion and the gear bending stress safety factor are above 1. However, the gear top land thickness constraint is not satisfied in all steps. Therefore, the iteration does not converge to the 413.469 mm center distance.

The optimum center distance can be obtained as 416.456 mm. The normal module is directly 4.1 mm and the pinion number of teeth is 38 and the gear number of teeth is 149 with the 23° helix angle and with the 416.456 mm center distance as seen from Table 5.4. The results of the Case 21 are filtered by taking the normal module, the pinion number of teeth, the gear number of teeth as 4.1 mm , 38 and 149, respectively. The addendum radii of the pinion and the gear are taken as 89.972 mm and 337.174 mm respectively. The dedendum radii of the pinion and the gear are taken as 79.728 mm and 326.929 mm, respectively. There are remaining seven gear pairs among the results of Case 21 when the design parameters are selected as mentioned above. The bending stress safety factor and the pinion top land thickness relation is given in Figure 5-9.

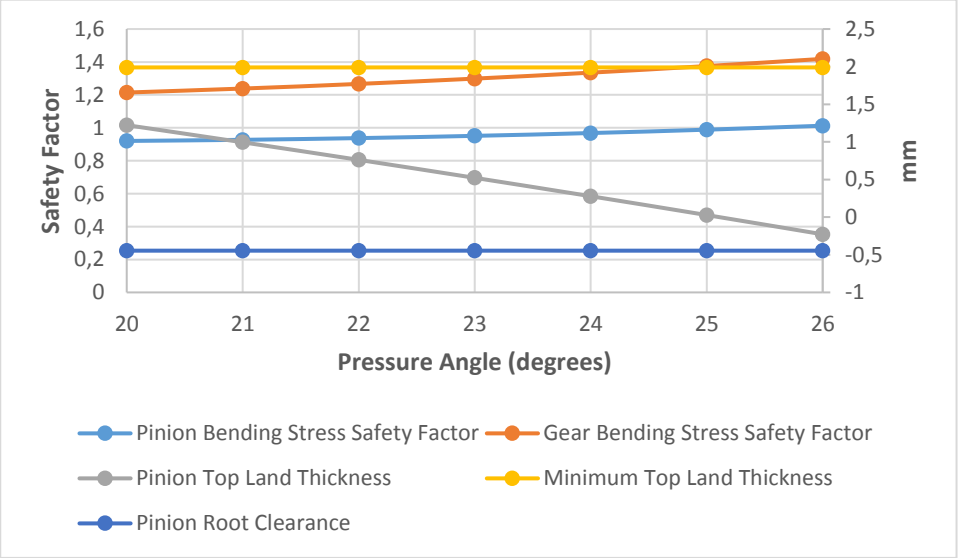

Figure 5-9 *Variation of safety factor, top land thickness and pinion root clearance vs pressure angle with -0.2 profile shifting coefficient* ($m_n = 4.1\ mm$, $z_1 = 38$, $z_2 = 149$, $\beta = 23^{\circ}$, $x_1 = 0$, $r_{a1} = 89.972\ mm$, $r_{a2} = 337.174\ mm$, $r_{f1} = 79.728\ mm$, $r_{f2} = 326.929\ mm$

As seen from Figure 5-9, the pinion top land thickness is below the required minimum top land thickness value. The pinion profile shifting coefficient must be increased to higher values. The pinion profile shifting coefficient is increased to 0.2. The following results given in Figure 5-10 are obtained.

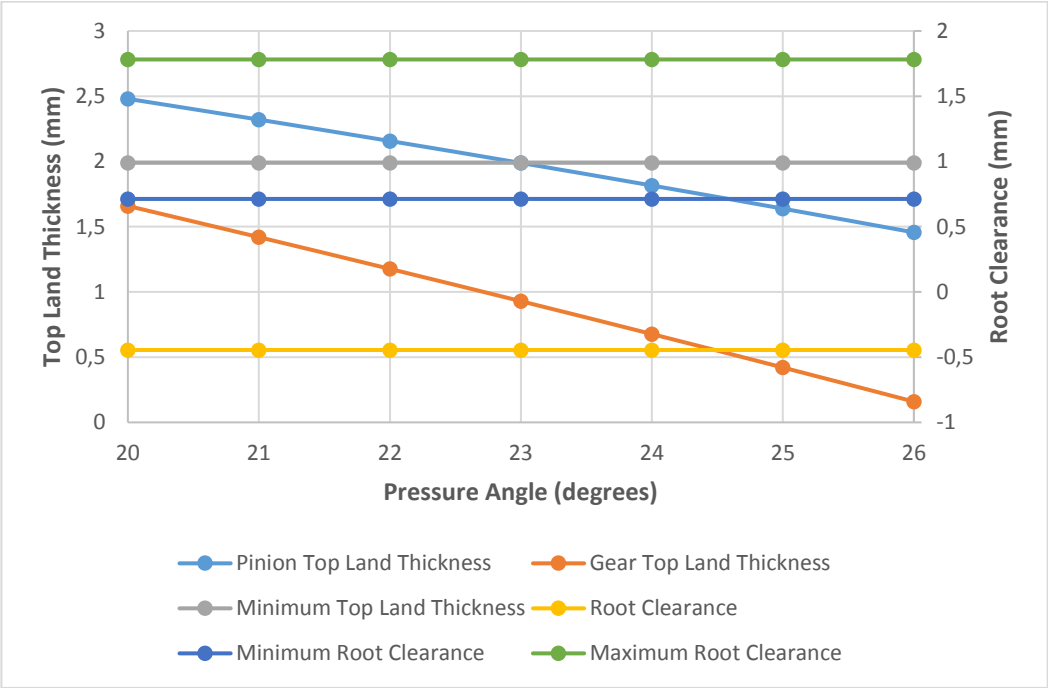

Figure 5-10 *Variation of top land thickness and root clearance vs pressure angle with 0.2 profile shifting coefficient* ($m_n = 4.1\,mm$, $z_1 = 38$, $z_2 = 149$, $\beta = 23^{\circ}$, $r_{a1} = 89.972\,mm$, $r_{a2} = 337.174\,mm$, $r_{f1} = 79.728\,mm$, $r_{f2} = 326.929\,mm$

As seen from Figure 5-10, the gear top land thickness criteria is not satisfied. The results are filtered to $416.456\,mm$ center distance. The pinion profile shifting coefficient are taken as 0 and 0.2. All the pressure angle and the addendum and the dedendum radii are implemented without any elimination. The obtained analysis results are filtered to satisfy all the constraints. However, the gear top land thickness criteria is not satisfied when all the other constraints are satisfied. The following results given in Figure 5-11 is obtained.

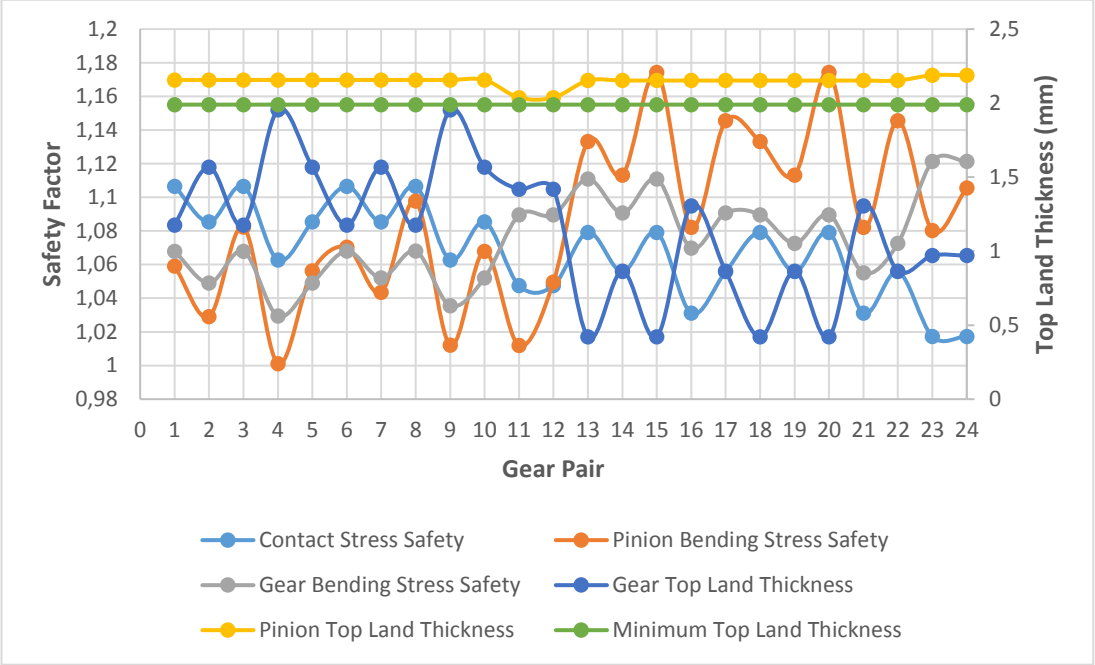

Figure 5-11 *Variation of safety factor and top land thickness* ($m_n = 4.1\ mm$, $z_1 = 38$, $z_2 = 149$, $\beta = 23^\circ$, $x_1 = 0, 0.2$, $r_{a1} = all$, $r_{a2} = all$, $r_{f1} = all$, $r_{f2} = all$

As seen from Figure 5-11, all the safety values are above 1. The pinion top land thickness criteria is also satisfied. However, top land thickness of the gear is below the minimum required top land thickness value in all analysis. Therefore, the iteration does not converge to the $416.456\ mm$ center distance.

5.3. Verification of the Bending Stress Geometry Factor Evaluation

The gear root evaluation is conducted and given in Chapter 2.1.1.6 and Chapter 2.1.1.7 for external and internal gear pairs respectively. The equations given in Chapter 2.1.1.6 are converted into the transverse plane. The gear root equations in transverse plane are:

$$\theta_{x1} = arctan\left(\frac{a_1}{b_1}\right) \tag{5.1}$$

$$R_{f1ty} + A_1 cos(\theta_1 - \theta_{x1}) - b_1 = 0 \tag{5.2}$$

$$a_1 + A_1 sin(\theta_1 - \theta_{x1}) - R_{f1tx} = 0 \tag{5.3}$$

$$a_1{}^2 + b_1{}^2 - \left(r_{f1} + A_1\right)^2 = 0 \tag{5.4}$$

$$\sqrt{\left(r_{f1} + A_1\right)^2 - r_{b1}{}^2} - A_1 - \sqrt{R_{f1n}{}^2 - r_{b1}{}^2} = 0 \tag{5.5}$$

The bending stress geometry factor evaluation is conducted by using the gear root equations in the transverse plane for the optimized gear pair obtained by Case 1 given in Table 4.4. The results of the bending stress geometry factor evaluation of the optimized gear pair in Case 1 are given in Table 5.7.

Table 5.7 *Comparison of the bending stress geometry factor of the optimized gear pair obtained by Case 1*

Parameters	***Kissoft***	***Current Study***
h_{f1}	6.70 mm	6.70 mm
h_{f2}	6.78 mm	6.75 mm
S_{F1}	7.44 mm	7.43 mm
S_{F2}	7.76 mm	7.74 mm
α_{nL1}	29.10°	29.10°
α_{nL2}	24.31°	24.31°
K_{ψ}	0.95	0.95
C_h	1.28	1.28
Y_1	0.637	0.635
Y_2	0.641	0.640
K_{f1}	1.578	1.491
K_{f2}	1.584	1.515
C_{ψ}	1	1
m_N	0.59	0.59
A_1	1.1516 mm	1.1516 mm
A_2	1.1941 mm	1.1942 mm
A_{1v}	0.6845 mm	1.1168 mm
A_{2v}	0.7745 mm	1.1539 mm
J_1	0.683 mm	0.721 mm
J_2	0.684 mm	0.716 mm
s_{t1}	352 MPa	332 MPa
s_{t2}	351 MPa	334 MPa

CHAPTER 6

CONCLUSIONS AND FUTURE WORK

The main concern of the current study is the optimization of cylindrical gear pairs. Normal module, helix angle, pinion number of teeth, gear number of teeth, addendum radius of the pinion, dedendum radius of the pinion, addendum radius of the gear, dedendum radius of the gear and pressure angle are design parameters. Root clearance, top land thickness, contact ratio, involute clearance and tiff clearance are considered as the geometrical constraints. Evaluation of contact stress, bending stress and scuffing probability are conducted as material based constraints. From Table 1.1 it is seen that studies conducted in the literature usually consider a few parameters as design parameters. However, ten design parameters are optimized by using the developed methodology by applying five geometrical constraints and three material based constraints in the current study. In the literature it is seen that nontraditional optimization techniques are used in the studies. However, it is given by Wu [3] that there is always the possibility of finding a local optimum in nontraditional optimization techniques. Additional methods must be implemented to overcome the possibility of local optimum. However, when the conducted studies in the literature are considered, it is seen that the optimization problems are usually consisted of a few design parameters and the number of constraint functions are not high as evaluated in the current study.

Furthermore, the rounded gear root evaluation is not conducted in the studies. However, the current study suggests an optimization method with rounded root evaluations by considering the arbitrary addendum and dedendum radii for the pinion and the gear. Therefore, using a nontraditional optimization technique can cause a local optimum solution in such a detailed gear optimization problem. In the current study, fine sizing method is implemented for optimization. All the possible gear sets

for the given range of the design variables are evaluated in fine sizing method. The constraints are applied for each of the gear pairs. The gear pairs which don't satisfy one of the constraints are eliminated. The possibility of the local optimum solution is eliminated since all the possible solutions are considered for given range of each design variables.

The most remarkable contribution of the current study is the evaluation of the root geometry and the bending stress geometry factor of the gear pairs which have rounded gear root. The gear root evaluation is conducted and given in Chapter 2.1.1.6 and Chapter 2.1.1.7 for external and internal gear pairs, respectively. The helical gears which are produced by grinding method have rounded gear root in the normal plane. However, when Table 5.1 and Table 5.2 are considered, it is seen that the evaluated bending stress geometry factor differs from Kissoft commercial tool. The gear root equations given in Chapter 2.1.1.6 are converted into the transverse plane and given in equations (5.1), (5.2), (5.3), (5.4) and (5.5). Evaluation of the root geometry and the bending stress geometry factor is evaluated in the transverse plane for the optimized gear pair obtained by Case1 given in Table 4.4. The obtained results are given in Table 5.7. It is seen from Table 5.7 that the maximum radii of the gear roots (A_1 and A_2) are the same in Kissoft and in the current study. Therefore, it is concluded that Kissoft evaluates the gear root in the transverse section. However, the helical gears which are produced by grinding method have rounded gear root in the normal plane.

Since the maximum radii of the gear roots are the same, it is expected that the stress correction factor for the pinion and for the gear (K_{f1} and K_{f2}) must be the same. However, it is seen that the maximum radii of the virtual gear roots (A_{1v} and A_{2v}) are different in Kissoft results and in the current study. The difference in the radii of the virtual gear roots comes from that Kissoft uses the methodology outlined in AGMA 908 [13] while the methodology given in Chapter 2.1.2.2.3 is used in the current study. However, the methodology given in [13] is applicable for the gears which have trochoidal gear root. Therefore, the methodology given in [13] does not cover the gears which are produced by grinding method.

The outlined methodology in the current study covers the effect of fully rounded gear roots and the backlash on the bending stress geometry factor evaluation. The lubrication regime is also considered in the contact stress evaluation. The outlined methodology differs from the other studies and Kissoft commercial tool by considering the fully rounded gear root, the lubrication regime and the gears produced by grinding method.

The proposed methodology in the current study is suitable for the gear pairs produced by nontraditional manufacturing methods and the optimized design parameters are nonstandard. The minimum weight consideration is the most important design constraint in aerospace applications. The minimum weight consideration requires an optimization methodology and nonstandard design parameters. In the current study, the minimum center distance optimization is implemented by obtaining the nonstandard optimized design parameters. There are lots of studies in aerospace applications to decrease the weight of an air vehicle. The proposed methodology has a crucial role in aerospace applications regarding the minimum weight considerations. However, the standard gear pairs which are designed without an optimization methodology are not the gear pairs which have the minimum center distance and the minimum weight. Therefore, the standard gear pairs are not suitable for aerospace applications.

The proposed methodology in the current study covers the optimization of the single pair of external and internal gear pairs. Optimization of the planetary stages can be implemented by using the same methodology as a future work. In the literature, there are some studies which evaluate the bending stress of the asymmetric gears as outlined in [10]. Therefore, the proposed optimization methodology can be also expanded into the optimization of asymmetric external and internal gear pairs. Evaluation of the gear root and the bending stress geometry factor with the $0.250\,mm$ normal circular backlash are conducted for different external and internal gear pairs. The obtained results are given in Table 6.1 and Table 6.2.

Table 6.1 *Gear root and bending stress geometry factor evaluation for external gear pairs with* $0.250\ mm$ *normal circular backlash*

Study	***1***	***2***	***3***	***4***	***5***
m_n	$3.2\ mm$	$4.1\ mm$	$3.2\ mm$	$3.8\ mm$	$3.2\ mm$
β	13°	17°	21°	21°	7°
x_1	0.2	0.2	0.2	0.3	-0.1
z_1	37	40	37	43	40
z_2	145	157	145	169	157
α_n	23°	23°	21.5°	24°	25°
a_w	$298.86\ mm$	$422.303\ mm$	$311.917\ mm$	$431.457\ mm$	$317.567\ mm$
$\boldsymbol{r_{a1}}$	$64.698\ mm$	$90.892\ mm$	$67.525\ mm$	$92.397\ mm$	$67.382\ mm$
$\boldsymbol{r_{a2}}$	$241.058\ mm$	$340.414\ mm$	$251.591\ mm$	$347.201\ mm$	$256.633\ mm$
$\boldsymbol{r_{f1}}$	$56.816\ mm$	$80.602\ mm$	$58.956\ mm$	$82.628\ mm$	$59.967\ mm$
$\boldsymbol{r_{f2}}$	$233.176\ mm$	$330.125\ mm$	$243.364\ mm$	$337.839\ mm$	$249.218\ mm$
A_1	$1.197\ mm$	$1.435\ mm$	$1.169\ mm$	$0.878\ mm$	$1.284\ mm$
A_2	$1.244\ mm$	$1.486\ mm$	$1.283\ mm$	$1.391\ mm$	$1.031\ mm$
A_{1v}	$1.196\ mm$	$1.432\ mm$	$1.166\ mm$	$0.875\ mm$	$1.284\ mm$
A_{2v}	$1.243\ mm$	$1.484\ mm$	$1.281\ mm$	$1.388\ mm$	$1.031\ mm$
J_1	0.677	0.690	0.632	0.694	0.611
J_2	0.671	0.685	0.645	0.660	0.691

Table 6.2 *Gear root and bending stress geometry factor evaluation for internal gear pairs with* $0.250\ mm$ *normal circular backlash*

Study	***1***	***2***	***3***	***4***	***5***
m_n	$7.1\ mm$	$4.7\ mm$	$7.1\ mm$	$4.5\ mm$	$7.1\ mm$
β	7°	11°	6°	11°	10°
x_1	0	-0.1	0	0.2	0
z_1	25	25	25	26	25
z_2	68	68	68	71	68
α_n	29°	28°	29°	26°	29°
a_w	$153.796\ mm$	$102.941\ mm$	$153.491\ mm$	$103.145\ mm$	$155.005\ mm$
$\boldsymbol{r_{a1}}$	$95.854\ mm$	$63.680\ mm$	$95.664\ mm$	$64.638\ mm$	$96.608\ mm$
$\boldsymbol{r_{a2}}$	$236.060\ mm$	$157.524\ mm$	$235.591\ mm$	$158.614\ mm$	$237.915\ mm$
$\boldsymbol{r_{f1}}$	$80.117\ mm$	$53.146\ mm$	$79.958\ mm$	$53.635\ mm$	$80.747\ mm$
$\boldsymbol{r_{f2}}$	$251.797\ mm$	$168.058\ mm$	$251.297\ mm$	$169.158\ mm$	$253.775\ mm$
A_1	$1.946\ mm$	$1.570\ mm$	$1.959\ mm$	$1.178\ mm$	$1.890\ mm$
A_2	$1.174\ mm$	$1.012\ mm$	$1.191\ mm$	$1.203\ mm$	$1.107\ mm$
A_{1v}	$1.944\ mm$	$1.566\ mm$	$1.958\ mm$	$1.175\ mm$	$1.887\ mm$
A_{2v}	$1.174\ mm$	$1.012\ mm$	$1.191\ mm$	$1.203\ mm$	$1.107\ mm$
J_1	0.640	0.879	0.625	0.914	0.679
J_2	0.803	1.152	0.786	1.116	0.850

REFERENCES

[1] Y. M. Mohan and T. Seshaiah, " Spur Gear Optimization by Using Genetic Algorithm, '' *International Journal of Engineering Research and Applications,* vol. 2, No. 1, pp. 311-318, Jan-Feb.2012.

[2] A. K. Singh, H. P. Gangwar, R. Saxena and A. Misra, " Optimization of Internal Spur Gear Design Using Genetic Algorithm, '' *MIT International Journal of Mechenical Engineering,* vol. 2, No. 1, pp. 22-30, Jan.2012.

[3] R. Wu, "Gear Weight Optimization Design Model Based on Disturbance and Simulated Annealing Algorithm, ''*Metallurgical and Mining Industry,* vol. 51, No. 8, pp. 502-507, 2015.

[4] V. Revar, D. Parmar and H. Shah, "Design, Modelling and Stress Analysis of High Speed Helical Gear on Basis of Bending Strength and Contact Strength by Changing Face Width and Helix Angle, ''*International Journal For Technological Research In Engineering,* vol.3, Issue 9, pp. 1975-1980, May 2016.

[5] A. L. Kapelevich and Y. V. Shekhtman, "Direct Gear Design: Bending Stress Minimization, ''*Gear Technology,* vol.20, No. 5, pp. 44-47 , September-October 2003.

[6] S. Padmanabhan, S. Ganesan, M. Chandrasekaran, and V. Srinivasa Raman, "Gear pair design optimization by genetic algorithm and FEA," *Proc. Int. Conf. Front. Automob. Mech. Eng. - 2010, FAME-2010,* No. November, pp. 301–307, 2010.

[7] Ram Gopal, Rajiv Suman and R.S. Jadoun, " Optimization of Helical Gear Design Using Genetic Algorithm for Center Distance, ''*International Journal of Advance and Innovation*, vol.4, Issue 3, pp. 543-548, 2016.

[8] Dr. Rajiv Suman, Ram Gopal, Anshika Gupta and Praveen Kumar Singh " Use of Genetic Algorithm for Center Distance to Optimize the Helical Gear Design, ''*Seminar on Advances in Technology to Mitigate the Effect of Natural Hazards, organized by The Institution of Engineers (India), Pantnagar Local Centre, March 2-3, 2017.*

[9] Paridhi Rai, Asim Gopal Barman, "Design Optimization of Spur Gear Using SA and RCGA, *''Journal of the Brazilian Society of Mechanical Sciences and Engineering,* vol.40, Issue 5, pp. 1-8, 2018.

[10] Mahir Gökhan Orak, "Investigation of Asymmetric Gear Tooth Bending Stress Formulation, *''Middle East Technical University,* March 2018.

[11] International Standard Organization, ''Gears – Cylindrical involute gears and gear pairs – Concepts and geometry ISO 21771,'' vol.01, no. September, p.31, 2007.

[12] American Gear Manufacturers Association, "Method for Specifying the Geometry of Spur and Helical Gears AGMA 913-A98," vol. 98, no. March, p. 4-8,12, 1998.

[13] American Gear Manufacturers Association, "Geometry Factors for Determining the Pitting Resistance and Bending Strength of Spur, Helical and Herringbone Gear Teeth AGMA 908-B89," vol. 89, no. August, p. 5-8,16 ,1989.

[14] American Gear Manufacturers Association, “Fundamental Rating Factors and Calculation Methods for Involute Spur and Helical Gear Teeth AGMA 2001-D04,” vol. 04, no. December, p. 9-18, 20-24,33-42, 2004.

[15] Engineering Sciences Data Unit, ‘‘The design of spur and helical involute gears. A procedure compatible with BS 436: Part 3: method for calculation of contact and root bending stress limitations for metallic involute gears ESDU 88033,’’ vol.3, no. June, p.32, 16, 2012

[16] American Gear Manufacturers Association, “Effect of Lubrication on Gear Surface Distress AGMA 925-A03,” vol. 03, no. January, p. 7-25, 2013.

[17] Stephen P.Radzevich, Dudley’s Handbook of Practical Gear Design and Manufacture, ’’ *CRC Press,* Second Edition, pp. 311-318, 2012.

[18] International Organization for Standardization, ‘‘Calculation of Load Capacity of Spur and Helical Gears ISO/DIS 6336-6.’’ no. September, p.15,16, 2005

APPENDICES

A. Overload factor, K_o

Overload factor,K_o, is given in [18]. Examples for driving machines with various characteristics are given in Table A.1.

Table A.1 Examples for driving machines with various working characteristics [18]

Working characteristic	Driving machine
Uniform	Electric motor (e.g. d.c. motor), steam or gas turbine with uniform operation [a] and small rarely occurring starting torques [b].
Light shocks	Steam turbine, gas turbine, hydraulic or electric motor (large, frequently occurring starting torques [b]).
Moderate shocks	Multiple cylinder internal combustion engines.
Heavy shocks	Single cylinder internal combustion engines.
[a] Based on vibration tests or on experience gained from similar installations. [b] See service life graphs, Z_{NT}, Y_{NT}, for the material in ISO 6336-2 and ISO 6336-3. Consideration of momentarily acting overload torques, see examples following Table B.1.	

In aerospace industry, gas turbines are generally used. Therefore, driving machine characteristic of the driving machine is specified as light shocks.

Table A.2 Examples of working characteristics of driven machine [18]

Working characteristic	Driven machines
Uniform	Steady load current generator; uniformly loaded conveyor belt or platform conveyor; worm conveyor; light lifts; packing machinery; feed drives for machine tools; ventilators; light-weight centrifuges; centrifugal pumps; agitators and mixers for light liquids or uniform density materials; shears; presses, stamping machines [a]; vertical gear, running gear [b].
Light shocks	Non-uniformly (i.e. with piece or batched components) loaded conveyor belts or platform conveyors; machine-tool main drives; heavy lifts; crane slewing gear; industrial and mine ventilators; heavy centrifuges; centrifugal pumps; agitators and mixers for viscous liquids or substances of non-uniform density; multi-cylinder piston pumps; distribution pumps; extruders (general); calendars; rotating kilns; rolling mill stands [c], (continuous zinc and aluminium strip mills, wire and bar mills).
Moderate shocks	Rubber extruders; continuously operating mixers for rubber and plastics; ball mills (light); wood-working machines (gang saws, lathes); billet rolling mills [c, d]; lifting gear; single cylinder piston pumps.
Heavy shocks	Excavators (bucket wheel drives); bucket chain drives; sieve drives; power shovels; ball mills (heavy); rubber kneaders; crushers (stone, ore); foundry machines; heavy distribution pumps; rotary drills; brick presses; de-barking mills; peeling machines; cold strip [c, e]; briquette presses; breaker mills.

[a] Nominal torque = maximum cutting, pressing or stamping torque.
[b] Nominal torque = maximum starting torque.
[c] Nominal torque = maximum rolling torque.
[d] Torque from current limitation.
[e] K_A up to 2,0 because of frequent strip cracking.

Since the gear pairs are considered in this study, working characteristic of the driven machine is specified as uniform.

After determining the characteristics of the driving and driving machine, overload factor is specified by using Table A.3

Table A.3 Overload factor, K_o [18]

Working characteristic of driving machine	Working characteristic of driven machine			
	Uniform	Light shocks	Moderate shocks	Heavy shocks
Uniform	1,00	1,25	1,50	1,75
Light shocks	1,10	1,35	1,60	1,85
Moderate shocks	1,25	1,50	1,75	2,00
Heavy shocks	1,50	1,75	2,00	W 2,25

As seen from Table A.3**,** overload factor is ′1.10′ for light shock driving machine and uniform driven machine.

B. Load Distribution Factor, K_m

In [14], the load distribution factor (K_m) is given as:

$$K_m = C_{mf} \tag{B.1}$$

For relatively stiff gear designs having gears mounted between bearings and relatively free from externally caused deflections, the following approximate method may be used:

$$C_{mf} = 1.0 + C_{mc}\left(C_{pf}C_{pm} + C_{ma}C_e\right) \tag{B.2}$$

Lead correction factor, C_{mc}, is 0.8 for gear with leads properly modified by crowning or lead correction.

The values for C_{pf} can be determined by the following equations:

when $F \leq 1.0$

$$C_{pf} = \frac{F}{10d_{w1}} - 0.025 \tag{B.3}$$

when $1.0 < F \leq 17$

$$C_{pf} = \frac{F}{10d_{w1}} - 0.0375 + 0.0125F \tag{B.4}$$

when $17 < F \leq 40$

$$C_{pf} = \frac{F}{10d_{w1}} - 0.1109 + 0.0207F - 0.000228F^2 \tag{B.5}$$

For values of $(F\ /\ (10d\_w1\ ))$ less than 0.05, 0.05 is used for C_{pf}.

C_{pm} is 1.0 for straddle mounted pinions with $S_1/S < 0.175$ and C_{pm} is 1.1 for straddle mounted pinions with $S_1/S \geq 0.175$.

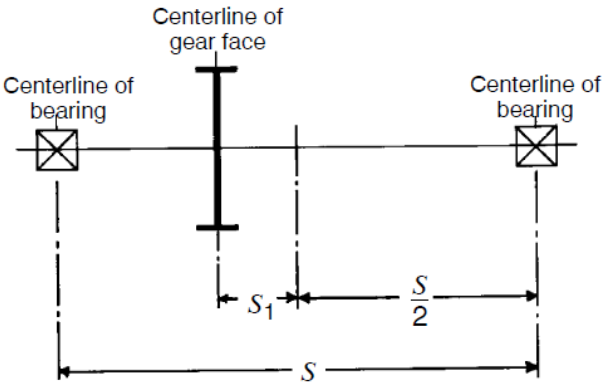

Fig. B.1 Evaluation of S and S_1 [14]

C_{pm} is taken as unity in this study.

The mesh alignment factor, C_{ma}, is given as:

$$C_{ma} = A + B(F) + C(F)^2 \tag{B.6}$$

Table B.1 Empirical constants; A, B *and* C [14]

Curve	*A*	*B*	*C*
Curve 1 Open gearing	2.47×10^{-1}	0.167×10^{-1}	-0.765×10^{-4}
Curve 2 Commercial enclosed gear units	1.27×10^{-1}	0.158×10^{-1}	-1.093×10^{-4}
Curve 3 Precision enclosed gear units	0.675×10^{-1}	0.128×10^{-1}	-0.926×10^{-4}
Curve 4 Extra precision enclosed gear units	0.380×10^{-1}	0.102×10^{-1}	-0.822×10^{-4}

Extra precision enclosed gear units are considered in this study.

C_e is 0.80 when the gearing is adjusted at assembly;

is 0.80 when the compatibility of the gearing is improved by lapping;

is 1.0 for all other conditions.

Super finished gears are considered in this study. Therefore, C_e is taken as 0.8.

C. Rim Thickness Factor

Rim thickness factor is given in Fig. A.2.

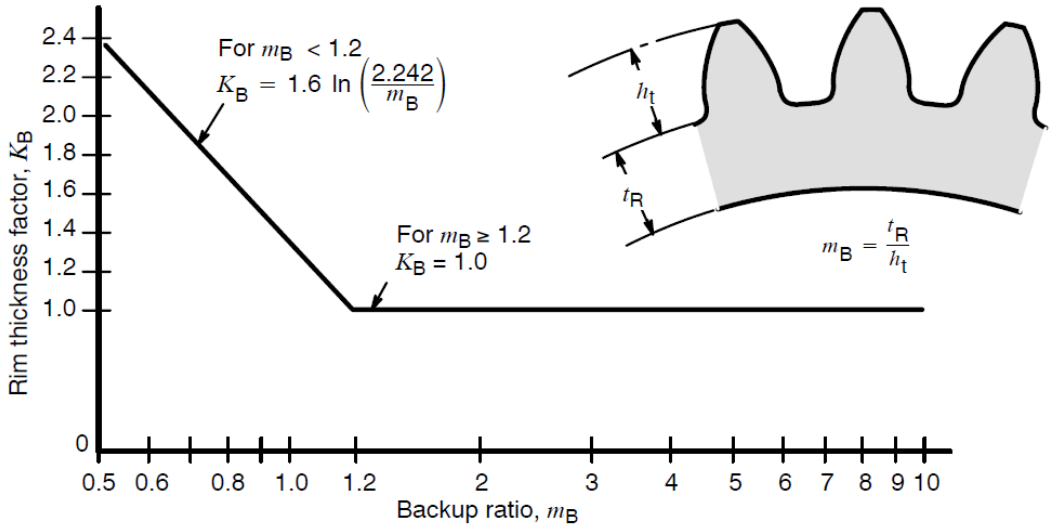

Fig. C.1 Rim thickness factor, K_B [14]

In this study, $\boldsymbol{m_B}$ is considered as higher than 1.2. Therefore, rim thickness factor is taken as unity.

D. Other Factors

According to [14], where gearing is manufactured using process controls which provide tooth accuracies which correspond to ‘very accurate gearing ‘, or where the design and manufacturing techniques ensure a low transmission error which is equivalent to this accuracy, values of K_v between 1.02 and 1.11 may be used, depending on the specifier’s experience with similar applications and the degree of accuracy actually achieved. Since aerospace gears have a very high level of accuracy, dynamic factor is taken as 1.02.

The size factor, K_s is related with non-uniformity of material properties. Since the gear materials used in the current study are Grade 3 quality, the size factor is taken as unity.

The surface condition factor, C_f is related with surface finish and residual stresses. Since the gear teeth are grinded from solid and shot peened, the tensile residual stresses on the gear teeth are avoided even the compressive residual stresses arise. Also since the super finish is applied on the gear teeth, the surface roughness is minimized. Therefore, C_f is taken as unity.

E. Scuffing Risk Evaluation

Scuffing risk evaluation is given in [16]. For random variables that follow normal (Gaussian) distributions, the following procedure can be used to calculate probabilities of failure in the range of 5 % to 95 %.

$$x = \frac{(y - \mu_y)}{\sigma_y} \tag{E.1}$$

$$Z_Q = 0.3989422804 e^{[-0.5(x)^2]} \tag{E.2}$$

Table E.1 Constant parameters for Scuffing Evaluation [16]

Parameter	*Value*
$\boldsymbol{b_1}$	0.319381530
$\boldsymbol{b_2}$	−0.356563782
$\boldsymbol{b_3}$	1.781477937
$\boldsymbol{b_4}$	−1.821255978
$\boldsymbol{b_5}$	1.330274429
$\boldsymbol{p}$	0.2316419

$$t = \frac{1}{1 + p|x|} \tag{E.3}$$

Evaluation of Q

if $|x| > 1.6448$, then:

$$Q = 0.05; \tag{E.4}$$

else

$$Q = Z_Q(b_1 t + b_2 t^2 + b_3 t^3 + b_4 t^4 + b_5 t^5) \quad \text{(E.5)}$$

Probability of failure

if $x > 0$, then:

$$probablity\ of\ failure = 1 - Q \quad \text{(E.6)}$$

else

$$probablity\ of\ failure = Q \quad \text{(E.7)}$$

F. Evaluation of Material Parameter

Material parameter is given in [16]:

$$G = \alpha E_r \tag{F.1}$$

Where

$$\alpha = k(\eta_M)^s \tag{F.2}$$

$$\alpha = k(\eta_M)^s \tag{F.3}$$

$$\eta_M = 10^g - 0.9 \tag{F.4}$$

$$g = 10^c(\theta_M + 273.15)^d \tag{F.5}$$

$$c = \log_{10}[\log_{10}(\eta_{40} + 0.9)] - 2.495752d \tag{F.6}$$

$$d = 13.13525 \log_{10}\left[\frac{\log_{10}(\eta_{100} + 0.9)}{\log_{10}(\eta_{40} + 0.9)}\right] \tag{F.7}$$

Viscosity and pressure-viscosity coefficient values for different lubricants are given in Table F.1. MIL – L – 23699E is considered in this study.

Dynamic viscosity of the oil at 40 ℃ is:

$$\eta_{40} = 22.56448\ mPa.s \tag{F.8}$$

Dynamic viscosity of the oil at 100 ℃ is:

$$\eta_{100} = 4.591235\ mPa.s \tag{F.9}$$

$$k = 0.006515 \tag{F.10}$$

Table F.1 *Data for determining viscosity and pressure-viscosity coefficient [16]*

Lubricant	ISO VG[1)]	η_{40}	η_{100}	c	d	k	s
Mineral oil	32	27.17816	4.294182	10.20076	−4.02279	0.010471	0.1348
	46	39.35879	5.440514	10.07933	−3.95628	0.010471	0.1348
	68	58.64514	7.059163	9.90355	−3.86833	0.010471	0.1348
	100	86.91484	9.251199	9.65708	−3.75377	0.010471	0.1348
	150	131.4335	12.27588	9.42526	−3.64563	0.010471	0.1348
	220	194.2414	15.98296	9.24059	−3.55832	0.010471	0.1348
	320	284.6312	20.60709	9.09300	−3.48706	0.010471	0.1348
	460	412.0824	26.34104	8.96420	−3.42445	0.010471	0.1348
	680	613.8288	34.24003	8.84572	−3.36585	0.010471	0.1348
	1000	909.4836	38.56783	9.25943	−3.52128	0.010471	0.1348
	1500	1374.931	49.58728	9.19946	−3.48702	0.010471	0.1348
	2200	2031.417	62.69805	9.15646	−3.46064	0.010471	0.1348
	3200	2975.954	78.56109	9.13012	−3.44157	0.010471	0.1348
PAO – based synthetic non–VI improved oil	150	128.5772	16.17971	7.99428	−3.07304	0.010326	0.0507
	220	189.9828	21.60933	7.79927	−2.98154	0.010326	0.0507
	320	278.3370	28.66405	7.63035	−2.90169	0.010326	0.0507
	460	402.8943	37.54020	7.49799	−2.83762	0.010326	0.0507
	680	600.0179	53.20423	7.16434	−2.69277	0.010326	0.0507
	1000	868.1710	68.60767	7.12008	−2.66528	0.010326	0.0507
	1500	1310.350	91.03300	7.07678	−2.63766	0.010326	0.0507
	2200	1933.070	118.0509	7.06113	−2.62221	0.010326	0.0507
	3200	2827.726	151.2132	7.06594	−2.61561	0.010326	0.0507
	6800	6077.362	244.5559	7.11907	−2.62091	0.010326	0.0507
PAG – based synthetic[2)]	100	102.630	19.560	6.42534	−2.45259	0.0047	0.1572
	150	153.950	27.380	6.19586	−2.34616	0.0047	0.1572
	220	225.790	40.090	5.76552	−2.16105	0.0047	0.1572
	320	328.430	56.710	5.49394	−2.04065	0.0047	0.1572
	460	472.130	77.250	5.35027	−1.97254	0.0047	0.1572
	680	697.920	113.43	5.06011	−1.84558	0.0047	0.1572
	1000	1026.37	163.30	4.85075	−1.75175	0.0047	0.1572
MIL–L–7808K Grade 3	12	11.35364	2.701402	9.58596	−3.82619	0.005492	0.25472
MIL–L–7808K Grade 4	17	16.09154	3.609883	9.08217	−3.60300	0.005492	0.25472
MIL–L–23699E	23	22.56448	4.591235	8.91638	−3.51779	0.006515	0.16530

NOTES:
1) ν_{40} (mm^2/s)
2) Copolymer of ethylene oxide and propylene oxide in 50% weight ratio.

G. Backlash and Tip Round Values

When the backlash is required, the following values given in Table G.1 can be used. For tip chamfer, the following values given in Table G.2 can be used.

Table G.1 *Recommended backlash values [17]*

Recommended Backlash Allowance for Power Gearing

Normal Diametral Pitch, P_{nd}	Center Distance, in. (3.93701×10^{-2} mm)						
	0–5	5–10	10–20	20–30	30–50	50–80	80–120
0.5	–	–	–	–	0.045	0.060	0.080
1	–	–	–	0.035	0.040	0.050	0.060
2	–	–	0.025	0.030	0.035	0.045	0.055
3	–	0.018	0.022	0.027	0.033	0.042	–
4	–	0.016	0.020	0.025	0.030	0.040	–
6	0.008	0.010	0.015	0.020	0.025	–	–
8	0.006	0.008	0.012	0.017	–	–	–
10	0.005	0.007	0.010	–	–	–	–
12	0.004	0.006	–	–	–	–	–
16	0.004	0.005	–	–	–	–	–
20	0.004	–	–	–	–	–	–
32	0.003	–	–	–	–	–	–
64	0.002	–	–	–	–	–	–

Table G.2 *Tip round values [17]*

Values for Tip Round and Edge Round and End Round

Diametral Pitch	Edge Round			Tip Round and End Round
	General Applications	Medium Strength	High Strength	
20 and finer	Burr brush edges	0.001–0.005	0.005–0.010	0.001–0.005
16	Burr brush edges	0.003–0.015	0.010–0.025	0.003–0.010
12	Burr brush edges	0.005–0.020	0.012–0.030	0.005–0.015
10	Burr brush edges	0.010–0.025	0.015–0.035	0.005–0.015
8	Burr brush edges	0.010–0.025	0.020–0.045	0.010–0.030
5	Burr brush edges	0.010–0.025	0.025–0.060	0.010–0.030
3	Burr brush edges	0.015–0.035	0.040–0.090	0.010–0.050
2	Burr brush edges	0.015–0.035	0.060–0.125	0.010–0.050

H. Optimization Flow Chart

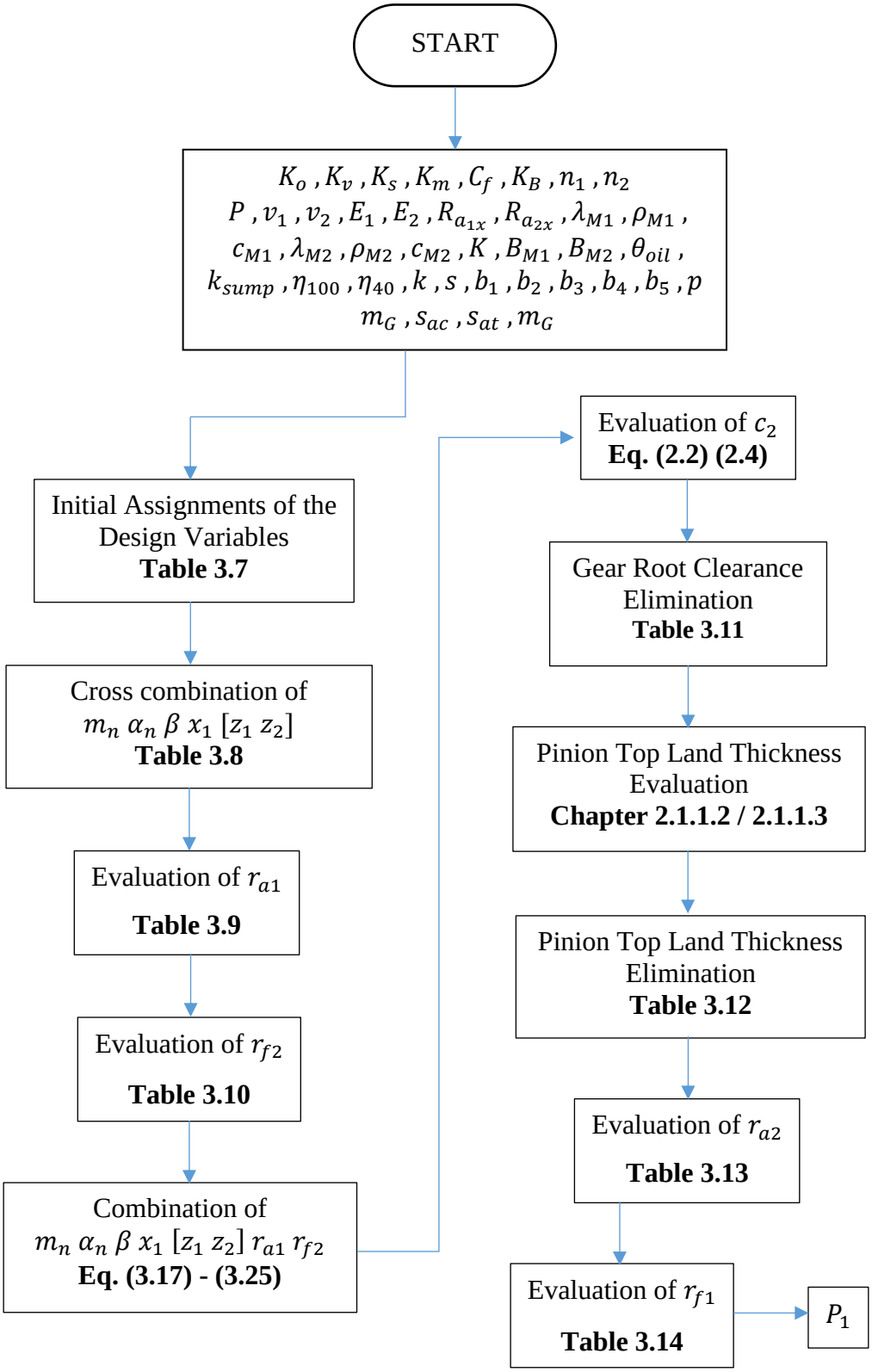

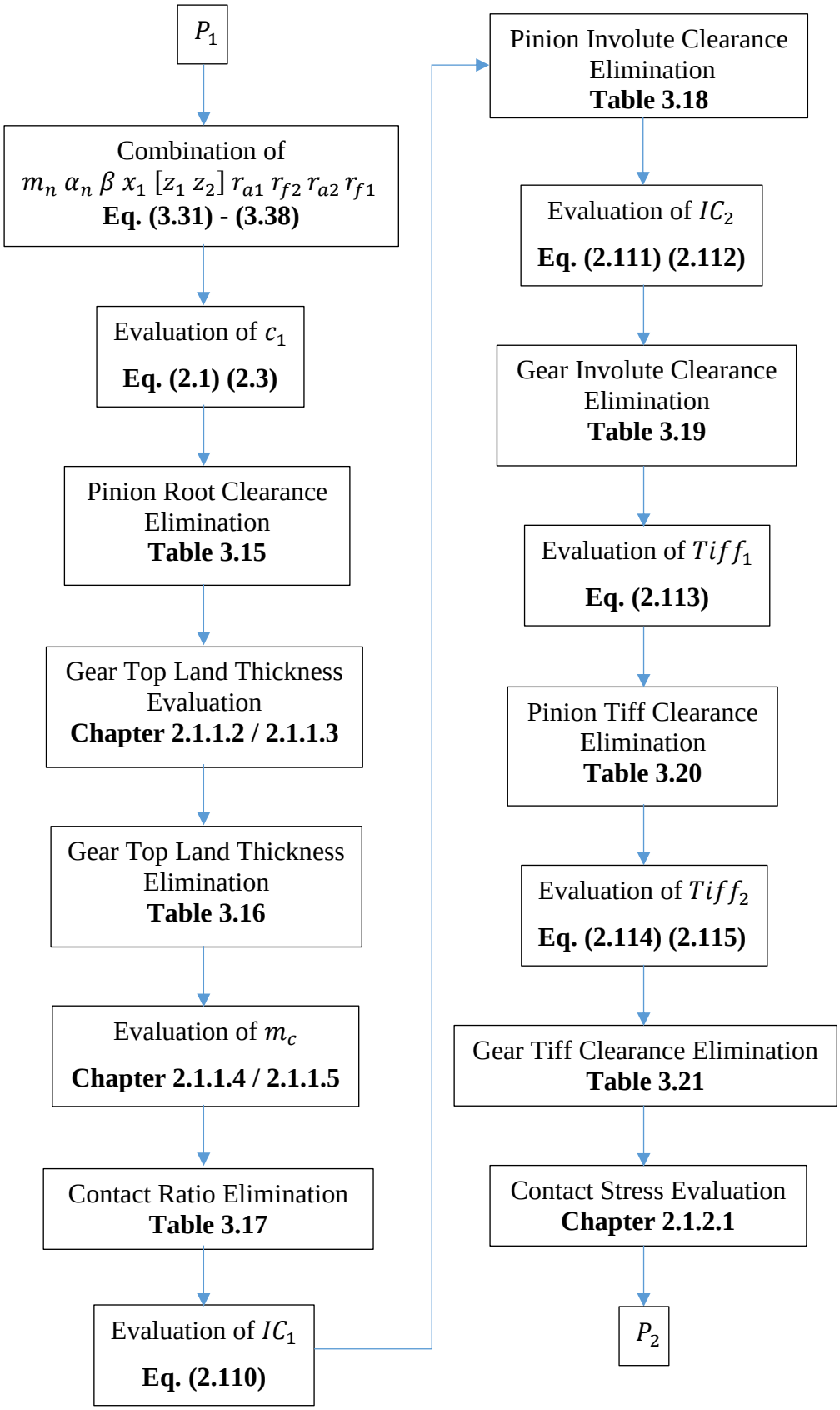
P_1
Combination of $m_n\ \alpha_n\ \beta\ x_1\ [z_1\ z_2]\ r_{a1}\ r_{f2}\ r_{a2}\ r_{f1}$ **Eq. (3.31) - (3.38)**
Evaluation of c_1 **Eq. (2.1) (2.3)**
Pinion Root Clearance Elimination **Table 3.15**
Gear Top Land Thickness Evaluation **Chapter 2.1.1.2 / 2.1.1.3**
Gear Top Land Thickness Elimination **Table 3.16**
Evaluation of m_c **Chapter 2.1.1.4 / 2.1.1.5**
Contact Ratio Elimination **Table 3.17**
Evaluation of IC_1 **Eq. (2.110)**
Pinion Involute Clearance Elimination **Table 3.18**
Evaluation of IC_2 **Eq. (2.111) (2.112)**
Gear Involute Clearance Elimination **Table 3.19**
Evaluation of $Tiff_1$ **Eq. (2.113)**
Pinion Tiff Clearance Elimination **Table 3.20**
Evaluation of $Tiff_2$ **Eq. (2.114) (2.115)**
Gear Tiff Clearance Elimination **Table 3.21**
Contact Stress Evaluation **Chapter 2.1.2.1**
P_2

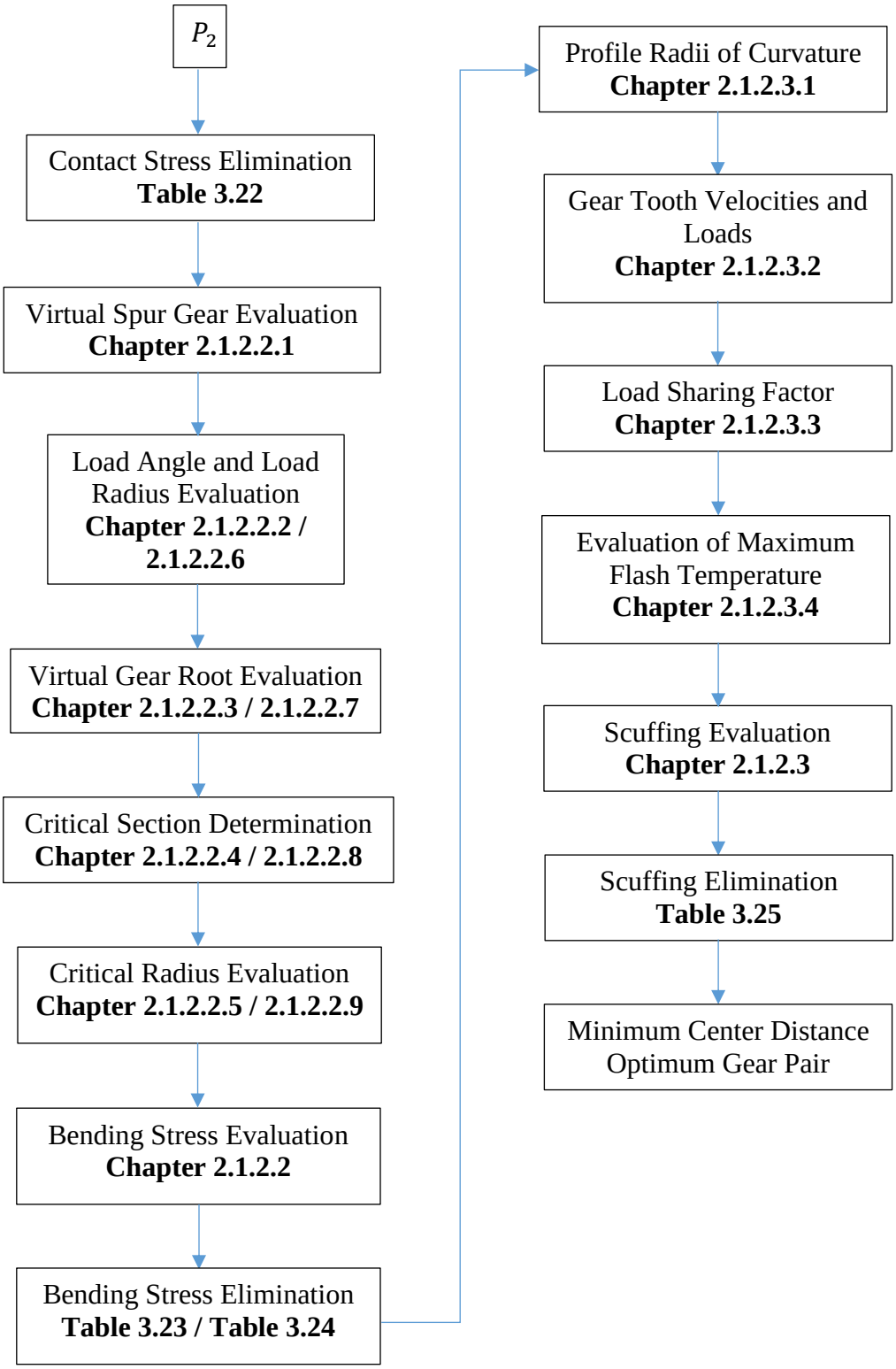
P_2
Contact Stress Elimination
Table 3.22
Virtual Spur Gear Evaluation
Chapter 2.1.2.2.1
Load Angle and Load Radius Evaluation
Chapter 2.1.2.2.2 / 2.1.2.2.6
Virtual Gear Root Evaluation
Chapter 2.1.2.2.3 / 2.1.2.2.7
Critical Section Determination
Chapter 2.1.2.2.4 / 2.1.2.2.8
Critical Radius Evaluation
Chapter 2.1.2.2.5 / 2.1.2.2.9
Bending Stress Evaluation
Chapter 2.1.2.2
Bending Stress Elimination
Table 3.23 / Table 3.24
Profile Radii of Curvature
Chapter 2.1.2.3.1
Gear Tooth Velocities and Loads
Chapter 2.1.2.3.2
Load Sharing Factor
Chapter 2.1.2.3.3
Evaluation of Maximum Flash Temperature
Chapter 2.1.2.3.4
Scuffing Evaluation
Chapter 2.1.2.3
Scuffing Elimination
Table 3.25
Minimum Center Distance Optimum Gear Pair